WindTech2015

The 2nd International Conference on Future Technologies in Wind Energy

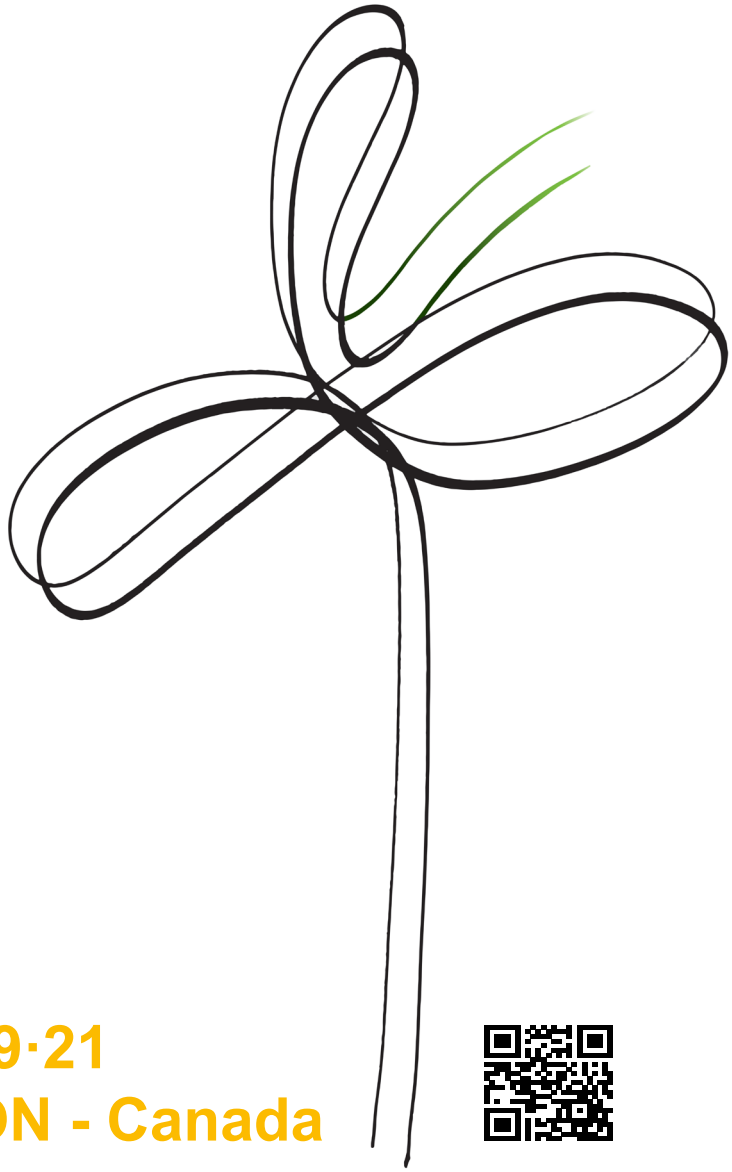

October 19-21

London, ON - Canada

BOOK of ABSTRACTS

© 2015 WindEEE Research Institute, Western University
2535 Advanced Avenue, London, Ontario, N6M 0E2, Canada

ISBN 978-0-7714-3099-2

Production : Adrian Costache
Production Assist : Jubayer Chowdhury, Ahmed Elatar, Maryam Refan, Dan Parvu, Djordje Romanic
Cover Art : Daniella Avila

Printed and bound in Canada

Contents

Welcome

The wind energy industry to date has faced both unprecedented successes as well as many challenges. Some of the new opportunities and challenges include improved reliability while ensuring overall performance, as well as opportunities and challenges related to offshore wind to name just a few.

WindTech2015 follows the success of the first International Conferences on Future Technologies in Wind Energy in 2013 to showcase impact research related to new technologies in wind energy and applications. In 2013 the Conference was held in Laramie, Wyoming, USA and co-organized by Jonathan Naughton and Ray Fertig of the University of Wyoming and Bent Sørenson and Durai Prabhakaran of DTU. This year's conference has as the venue London, Ontario, Canada and it is co-organized by WindEEE Research Institute at Western University, Canada, Cornell University and University of Wyoming in USA as well as by Danish Technical University (DTU), Denmark. The name WindTech was adopted as the name with the intent to organize a series of conferences to be held every two years. The intention is to organize conferences that, while maintaining the overarching topic of Wind Energy Technology, they embrace different them54es for every conference.

The main theme of WindTech2015 is wind energy related experiments and the instrumentation required to carry out those experiments. The experiments and instrumentation include both full scale (with one dedicated session this year) and laboratory (with two dedicated sessions this year). These sessions are complemented by a large palette of sessions in wind farm tools, modelling and simulations and rotor and blade design.

We are delighted to welcome so many of you here, especially those who made long journeys, to share your expertize and cutting edge results from your wind energy research. Can we encourage you to get on board with WindTech looking forward and whether you and your institution are interested in participating in, hosting or sponsoring WindTech 2017?

The host of WindTech2015 is the Wind Engineering Energy and Environment (WindEEE) Research Institute at Western University in Canada. WindEEE RI was established in 2011 as a clear recognition of new opportunities related to the emergence of the novel WindEEE Dome facility and the extensive collaborations this mega-project has generated at Western among several Faculties and with Canadian and International partners.

Western University is internationally recognized as the leading global university in wind engineering and we have identified "resiliency in the global built-habitat against natural hazards" as an area of strategic importance. Western's strength in wind research comes from strong, interdisciplinary teams of researchers from several faculties, including Engineering, Science, Social Science and the Richard Ivey School of Business. The University is also the only institution in Canada currently offering a graduate program in wind engineering. With a full-time enrolment of 32,000, Western University is a leading research-intensive university with a full range of academic and professional programs.

The university campus is in London Ontario, a thriving city of approximately 500,000, located midway between Toronto and Detroit. With parks, river valleys, tree-lined streets, and bicycle paths, London is known as the "Forest City" and boasts an international airport, galleries, theatre, music and sporting events. The venue of WindTech2015 is the Ivey Spencer Leadership Centre. As southwestern Ontario's only IACC-Approved conference hotel, this historic Georgian estate is the ideal location for meetings and overnight accommodations.

We would like to welcome you to London, Ontario and the WindEEE Research Institute at Western!

The Organizing Committee

Horia Hangan / WindEEE Research Institute, Western University

Jonathan Naughton / Wind Energy Research Center, University of Wyoming

Rebecca J. Barthelmie / Sibley School of Mechanical and Aerospace Engineering, Cornell University

Jakob Mann / Department of Wind Energy, Danish Technical University

Invited Speakers

Alberto Zasso | Scale Model Technology for Wind Energy: Numerical vs Experimental Validation in Wind Tunnel

Alberto Zasso having received a PhD in Mechanical Engineering in 1989, is now Full Professor in Applied Mechanics at Politecnico di Milano, chairing the courses of Applied Mechanics, Mechanical Vibrations (BSc Mech. Eng.), Dynamics of Mechanical Systems, being Lecturer on Wind Engineering (Building Aerodynamics, Structures Aeroelasticity) (MSc Mech. Eng.), responsible for the course "Atmospheric Boundary Layer, fundamental physics and modelling" (PhD Mech. POLIMI). His research is in the field of Structures Dynamics due to Wind Interaction applied to long-span bridges and high rise buildings, bluff body aerodynamics and vortex shedding induced vibrations. The key research became recently wind energy and CFD with focus on aerodynamic boundary layer numerical modelling and wind tunnel scale model validation of CFD wind interaction numerical modelling. He made experience on wind tunnel testing of horizontal axis (scaled models) and vertical axis (full scale prototypes) wind turbines, as well as implementation on HPC of CFD LES modelling of horizontal axis wind turbines. The scientific activity resulted in more than 100 publications at National and International level. He has been responsible for the design and realization of the Boundary Layer Wind Tunnel at Campus Bovisa, being at present the Director of the facility. Member of TPWind the European Wind Energy Technology Platform and POLIMI Representative at EERA JP Wind Energy, he participated to relevant international projects: member of the Panel of Specialists for the P.M.C. of Stretto di Messina Suspension Bridge, member of the design team of the BB3 Third Bosphorous Bridge for aerodynamics, leader of the POLIMI team awarded by PRACE-INCOME4WINDFARMS-Innovative HPC Computational Methods for Wind Farms, partner of the EU project LIFES50+ on offshore floating wind turbines.

David Hickey | Business Perspective and Useable Innovation

Based in Oakville, Ontario, David Hickey is the Vice President of Wind Power and Renewables Division for Siemens Canada Limited and is responsible for all strategy, sales, supply chain, project management and operations of the Division throughout Canada.

David has broad experience in leadership roles across the Wind Power and Fossil Power Generation portfolios with an emphasis in Project Management in Canada, the United States, and Scotland. Before joining Siemens in 2001, David was a Project Manager/Quantity Surveyor for various Property/Residential Developers in Scotland.

David holds a Bachelor’s degree in Quantity Surveying from Glasgow Caledonian University in Scotland.

David Maniaci | Wake Validation Experiment Planning for the SWiFT Facility

David Maniaci is the Rotor Blade and Wind Plant Aerodynamics Lead in the Wind Energy Technologies Department at Sandia National Laboratories in Albuquerque, NM. His current research includes the verification and validation of models that capture wind turbine wake dynamics, studying the effects of leading-edge erosion and soiling on airfoil and rotor performance, and the functional scaling and design of rotor blades. He received a Ph.D. in Aerospace Engineering from the Pennsylvania State University, where he was an instructor of aircraft design for several years and performed research in applied aerodynamics, wind tunnel testing, and wind turbine aerodynamics.

Doug Cairns | Business Perspective and Useable Innovation

Doug Cairns is a Professor of Mechanical Engineering of the Mechanical & Industrial Engineering Department at MSU. Prior to coming to MSU, he was Manager of Composites Technology at Hercules Materials Company (Now Hexcel) where he conducted research on composite materials applied to primary structure. He has a B.S. and M.S. from the University of Wyoming, and a Ph.D. in Aeronautics and Astronautics the Massachusetts Institute of Technology. He is a Member of ASME (Composite Materials Subcommittee), AIAA (past Materials Technical Committee Chairman). He is Chairman of the Mechanical Engineering Graduate Studies Committee.

His current professional interests include the understanding of advanced materials as applied to primary structure and understanding the materials, manufacturing, and structural performance link for new engineering systems. Dr. Cairns has funding from the Office of Naval Research, the National Renewable Energy Laboratory - Wind Technology Center, and the U.S. Air Force. Prof. Cairns is the Chief Engineer for Radius Engineering in Salt Lake City, Utah and consults for several industrial and private sector partners.

Peter Clive | Application of Scanning LiDAR in Wind Energy Research

Peter has been associated with the wind power industry since taking his PhD in physics in 2002. He has had a central role in the development of the Galion Lidar, the 2nd generation wind Lidar system. This system enables wind fields to be surveyed with previously unobtainable detail and precision, revealing flow characteristics and structures that have a significant impact on the productivity and longevity of wind power assets. Peter also pioneered the introduction of response deficit analysis into wind turbine performance assessment, allowing the expertise and experience of wind analysts to be leveraged in the most focused and cost effective manner. His interests also include innovative resource assessment techniques that extract all the available information from the long and short term datasets from target and reference sites, minimizing project uncertainty and boosting project value. Peter has published widely on the subject of Lidar and has addressed many conferences around the world.

Hassan Peerhossaini | Laminar Mixing for Energy Efficiency: Theory and Experiment

Dr. Hassan Peerhossaini is Distinguished Professor of Fluid Mechanics and Heat Transfer at the University of Paris (France) where he directs the Paris Interdisciplinary Energy Research Institute (PIERI). His research focuses on the physics of turbulence in reactive flows, hydrodynamic stability and transition to turbulence, active fluid dynamics, convective heat transfer, heat transfer and process intensification, energy efficiency, bio-resourced energy, and in particular on chaotic advection and its technological applications. His research interests lie also in interdisciplinary approach to energy systems and its social and economic impacts. He is the author of more than 450 publications including refereed archival papers, full length proceeding papers and technical reports. He received the ASME 2013 Lewis F. Moody award for his work on mixing. H. Peerhossaini has been associate editor of the ASME Journal of Fluids Engineering (2007-2013) and is currently associate editor of the Journal of Applied Fluid Mechanics.

Dr. Peerhossaini is a member of the French “Haut Comité de Mécanique”, scientific delegate of the French “Haut Conseil d’Evaluation de Recherche et Enseignement Supérieur”, Director of the “Energy of Tomorrow” program of Sorbonne Paris Cité, and member of several national and international scientific committees. He has been Deputy Director of the interdisciplinary energy program of CNRS.

Horia Hangan | New multi-scale physical simulations for Wind Energy in the WindEEE Dome

Dr. Horia Hangan is a Professor in the Department of Civil Engineering and Environmental at Western University and the Director of the Wind Engineering, Energy and Environment (WindEEE) Research Institute (www.windeee.ca).

In 2009, Professor Hangan received a 30 million dollar grant by the federal (Canada Foundation for Innovation) and provincial (Ontario Research Fund) funding agencies to design and built the WindEEE Dome. WindEEE is a world novel facility meant to reproduce and study the impact of three-dimensional and time dependent wind systems on the man-made and natural habitat.

Professor Hangan's research is in the simulation and impact of high intensity winds (downbursts and tornados), wind energy (wakes, sitting in complex terrain, wind turbine blade aerodynamics) and wind environmental impacts (urban wind environment, atmospheric pollution-dispersion, wind-driven rain and snow). He authored 2 book chapters and more than 200 journal and conference publications, acts as reviewer and is part of the Editorial Board of several international journals such as Journal of Fluid Mechanics, AIAA Journal, Journal of Fluids and Structures, ASME Journal of Fluids Engineering, ASME Journal of Solar (and Wind) Energy, Journal of Wind Engineering and Industrial Aerodynamics. He is member of several professional organizations such as the Board of Directors of the Canadian Society for Mechanical Engineering (CSME), Task Committee Leader of the ASCE on Non-synoptic winds, the Technical Committee of the National Institute Standards and Technology (NIST). He is presently on the Western University Research Board.

Jakob Mann | Experimental Investigations of Flow Over Terrain for Wind Energy

Jakob Mann got his Master degree in Astrophysics in 1990 from Aarhus University, Denmark and his PhD in 1994 about micrometeorology from Aalborg University, Denmark, for work done at Risø National Laboratory on various aspects of atmospheric turbulence. Jakob is now Professor of Wind Energy and Atmospheric Turbulence at the Technical University of Denmark where he also works with Doppler lasers. He is currently president for the European Academy of Wind Energy providing high quality conferences on wind energy and PhD seminars for all wind energy students in Europe.

As a part that work Jakob is heading an effort to launch a new open-access journal called Wind Energy Science. Starting 2015, Jakob heads the New European Wind Atlas project with the goal of providing experimentally validated models and data for wind turbine site assessment all over Europe.

Jonathan W. Naughton | Coordination of Measurement and Modeling for Validation of Wind Farm Simulations

Jonathan W. Naughton has been a faculty member in the Mechanical Engineering Department at the University of Wyoming since 1997 and is currently a Professor and Director of the Wind Energy Research Center. Dr. Naughton obtained his B.S. from Cornell University and his Ph.D. from the Pennsylvania State University in the area of compressible fluid dynamics. Prior to joining the UW faculty, Dr. Naughton worked at NASA-Ames Research Center for four years. During the 2004-2005 academic year, Dr. Naughton was a visiting faculty at Chalmers Technical University in Gothenberg, Sweden where he worked with the turbulence research laboratory. Dr. Naughton's current research includes the development of skin-friction measurement techniques and turbulent flow measurement, modeling and control with applications to jet flows, wake flows, base drag reduction, unsteady blade aerodynamics, and atmospheric boundary layer modeling. As the Wind Energy Research Center has grown, Dr. Naughton spends an increasing amount of time interacting with industry, government labs, state organizations, and academic institutions involved in developing the understanding and technology necessary for expanding the penetration of wind energy into the electricity market with a particular focus on the development of Wyoming wind resources. Faculty from the center were recently awarded a 4.25 million dollar grant considering the interaction between wind farm efficiency, transmission stability, and economics of transmission**.**

Dr. Naughton is an active member of the American Physical Society, the American Helicopter Society, and the American Institute of Aeronautics and Astronautics. In the latter society, Dr. Naughton is an Associate Fellow and served as the Chair of the Aerodynamic Measurement Technology Technical Committee from 2008-2010. He is married to Leann and has two sons, Kian and Evan. Dr. Naughton is also an Alpine Trainer with the Professional Ski Instructors of America - Rocky Mountain Division.

Marianne Rodgers | Research Activities on an Operating Wind Farm

Dr. Marianne Rodgers has been the Scientific Director at the Wind Energy Institute of Canada in North Cape, PEI since March, 2014. Prior to joining WEICan, Marianne researched many types of alternative energies, including fuel cells, batteries, and photovoltaics, at the Florida Solar Energy Center in Cocoa, Florida. Marianne holds a B.Sc. in chemistry from St. Francis Xavier University in Antigonish, NS and a Ph.D. in chemistry from Simon Fraser University in Burnaby, BC. Marianne’s research in alternative energy has resulted in more than 40 publications and more than 40 invited and conference presentations.

Michael Harris | Lidar in the Wind Industry: from the Lunatic Fringe to Mainstream Acceptance

Michael Harris has played a pioneering role in the development of lidar for the wind industry. He received a Class 1 degree in Physics from Oxford University in 1980; following his PhD in Atomic Physics from the University of Newcastle, he worked at the Joint Institute for Laboratory Astrophysics (JILA), Boulder, Colorado, and at the University of Essex. He joined DRA (now QinetiQ) Malvern in 1993, and became a Fellow of the Institute of Physics in 2001. He has contributed to the invention and design of a variety of lidar systems including the ZephIR laser anemometer. Until 2008 he was Technical/Team Leader for Remote Sensing at QinetiQ Malvern, and is currently Chief Scientist at ZephIR Lidar, where he continues to develop and promote laser anemometry for use in the wind energy industry.

Rebecca J Barthelmie | An Overview of the PEIWEE Experiment 2015

Rebecca J Barthelmie is a Croll Fellow and Professor in the Sibley School of Mechanical and Aerospace Engineering at Cornell University. Her research encompasses many aspects of wind energy but focuses on resources and wind turbine wakes with an emphasis on large wind farms. She is author of more than 110 journal papers, 11 book chapters and 400 conference papers and reports. She is co-chief editor of the journal Wind Energy, and on the science and technical committees of many wind energy conferences. At Risø National Laboratory from 1993-2006 she worked on more than 10 offshore wind farms in Europe in various roles including resource measurement, modeling and consultancy. She led several large international projects including 'Efficient Development of Offshore Wind Farms' and was the leader of the 'Flow' workpackage in the large international project 'UPwind' funded by the European Commission. In 2009 she received the annual scientific award from the European Wind Energy Academy for 'her extraordinary efforts and achievements in the field of wind energy research'. She is currently the lead on a number of research projects funded by the Department of Energy and National Science Foundation in the USA focused on wind turbines wakes and resource characterization in large wind farms on- and offshore.

Scott Schreck | Controlled Inflow Experiments for A2e Wake Modeling and Validation

Scott Schreck joined NREL's National Wind Technology Center in 1998, and since then has served in diverse roles within the center, ranging from basic and applied research to utility scale technology development. At present, he leads various large-scale experimental efforts, supported by both DOE and industry partners, which are aimed at understanding the fluid mechanics of the wind turbine, wind plant, and atmosphere, as the determinants of energy production and machine structural loads.

Early in his career at NREL, Scott's responsibilities included planning and analyses of experiments in the NASA Ames 80' x 120' wind tunnel, as well as establishment of International Energy Agency Annex 20, a multinational consortium of turbine aerodynamics researchers from Asia, Europe, and North America for developing and validating turbine aerodynamics models. Subsequently, Scott managed the Low Wind Speed Technologies program, DOE's $40M multiyear effort for utility scale wind energy technology development. This effort consisted of a portfolio of industry-NREL subcontracts for developing wind turbine prototypes and components, and for conceptualizing long range technologies.

Before coming to NREL, Scott was an Air Force officer and led a variety of defense science and engineering programs. These included the USAF Seiler Research Laboratory/Air Force Academy unsteady aerodynamics research program, a joint effort aimed at aircraft maneuverability enhancement. His final assignment was with the Air Force Office of Scientific Research where he managed the Computational Mathematics Program, a multidisciplinary program that supported university, industry, and Air Force laboratory computational research efforts in fluid dynamics, combustion, structures, materials, nanotechnology, multidisciplinary design optimization, and parallelization.

Tanay Sidki Uyar | Transition to Ecological and Democratic Societies using 100% Renewable Energy Community Power

Dr. Uyar has been a Professor of Renewable Energy at Marmara University since 2001, where he heads the Faculty of Engineering. He also serves as President of Eurosolar Turkey and Conference Chair of IRENEC 2013. From 1994-2001, he was an Assistant Professor at Kocaeli University on the Faculty of Technical Education at the Department of Electrical Education. Previous professional experience includes being a Senior Research Scientist during TUBITAK, Scientific and Technical Research Council of Turkey, Marmara, serving as a member of the Energy Systems Research Department at the Scientific and Industrial Research Institute, and holding the position of Director of the Chamber of Electrical Engineers Istanbul Branch from 1976-1978. He completed his formal education in Istanbul, Turkey, receiving his BSc and MSc (the latter in Nuclear Engineering) from Boğaziçi University, Faculty of Engineering, Department of Electrical Engineering. He received his PhD from Yildiz Technical University, Mechanical Engineering Department. Dr. Uyar also serves as Vice President of the World Wind Energy Association, Board Member of the International Solar Energy Society, Board member of the World Bioenergy Association, and Member of the World Council for Renewable Energy.

Torben Mikkelsen | 3D Wind Field Measurements obtained with DTU Wind Energy's Space and Time Synchronized WindScanners

Professor Torben Mikkelsen from DTU Wind Energy Denmark engages with wind remote sensing measurement systems for wind energy research, in particular atmospheric boundary-layer wind and turbulence research. Torben Mikkelsen is engaged with research and technological developments in the Test and Measurement Section in the Wind Energy Department at the Technical University of Denmark, DTU.

As daily leader of the WindScanner Research and Innovation team he is engaged with the development of remote sensing-based research infrastructure experimental research facility called WindScanner, cf. www.windscanner.dk and www.WindScanner.eu.

He is also engaged with scientific instrument development, in particular with the development of innovation products such as the wind lidar based WindScanners for turbine inflow (SpinnerLidar) and other exiting remote sensing devices, including also small "Lidic telescopes" for wind tunnel reference measurement and wind industry applications.

Professor Mikkelsen received his PhD from the Technical University of Denmark in 1983, followed by a Postdoc position as Associate research professor at the Naval Postgraduate School, 1985-1986 in Monterey, Ca USA, Departments of Meteorology and Physics. He became full professor at DTU in 2011. His scientific background is plasma physics, atmospheric sciences, atmospheric dispersion and atmospheric boundary-layer wind and turbulence.

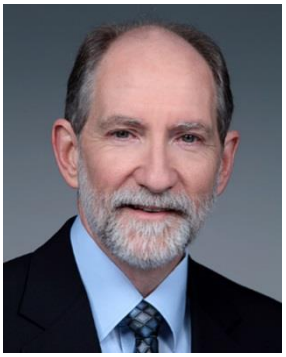

William Shaw | Wind Plant of the Future: DOE's A2e Initiative

Dr. Shaw is a Staff Scientist at the U.S. Department of Energy's (DOE's) Pacific Northwest National Laboratory. In a career spanning three decades he has specialized in turbulence and structure of the atmospheric boundary layer, including air-sea interaction and boundary layers in complex terrain. In the last decade, he has focused on boundary layer processes affecting wind energy. He has published nearly 50 articles in peer-reviewed journals. His recent work has included a one-year assignment in 2010–11 at DOE headquarters providing technical and programmatic support to DOE's Wind and Water Power Program. He currently serves on the Executive Management Committee of DOE's Atmosphere to Electrons (A2e) Initiative as the laboratory lead for the atmospheric sciences component of that program across the DOE national laboratories.

Abstracts

Dynamic Modeling and Simulation of a Wind Turbine

A. Hazal Altuğ
Research Asst., Ankara, Turkey

İlkay Yavrucuk
Assoc. Prof., Ankara, Turkey

Introduction

Installed wind capacity is increasing around the world [1]. Wind turbine research is equally on the rise. One such area of research is the development of real-time running dynamic models. In this paper a generic dynamic model for a three-bladed horizontal axis wind turbine for its operational envelope is developed using Blade Element Momentum (BEM) Theory. Verification of the model is performed by comparing results with the commercial software of LMS Samtech, Samcef for Wind Turbines (S4WT) [2].

Body

The BEM Theory is used to model aerodynamic forces and moments acting on blades as distributed loads. Blades are assumed rigid, wind is assumed uniform and wind shear is ignored. Hub and tip losses are included [3]. Axial and tangential induction factors are calculated by iteration [4]. In order to calculate aerodynamical forces, relative wind velocity and angle of attack of an element, shown in Fig. 1, is calculated. Moment affecting each element is found by cross product of displacement and force vectors. Total moments acting on a blade are found by integration and repeated for all three blades while changing the azimuth angle defined for that blade. Total aerodynamic torque acting on the rotor shaft is then calculated by making necessary axis transformations to total aerodynamic moments on blades. Aerodynamic power output of the model is calculated using aerodynamic torque. Also power coefficient is calculated to confirm the model does not exceed Betz limit. The dynamic model is developed in the MATLAB/Simulink environment.

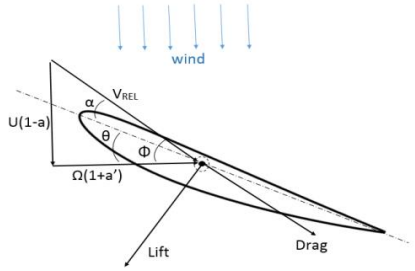

Fig. 1 Velocities and Forces on a Blade Element

The verification of the code is done for a wind turbine modeled in S4WT [5]. Three different load cases were used; below-rated, rated, and above-rated. Rotational speed is assumed constant and gravitational forces are ignored.

Firstly, the simulation is performed using the Samcef software. Then, the same wind scenario is applied to the model using same turbine properties. For each blade section, axial and tangential induction factors, tip hub losses, angle of attack, inflow angle, lift and drag coefficients and normal and tangential forces are collected for each element. Total aerodynamic torque, power and power coefficients of rotor are calculated for each wind load case and added.

Torque, Power and Cp related results are shown in Table 1. Both power and power coefficient are calculated using torque.

	Below Rated		Rated		Above Rated	
	Samcef	Hazal	Samcef	Hazal	Samcef	Hazal
Torque (Nm)	4.3E4	3.83E4	1.18E6	1.34E6	2.45E6	2.68E6
Power (W)	5.89E4	5.21E4	1.85E6	2.11E6	3.76E6	4.21E6
Cp	0.29	0.26	0.347	0.39	0.152	0.17

Table 1 Comparison of Torque, Power and Power Coefficients

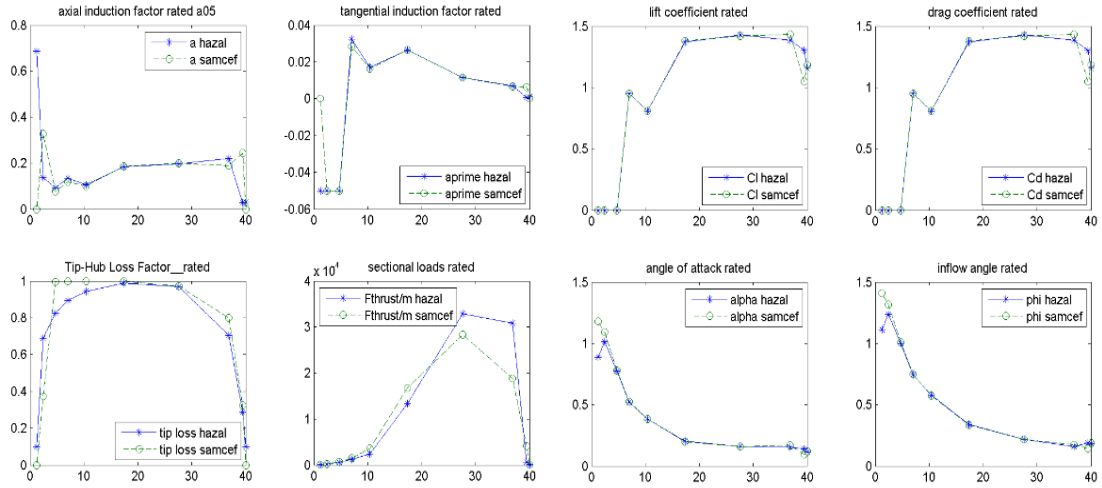

Fig. 2 Comparison of Sectional Properties for Rated Load Case

Comparison plots for the case of rated load are shown in Fig. 2. At tip sections, hub-tip losses are different from S4WT values. This makes lift, Cl, and drag, Cd, coefficients different with a chain reaction; losses affect axial and tangential induction factors, which then affect inflow angle and angle of attack and finally Cl, Cd values are affected since aerodynamic coefficients are a function of angle of attack. This could be because of the difference in the assumptions of aerodynamical losses which are applied as a correction to BEM theory.

Details used to create the dynamic model and results for the below-rated and above-rated load case simulations will be explained in the final paper.

Acknowledgments

This study is supported by METU Center for Wind Energy (MetuWind). Their support is greatly appreciated.

References

[1] G. W. E. Council. Wind in numbers. http://www.gwec.net/ global-figures/wind-in-numbers/.
[2] S4WT. Lms Samtech Samcef Wind Turbines. http://www.plm.automation.siemens.com/en_us/ products/lms/samtech/samcef-wind-turbines.shtml, 2015.
[3] P. J. Moriarty and A. C. Hansen. AeroDyn theory manual. National Renewable Energy Laboratory Golden, Colorado, USA, 2005.
[4] J. F. Manwell, J. G. McGowan, and A. L. Rogers. Wind energy explained: theory, design and application. John Wiley & Sons, 2010.
[5] Bonnet. SWT V3.302 Stationary Aerodynamics Validation 2013.

Scanning and Nacelle-Based Wind Lidars for Measuring Wind Turbine Wakes

A Cassola
University of Strathclyde, Glasgow, UK
Oldbaum Services, Stirling, UK

M Stickland
University of Strathclyde, Glasgow, UK

A Oldroyd
Oldbaum Services, Stirling, UK

Abstract

Wind turbine wakes have been of great interest to the wind energy community for many years. Measuring real life wakes poses many technical and economic challenges, especially offshore, however a greater understanding of them could lead to improved wind farm designs which would translate into, among other benefits, increased energy. Recent developments in remote sensing technology for wind energy, in particular light detection and ranging (lidar) devices, brought along new opportunities for measuring full scale wakes.

Nacelle-mounted and scanning lidar devices were deployed on an offshore wind farm site in Denmark for one year with the intent and purpose of measuring wind turbine wakes. Four nacelle-mounted two-beam lidars stood in pairs atop two wind turbine nacelles in a forward and backward facing configuration. Each pair took readings at approximately hub height at a total of twelve range gates and at a maximum distance of 400 m upstream and downstream of their respective turbine. For a short period the aft lidars were configured to measure along just one line-of-sight pointing directly behind the turbines. Two long-range scanning lidars detected winds from different locations at the edge of the farm up to a distance of 6 km. They scanned inside the farm, seeing nearly all turbines, as well as outside of it.

The vast amounts of data collected were used to analyse single wind turbine wakes for the case of free stream upstream wind. All the lidars recorded data at a sampling rate of 1Hz (the single beam aft facing lidars measured at 4Hz) and different novel data manipulation processes were created for each lidar type. The various data outputs were used to analyse the wakes for different free stream conditions but also to compare and contrast results from the two lidar types and to analyse comparisons.

The results presented show how the wind speed deficit and turbulence intensity values varied with distance downstream of a turbine for the different free stream wind conditions seen, as well as with distance laterally and vertically through from the turbine rotor. Results for wind speed profiles from both lidar types compare well in general for certain optimal spatial binning schemes applied when processing the scanning lidar data. This shows that these forms of wind data acquisition are very promising for wake measurements but also for other wind energy applications.

Windtell: Wind Farm Analytics

Austin Crough
Turbulence and Energy Lab, University of Windsor, Canada

Philip McKay
Turbulence and Energy Lab, University of Windsor, Canada

Rupp Carriveau
Turbulence and Energy Lab, University of Windsor, Canada

David Ting
Turbulence and Energy Lab, University of Windsor, Canada

Marianne Rogers
Wind Energy Institute of Canada, PEI, Canada

Introduction

The flow fields around a single wind turbine are multifaceted. Diverse inflow conditions, frequently colored with degrees of shear and turbulence, will pass through the machine and produce downstream wake structures of at least comparable complexity. Commercial wind farms are made up of many machines that rarely operate in isolation. Interaction between single machines, or groups of machines; can have consequences on individual turbine, and total farm performance. These effects are not well understood, and are of interest to both fundamental and applied communities. Such effects can be dependent on many different external factors and scales, difficult to simulate in a wind tunnel or computational model. What is required is a field-scale laboratory. Contemporary wind turbines monitor hundreds of variables from their physical environment every second. Large commercial wind farms can be made up of more than one hundred such "instruments" set up over large distances. The challenge is in managing and strategically mining the big data that is available. Windtell is a non-structured query language (NOSQL) database tool developed to enable both farm operators and researchers to better benefit from the wealth of data produced by commercial wind farms.

In this abstract, a sample output of the tool is demonstrated. The database is used to examine the most commonly studied group dynamic in wind farms; wake induced effects [1,2]. In this instance, the tool was focused on two neighboring machines to explore how closely their power generation compared for similar yaw angles.

Body

Two 2.3MW, 93 m rotor, turbines (T8 and T9), are selected from a 200 MW wind farm on the north coast of Lake Erie. The farm is located in Kent County; which has the lowest proportion of tree cover in Ontario. This part of the County has an elevation differential of less than 1 m. Machines T8 and T9 form a line of that deviates 30^{o} CCW from North and runs to edge of Lake Erie to the South. The units are spaced roughly 7 rotor diameters apart.

Two years of continuous yaw angle and corresponding power production data sampled at 0.33 Hz were averaged into 10 minute packets. This data was used to produce a plot of turbine power against yaw angle, in this case for a single wind speed of 10 m/s. Fig. 1 portrays a type of "power rose" that illustrates the average power produced for each yaw angle over two years for each of T8 and T9. Initial review of Fig. 2 indicates that despite their relatively similar location on the farm, their power production varies notably based on the yaw angle of the machines.

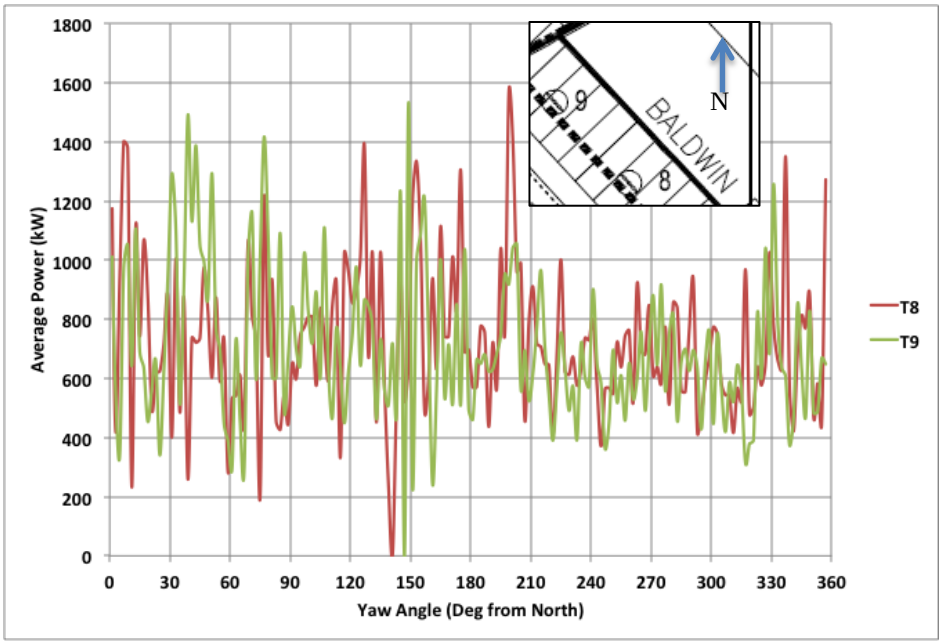

Fig. 1. Average Power (kW) vs. Turbine Yaw Angle (Deg from North) for a Wind Speed of 10 m/s. Data collected at 0.33 Hz averaged into 10 minute packets over 2 years.

Closer review of Fig. 1 reveals some anticipated features including suspected wake-induced losses at collinear nacelle alignments. At 30 degrees T9 is directly upwind of T8, and is evidently making more power. At 210 degrees the reverse is true as expected. However, in between, and outside of these points the effects are largely unpredicted. The two signals do not appear to track each other well. This would suggest, that while being situated in relatively similar surroundings their inflow wind fields are quite different. Further, the discrepancies change with changing wind speed (not shown here). This raises interesting questions about the connected interaction of wind turbines across a farm. Mined data like that shown in Fig. 1 produced from the massive data sets generated by wind farms every day could provide opportunities for owners to learn more about the performance of their farms. Further, it could better enable the research community to explore atmospheric behavior in elevations affected by wind farms, and better understand the consequences of interaction between these dynamic machines.

Acknowledgments

JJ Davis and Kruger Energy, NSERC, Ontario Centres of Excellence.

References

[1] McKay, P, Carriveau, R, S-K Ting, D. Wake impacts on downstream wind turbine performance and yaw alignment. *Wind Energy*. 2012. 16(2): 221-234.

[2] Barthelmie, RJ, Pryor SC, Frandsen ST, Hansen KS, Schepers JG, Rados K, Schlez W, Neubert A, Jensen LE and Neckelmann S. Quantifying the Impact of Wind Turbine Wakes on Power Output at Offshore Wind Farms. *Journal of Atmospheric and Oceanic Technology*. 2010. 27: 1302-1319.

Inverse Wind Turbine Blade Design for Scaled Wake Testing

Arash Hassanzadeh
University of Wyoming, Laramie, WY, USA

Jonathan W. Naughton
University of Wyoming, Laramie, WY, USA

Introduction

Turbine wake interactions affect wind turbine performance and lifetime. For improved wind farm performance, a better understanding of wake behavior is necessary. Many details regarding wind turbine wakes are still not fully understood, since detailed experimental wake studies, especially reasonable size turbines with no blockage and scaling issues, are rare. Such experiments are necessary to allow for better understanding of wake behavior and to provide a means for validating computational models.

A number of experimental studies have been carried out to better understand and predict turbine wakes [1-2]. A comprehensive review on wind turbine wake research is given by Vermeer et al. [3]. However, wind tunnel experiments are mostly conducted for wind turbines that are geometrically scaled down, thus working at relatively low Reynolds numbers compared to the full scale phenomena that consequently results in scaling effects. As a result, the wake produced by the model is likely to suffer from scale effects [3]. To address this problem, recent work done at the Sandia National Laboratory has focused on the design of a blade for a scaled wind turbine to produce a wake similar to that of a large wind turbine [4]. In the design process, they relaxed geometric and Re scaling, but matched dimensionless circulation for full-scale and sub-scale wind turbine.

The objective of this work is to design a sub-scale wind turbine blade that generates a wake comparable to that of an industrial scale large wind turbine. As the wake arises from interaction between the flow and the blade, and the wake dynamics and stability are affected by load distributions on the blade, matching normalized forces for full-scale and sub-scale wind turbine should result in similar wake structure.

Approach and Example Design

Using normalized normal and tangential load distributions, a blade element momentum theory (BEMT) inverse design approach is employed to determine the blade chord and twist angle distributions. To start the process, the large wind turbine's normalized normal and tangential forces are considered as prescribed parameters, and an inverse design approach is used to determine the sub-scale wind turbine blade shape. In BEMT, the forces on the blade are assumed to act over discrete elements of the blade, and there is no radial flow and no direct interaction between the elements. The forces on the blades are determined by the lift coefficient C_l and drag coefficient C_d of the airfoils, which were determined using XFOIL. A flowchart of this procedure can be found in Fig. 1, which provides the 13 steps used to determine the geometry of each element of the blade.

In our case study, the normal force (F_n) and tangential force (F_t) distributions across the blade of the large wind turbine, the NREL 1.5 MW turbine, are specified. The NREL design code FAST [5] is used in this example to specify these distributions. These forces are then normalized with the turbine's thrust and torque respectively. By matching the normalized load distributions for full-scale (NREL 1.5MW) and sub-scale (2m diameter) wind turbine, the sub-scale load distribution is found. The airfoil geometry along the sub-scale blade was chosen to be similar to that of a commercial wind turbine starting with thick airfoils near the blade root and transitioning to thin airfoils near the blade tip. Five high Reynolds number DU-airfoils ranging in maximum relative thickness from 18% to 35% chord were chosen for this design. Using the loads and airfoil shapes, the blade geometry was determined using the approach in Fig. 1. Fig. 2 shows a solid model of the resulting blade design. It can be seen that the blade shape is similar to the modern wind turbines blade shapes.

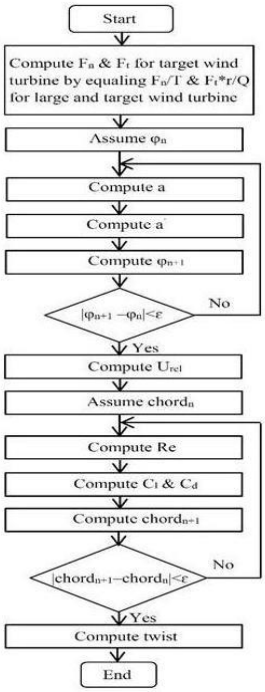

Fig. 1 Flowchart of the code for designing the blade

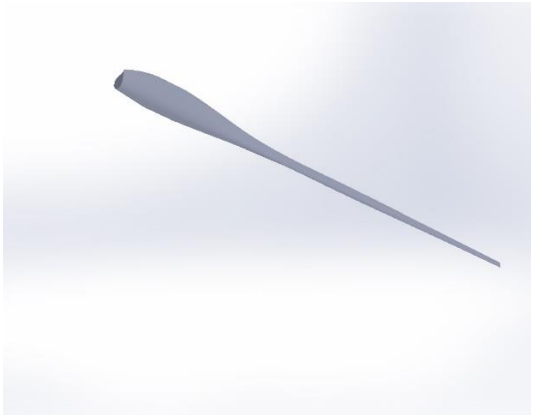

Fig. 2 Solid model of the blade shape

Acknowledgments

This work was supported by the U.S. Department of Energy, Office of Science, Basic Energy Sciences, under Award # DE-SC0012671.

References

[1]Adaramola MS, Krogstad PA. Experimental investigation of wake effects on wind turbine performance. Renewable Energy, 36 (2011), pp. 2078–2086.
[2]Hu H, Yang Z, Sarkar P. Dynamic wind loads and wake characteristics of a wind turbine model in an atmospheric boundary layer wind. Experiments in Fluids 2012;52:1277-94.
[3]Vermeer L J, Sorensen J N and Crespo A. Wind turbine wake aerodynamics Aerospace Sciences 2003; 39:467–510.
[4]Kelley C, Berg J. Sub-scale Inverse Wind Turbine Blade Design Using Bound Circulation. http://meetings.aps.org/link/BAPS.2014.DFD.L30.2
[5]Jonkman JM, Buhl ML. FAST User's Guide; Technical Report NREL/EL-500-38230; National Renewable Energy Laboratory: Golden, CO, USA, 2005.

High Resolution Vertical Wind Profile Measurements

Anders Tegtmeier Pedersen, Nikolas Angelou, Torben Mikkelsen
DTU Wind Energy, Risø Campus, Frederiksborgvej 399, 4000 Roskilde, Denmark

Introduction

DTU Wind Energy develops and deploy high-resolution short-range WindScanners for research in wind energy and boundary-layer meteorology, cf. www.windscanner.dk [1,2]. In September 2014 a signal-to noise improved and low wind speed featured new WindScanner, to be supplied to the WindEEE research facility in Ontario, Canada, was ready for testing. WindScanner measures the line-of-sight projected wind component of the 3D wind velocity vector of atmospheric flow. For measurement of the vertical wind component the WindEEE WindScanner was starred vertically into the air flow above DTU Risø Campus during a sunny slightly convective afternoon. One goal was to evaluate the lidar's ability to measure wind speeds close to zero wind including zero crossings, and therefore the vertical *w*-component as function of height was measured.

In this contribution we present the resulting high spatial and temporal resolution vertical wind component measurements up to a height of 140 m, obtained by scanning back and forth continuously along a vertical line. Vertical wind speed measurements of turbulent coherent structures in the atmosphere in 2D space-time field plots are shown, and also analysis of the measurements with respect to vertical wind speed mean and turbulence will be given. The effect of the lidar's sampling volume and its dependency on measurement range (in this case height) will also be discussed.

Lidar System and Experiment

The WindEEE WindScanner is a continuous-wave (CW) Doppler lidar with a two degree of freedom steerable laser beam scan head and adjustable measuring range. Discrimination between positive and negative wind speeds is obtained via an in-phase and quadrature detector system [3,4]. In order to measure the *w*-component the laser beam was aligned to point vertically upwards and the motor controlling the focus range set to scan linearly back and forth in 2 s, meaning that each height were visited once per second. The linear motion of the focus motor results in a hyperbola motion of the focus point ranging from 6-140 m in this experiment. The lidars line-of sight probe length increases as the measurement range squared and was estimated to vary from 0.045-25 m for the range used. Wind speeds were sampled at a rate of 102 Hz and in total data were collected for approximately 60 min.

Fig. 1 The WindEEE WindScanner at DTU Risø Campus.

Results

Fig. 2 shows an example of the vertical wind component measured as function of time and height. The presence of large coherent structures is evident particularly at the elevated heights, where also the length scale of the vertical wind component turbulence is known to increase with height.

At ground level, between heights of 6 and say 20 meters, fine scale coherent structures are evident. At these low heights, the probe length of the WindScanner lidar is small compared to the length scale of the turbulence, which is of the order of the measurement height itself. At 10 m height the wind lidar probe length is only about 0.12 m. At 100 m measurement height, however, the length scale of the turbulence is also about 100 meters, whereas the probe length of the WindScanner increases to about 13 m.

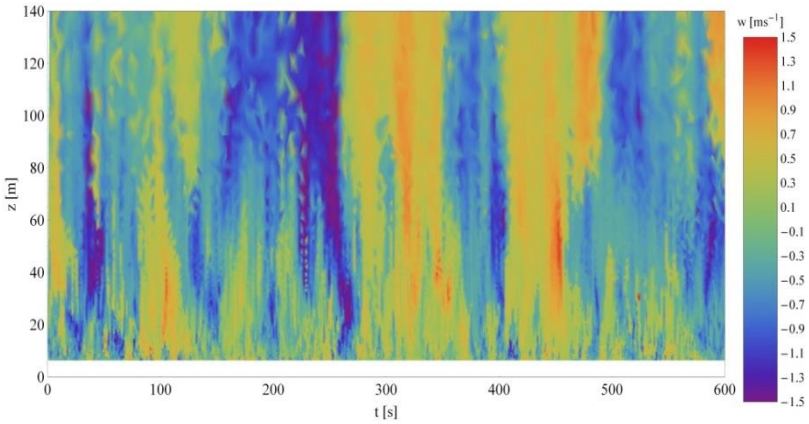

Fig. 2 Vertical wind profile measurements. The plot shows vertical wind speed measured between 6 and 140m height during a 10-min period.

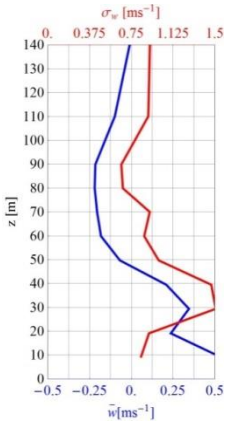

Fig. 3 Mean and standard deviation profiles.

In Fig. 3 we present the measured vertical mean $\bar{w}$ and turbulence σ_w profiles as function of height over DTU Risø campus. The measurements are from ground level from the western side of Building 100, cf. Fig.1. Although the mean horizontal wind speed was low, 4-5 m/s, and sunny afternoon convective atmospheric stability conditions prevailed, the mean horizontal wind direction was predominantly South-westerly. From SW wind direction, the wind passes over an up to 20 m tall and 1 km long alley, in addition to several nearby 2 story buildings. The profile measurements were consequently gathered over rather complex terrain. The WindScanner Doppler measurements are positive when approaching the lidar. The vertical mean wind profile (blue curve) consequently shows ascending wind speed aloft DTU Campus at heights between 50 and 120 m, consistent with the gently windward upsloping terrain. Near the top of the measurement range, at 140 meters, the vertical wind speed tends to zero, as anticipated. The vertical turbulence profile (red curve), however, exhibits increased turbulence levels in the air aloft the alley between 20 and 50 meters. This is believed to be due to internal boundary layer turbulence generated locally within an internal boundary layer by wind shear heat flux as the air flow passes inland from the Roskilde Fjord only 500 meters upwind. Above the 50 m height level, the vertical turbulence level is almost constant as also anticipated in a convective surface layer.

Acknowledgments

University of Western Ontario, Canada is gratefully acknowledged for supporting DTU Wind Energy to provide WindEEE with a WindScanner under contract UWORFPSR-01245 Supply of a Light Detection and Ranging (Lidar) System.

References

[1] T. Mikkelsen, J. Mann, and M. Courtney, "Wind Scanner: A full-scale Laser Facility for Wind and Turbulence Measurements around large Wind Turbines," in *EWEC 2008* (EWEA - The European Wind Energy Association, 2008), p. 10.
[2] T. Mikkelsen, "Lidar-based Research and Innovation at DTU Wind Energy – a Review," J. Phys. Conf. Ser. **524**, 012007 (2014).
[3] C. F. Abari, A. T. Pedersen, and J. Mann, "An all-fiber image-reject homodyne coherent Doppler wind lidar," Opt. Express **22**, 25880 (2014).
[4] A. T. Pedersen, C. F. Abari, J. Mann, and T. Mikkelsen, "Theoretical and experimental signal-to-noise ratio assessment in new direction sensing continuous-wave Doppler lidar," in *Torque 2014* (IOP Publishing, 2014), Vol. 524, p. 012004.

Potential Inaccuracies in Energy Estimates from Standard Wind Turbine Power Curves

A. Salisbury, K. Visser
Clarkson University, Potsdam, NY USA

Introduction

The viability of the empirically determined wind turbine power curve as a means to predict annual energy output was examined. Both the impact of time period and number of averaged binned data points required were investigated using a ducted wind turbine (DWT) tested at the Clarkson University Wind Turbine Test Site. The wind speed at each data point was used with the empirically determined curve to determine the expected energy produced each day and compared to the recorded energy to determine the accuracy of using the standard empirical power curve. Results indicated an over-prediction of the energy by more than three times the recorded energy output at given times. An alternate power curve derivation was proposed to increase prediction accuracy based on a third order curve fit of the entire empirical power data. Analysis indicated that the suggested power curve was significantly more accurate than the time average power curve.

Estimating Wind Energy

Accurate renewable energy estimates are key for an effective reduction of carbon based energy sources an acceptance of renewable energy strategies. In the small wind turbine market, consumer response has indicated that small wind turbines often fail to achieve the rated power of the turbine based on manufacturer provided data (Gipe [1]). The most common method for predicting the annual energy output of a turbine is to create a representative power curve of the wind turbine, based on time averaged test results of a turbine, and to apply a wind probability distribution curve based on local annual characteristics to this data to determine the energy.

The literature indicates that extensive work has been done on determining the effectiveness of different probability distributions (PDFs). The Weibull, the Rayleigh and Lognormal probability distribution functions are the most widely used functions (Celik [2]). There is also a large amount of uncertainty dealing with the prediction of the wind due to uncertainty in measurement, changes in air density, difficulty in choosing proper Weibull parameters and uncertainty over the long term period (Lackner et al, [3]).

These previous analyses assume, however, that the given power curve is representative of the turbine performance. Therefore, this study focused on the energy estimate accuracy by examining whether the power curve did indeed predict the actual energy output based on measured data, at least in the short term.

Results and Discussion

Experimental data for the present study was acquired on an experimental DWT, Fig. 1, tested at the Clarkson University Wind Turbine Test Site. Loads were applied with a variable resistance bank, with power and meteorological data acquired at a rate of one hertz.

Fig. 1 WindTamer DWT

The average power curve was determined using a time averaging methods as outlined by Gipe [1]. A standard practice for small wind turbines is to use one minute time averaging (AWEA [4]). The averaged data was then sorted into wind speed bins, each bin corresponding to integer values of the wind speed. The result of this analysis for one day is shown in Fig. 2. The average power output for each wind speed bin, over all the data for each load setting, then corresponds to the power to be used in the power curve for that load setting. This study varied the number averages required from 6 to 30 to gain a larger understanding of the impact of the number of binned averages on the prediction

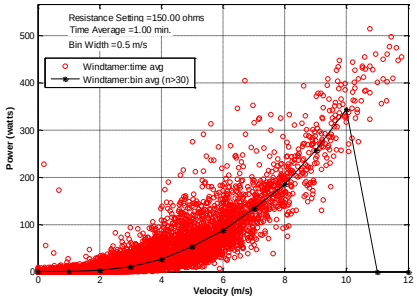

Fig. 2 Daily Turbine Power Curve

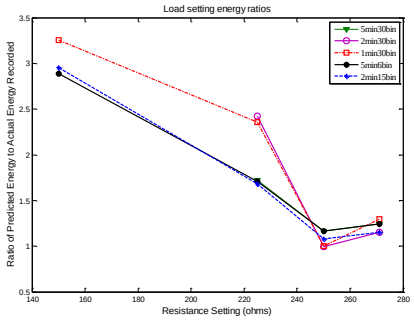

Fig. 3 Load Setting Energy Ratio

accuracy. The final power curve was created by taking the highest power output from each of the loads for each wind speed.

The ratio of predicted energy to recorded energy production was used as a means to evaluated the accuracy of the power curve's predictive capability. As indicated in Fig. 3, there appears to be a relationship between load setting and accuracy of the prediction. At a high resistance, low load per se, the data indicated greater accuracy, whereas for low resistances, or high load, the accuracy decreased. This further indicates a possible correlation between wind speed and prediction accuracy, as higher loads are used higher wind speeds. The average daily accuracy was shown to vary between .99 and 3.26.

An alternate method of simply fitting a cubic function to all the measured data was investigated in an effort to increase prediction accuracy, and to simplify the power curve creation process. Fig. 4 shows a comparison between the cubic fitted power curve and the empirically binned and averaged power curve. It was observed that the proposed power curve has lower predicted power output for all wind speeds.

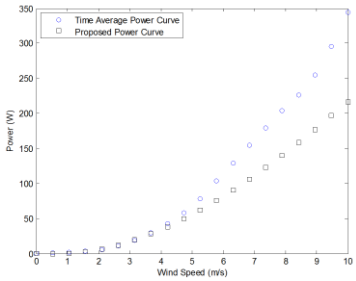

Fig. 4 Power Curve Behavior

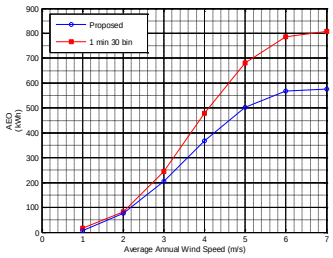

Fig. 5 Annual Energy Predictions

The effect of modifying the turbine power curve on the predicted annual energy production of the turbine was drastically lower, as expected. A Rayleigh PDF yielded the results in Fig. 5. It was found that the annual energy production estimate for the new power curve was 26% lower than the time average power curve, when using an average annual wind speed of 5 m/s. It was also found that the difference in predicted annual energy output between the two power curves was dependent on the average annual wind speed.

References

[1] Gipe, P. "Testing the Power Curves of Small Wind Turbines." Available at: http://www.wind-works.org/articles/PowerCurves.html (Accessed November 20,2012)
[2] Celik, A. 2003. "Assessing the suitability of wind speed probability distribution functions based on wind power density." *Renewable Energy* 28(10): 1563-1574..
[3] Lackner, M.A., A.L. Rogers, and J.F. Manwell. 2007. "Uncertainty analysis in wind resource assessment and wind energy production estimation." *45th AIAA Aerospace Sciences Meeting and Exhibit, AIAA-2007-1222,* , p. 1-16.
[4] "AWEA Small Wind Turbine Performance and Safety Standard." AWEA 9.1-2009.

Effective Velocity Model Improved Actuator Line Approach for HAWT and VAWT Applications

Alberto Zasso
Politecnico di Milano – Dipartimento di Meccanica, Milano, Italy

Paolo Schito
Politecnico di Milano – Dipartimento di Meccanica, Milano, Italy

Luca Bernini
Politecnico di Milano – Dipartimento di Meccanica, Milano, Italy

Introduction

The numerical method is implemented as an actuator-line approach in the open-source framework OpenFOAM®[1]. The key point of the problem is the correct definition of the wind incidence angle and wind speed that is responsible for the load on the blade. Standard approach relies on Blade Element Momentum theory to define the actual wind speed and incidence angle that produces a certain load. This approach is useful for structural calculations, but CFD provides very detailed flow fields that are useful for a more physical description of the local wind. Current AL models calculate the aerodynamic forces generated by a section of the blade, using as reference the wind evaluated in a single point, at some distance upstream of the rotor plane [2] or located in the region close to the blade section [3] [4]. These methods are quite diffused, however the results in terms of wind turbine power prediction can be improved; in general the thrust acting on the rotor is reproduced with a good accuracy.

The goal of this paper is the definition of a model able to define the relationship between flow characteristics around a wind turbine blade section and the forces acting on the airfoil: this model will be called Effective Velocity Model, since it aims to evaluate from local inflow velocity fields the equivalent undisturbed velocity incident to the airfoil and then use this value to correctly interpolate the airfoil tabulated polar curve and define the forces acting on the blade section.

VAWT and HAWT Applications

The development of aerodynamic models for VAWTs has been hindered by the inherent complexity of the flow. In the last few years, lots of efforts have been spent to develop much more refined turbine models which can correctly reproduce the interaction of the flow with turbine rotors. The motivation of such efforts is the need to develop models that can better predict the behavior of turbines in order to optimize their performances.

In the current paper a CFD approach is adopted, based on well-known Actuator Line (AL) model and implemented in OpenFOAM. The wind turbine is not entirely modelled as in the fully-resolved CFD simulations, but the effects of the interaction between air and blades are introduced directly in the Navier-Stokes equations as a source term. The simulation mesh does not contain the blade profile, thus a coarser mesh is adopted, causing a reduction of the computational costs and simulation time.

AL can simulate the overall performances without huge computational costs and allows to reproduce tip vortex and wind turbine wake. Hence, it might be useful in simulation of wind farms.

The source forces are introduced in the cells that are intersected by the actual position of the blades. Despite the fact that it was developed for HAWT simulations, AL model can be extended to VAWT ones with the same characteristics, the differences lie in the lifting line positions and how the aero dynamic forces are computed from the incoming wind. In this code it is possible to implement independent pitch control (IPC) for maximizing the energy harvesting and the reduction of cyclic loads on HAWT, while IPC may promote self-starting capabilities

on H-Darrieus type VAWT. Fig. 1 shows the representation of the blades in the AL simulation of a VAWT and of a HAWT and the reproduction of the wake by means of contours of iso-vorticity.

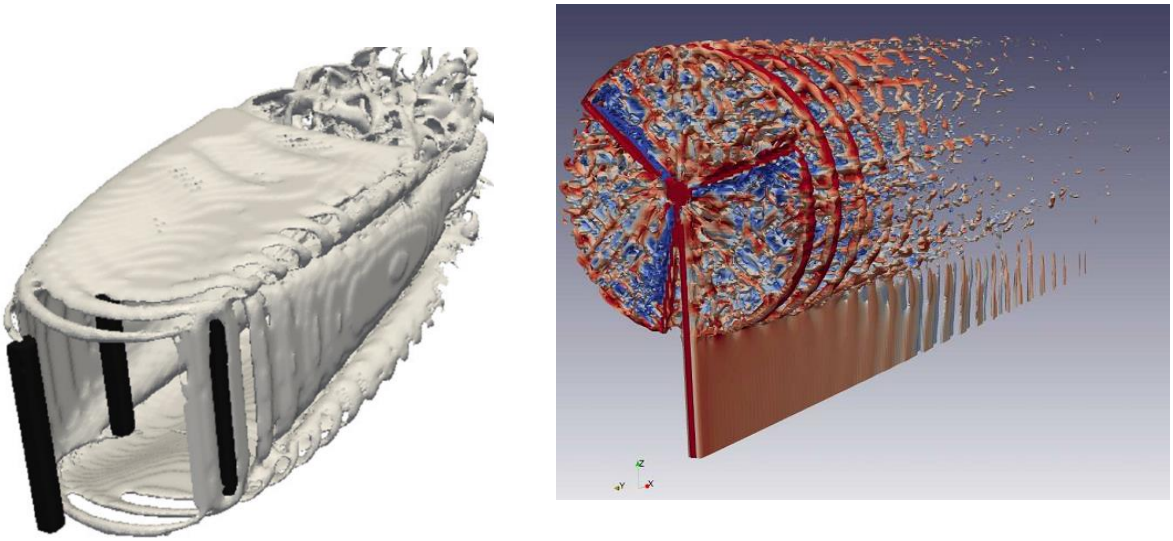

Fig. 1 Vertical axis wind turbine (left); Horizontal axis wind turbine (right)

References

[1] The OpenFOAM Foundation, *www.openfoam.org*
[2] Wu Y, Porté-Agel F. *Large-eddy simulation of wind-turbine wakes: Evaluation of turbine parametrisations. Boundary - layer meteorology*. 2011;138(3):345-366.
[3] Martinez L, Leonardi S, Churchfield M, Moriarty P. *A comparison of actuator disk and actuator line wind turbine models and best practices for their use. In: American Institute of Aeronautics and Astronautics*; 2012. 10.2514/6.2012-900.
[4] Troldborg N. *Actuator line modeling of wind turbine wakes.* [PhD Thesis]. Technical University of Denmark, Lyngby, Denmark; 2008.

Scale Model Technology for Wind Energy: Numerical Vs Experimental Validation in Wind Tunnel

Alberto Zasso
Politecnico di Milano – Dipartimento di Meccanica, Milano, Italy.

Marco Belloli
Politecnico di Milano – Dipartimento di Meccanica, Milano, Italy.

Hermes Giberti
Politecnico di Milano – Dipartimento di Meccanica, Milano, Italy.

Ilmas Bayati
Politecnico di Milano – Dipartimento di Meccanica, Milano, Italy.

Luca Bernini
Politecnico di Milano – Dipartimento di Meccanica, Milano, Italy.

Introduction

Wind energy is growing enormously, consistently with the continuous energy supply demand, moving to Multi-Megawatt and floating offshore horizontal axis wind turbine's concepts. In this scenario, research and development are playing a key-role in decreasing the overall cost of energy as well as increasing the efficiency and the reliability of such complex machines. From this perspective experimental data are necessary for calibrating multidisciplinary and predictive numerical tools, serving also as reference for new generation wind turbines. To this aim, full-scale experiments, which would apparently represent the greatest information from engineering and operational (decision-making) point of view, suffer from drawbacks such as difficulties in the definition of the inlet boundary condition, along with environmental conditions that are not available "on request". This brings about the need of a large amount of time to collect a set of data that are representative for the overall operating condition of the machine, beside the non-negligible cost in carrying out these measurements themselves and for such a long period. This generally goes with a limited access to the proprietary data (machine design and wind farm's management data).

Wind tunnel tests represent a good solution in that allows to test scale models and to gather reliable data in a controlled environment with known boundary conditions, making also more consistent the comparison with the numerical counterpart of the same test. In addition, the greatly larger number of different test conditions in enormously shorter amount of time, allows to span completely the operational range of the machine. Modern era miniaturized mechatronics, as well as materials technology improvements, allow to build wind tunnel scale model of wind turbine that very close to the full scale machines, in their functional capabilities. This turns out in testing significant control strategies, say Individual Pitch Control of the blades (IPC), as well as new optimized aero-elastic features, Fig.1.

As the new concepts of Multi-Megawatt wind turbines are mainly offshore, basin tests are necessary to be combined and compared with wind tunnel tests. However, this brings about some issues in the scaling process. More specifically, Froude number similitude (full/model scale), which characterize ocean basin tests, due to the presence of gravity based forcing (waves), can't be adopted in the wind tunnel tests, since it would be responsible, along with the Tips Speed Ratio (TSR) aerodynamic similitude, of too low wind tunnel wind speeds. This would cause excessively low measured forces on the model itself. On the contrary, having higher velocity scale factors, goes with higher rotational speed of the wind turbine model and then higher frequency band required from the IPC

motors for the blade pitch control. Furthermore, Reynolds similitude, which is hardly reached in wind tunnel tests, is handled by scaling blades also accounting for the re-design of the set of the airfoils adopted, with respect the full scale blade, also trying to optimize the overall trust of the rotor to be as closest as possible, in terms of similitude, with respect to the full scale.

Moreover, new perspectives of testing models of floating offshore wind turbines in ocean basin/ wind tunnel tests relies on Hardware-In-The-Loop approach, that turns out in hybrid testing approach (measured/simulated) [1,2]. Therefore, the aerodynamic input in ocean basin tests are simulated in real time as well as the motion of the floating platform for the wind tunnel counterpart, Fig.2 [3]. This approach allow overcoming scaling issues coming with testing structures affected by aerodynamic and hydrodynamic loads together. Ongoing European projects as LIFES50+ that involves, among industrial and academic partners, facilities as Marintek (Ocean basin) and PoliMi (Wind Tunnel) [4] intend to investigate thoroughly this HIL-based experimental approach as the new frontier for studying aero-hydrodynamics of floating wind turbines.

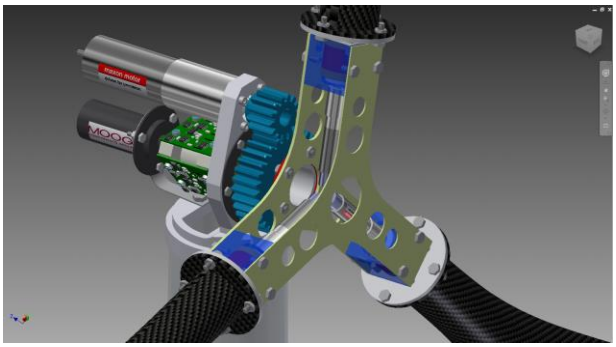

Fig. 1 Assembly of the nacelle of a Multi-Megawatt wind turbine scaled model (1/75).

Fig. 2 Hexapod: 6 degree of freedom robot to simulate the motion of a wind turbine for HIL-wind tunnel hybrid tests.

References

[1] Bayati I., Belloli M., Facchinetti A., Giappino S., ”Wind Tunnel Tests on Floating Offshore Wind Turbines: A Proposal for Hardware-In-The-Loop Approach to Validate Numerical Codes”. Wind Engineering, vol.37, N.6, 2013.
[2] Bayati I., Belloli M., Facchinetti A.,”Verification and Implemenation of a State-Space hydrodynamic model for wind tunnel-HIL application on FOWT”, DeepWind R&D Conference, February 2015, Trondheim, Norway.
[3] Bayati I., Belloli M., Ferrari D., Fossati F., Giberti H., ”Design of a 6-DoF Robotic Platform for Wind Tunnel Tests of Floating Wind Turbines”, Energy Procedia, pp. 313-323, 2014.
[4] Diana G., De Ponte S., Falco M., Zasso A., ”A new Large Wind Tunnel For Civil Environmental And Aeronauitcal Application”, Journal of Wind Enegineering and Industrial Aerodynamics, 74-76, 553-565, 1998.

Ducted Wind Turbines: More Efficient than Open Rotors?

B. Helenbrook and K. Visser
Clarkson University, Potsdam, NY USA

Stuart Wilson
Griffith University, Queensland, Australia

Introduction

A computational study was conducted to optimize the design of a slotted Ducted Wind Turbine (DWT) and provide guidance for a full-scale prototype. Seven variables were investigated: duct and flap angles of attack, gap ratio, rotor position, pressure drop factor, flap gap and flap overlap. It was observed that the optimum rotor placement was towards the trailing edge of the DWT, not in the highest velocity position, as is often surmised. Most importantly, however, the optimized output power coefficient exceeded that of a conventional rotor based on the projected frontal area, namely the exit area of the duct, indicating a ducted rotor to be theoretically more efficient than an open rotor.

Ducted Wind Turbine

DWTs are created by enclosing a horizontal axis wind turbine (HAWT) within a duct, often an airfoil revolved around the rotor axis. The presence of the duct increases the mass flow rate through the turbine resulting in an increase in the power coefficient proportional to the mass flow, (Gilbert and Foreman, [1]; Hanson, [2]; de Vries, [3]) as illustrated in Fig. 1. The theoretical maximum open rotor power extractable, from the rotor diameter stream tube, is 59.3% and is known as the Betz limit [4]. The power coefficient is defined as:

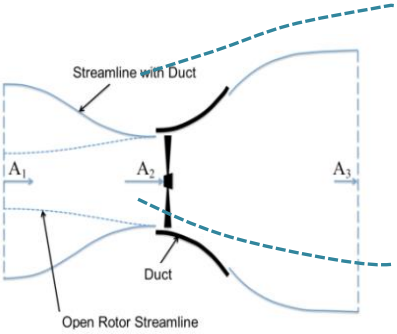

Fig. 1 Ducted Turbine Streamtube

$$Cp = \text{power extracted/power in the wind} = 2P/\rho V_o^3 \pi R^2$$

where $Cp_{max} = Cp_{Betz} = 0.593$. With an increased mass flow rate and velocity, a DWT increases the amount of generated power and Cp values can exceed the Betz definition, when based on the rotor area πR^2. Gilbert and Foreman suggested a Cp as high as 1.57, defining an 'augmentation ratio' of $Cp_{DWT} / Cp_{Betz} = 2.65$. Many studies have investigated the feasibility of DWTs (Hu et al, [5]; Igra O., [6]; Hansen et al, [7]; Werle and Presz [8]; Van Bussel, [9]; Oman, [10]; Moeller and Visser [11]; Jedamski and Visser, [12]; Venters; [13]) driving research in this area, however to date, no commercially viable design has realized these values.

Numerical Results

The parameters investigated are illustrated in Fig. 2. A baseline geometry was established based of a main duct lifting surface chord of 1.0m, a flapped chord length of 0.5m, and a rotor diameter of about 2.1m, resulting in a fineness ratio, length to diameter, of approximately 0.60. The results of the parametric investigation determined the best design parameters to be:

- Main surface angle of attack: Clarkson AP1 airfoil at 10°
- Flap angle of attack: AP1 airfoil at 34°
- Gap Ratio: 0.034 (1 - rotor diameter / duct diameter)
- Rotor Position: 59% of duct length
- Flap Gap: 0.023m, Flap Overlap: 0.149m

It should be noted that the purpose of the study was not to compute absolute numbers, but to provide direction for a prototype to be constructed for field testing. The FLUENT flow field solution, using a κ-ε turbulence model of the optimized design, is presented in Fig. 3. An averaged wind velocity of 1.15 of upstream was observed at the rotor, compared to an optimized open rotor velocity of 2/3. The augmentation factor was 2.16, yielding a *Cp* of 1.28. A sketch is shown in Fig. 4 of the geometry.

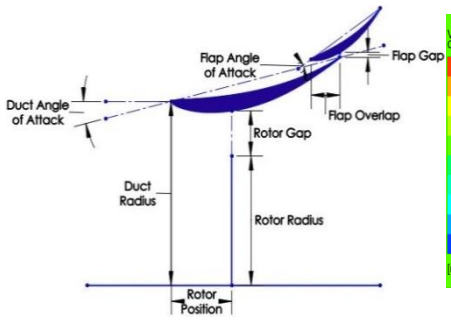

Fig. 2 DWT Geometry

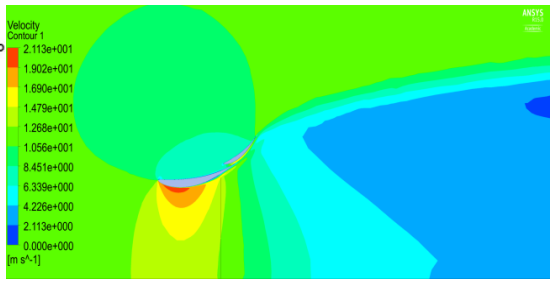

Fig. 3 Optimized Numerical Flowfield Solution

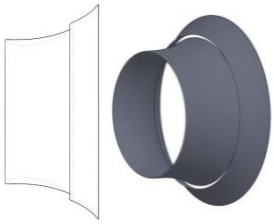

Fig. 4 Optimized Duct

The most interesting results, however, come about by examining the power coefficient, not in terms of the swept rotor area, but instead by projected frontal area, defining an equivalent DWT "Betz coefficient". The present duct had a PFA of 6.6m^2 yielding a Cp_{PFA} = 0.647, *greater than the longstanding 59.3 % limit.* In fact, an open wind turbine would require a rotor diameter of 3.03m, with an area of 7.2m^2, in order to produce the same power as the current DWT rotor. Work is continuing towards building a prototype for testing.

References

[1] Foreman, K. M., Gilbert, B. L., and Oman, R. A., "Diffuser Augmentation of Wind Turbines", Journal of Solar Energy, Vol. 20, No. 4, April 1978, pp.305-311.
[2] de Vries, O., "Fluid Dynmaic Aspects of Wind Energy Conversion", AGARDograph No 243, Advisory Group for Aeronautical Research and Development, 1979
[4] Betz, A., "Introduction to the Theory of Flow Machines", Pergamon Press, 1966
[5] Hu, SSu-Yuan and Cheng, Jung-Ho. "Innovatory Designs for Ducted Wind Turbines". Renewable Energy. 33 (2008):1491-1498.
[6] Igra O. "Reseach and Development for Shrouded Wind Turbines". European Wind Energy Conference EWEC84, Hamburg, 1984; 236-245.
[7] Hansen, M. O. L., N. N. Sorenson, and R. G. J. Flay. "Effect of Placing a Diffuser around a Wind Turbine". Wind Energy. 3 (2000): 207-213
[8] Werle, M.J. and W. M. Presz Jr., W. M., "Ducted Wind/Water Turbines and Propellers Revisited." Journal of Propulsion and Power, 24(5):1146-1150,
[9] Van Bussel, G. J. W., "The Science of Making more Torque from Wind: Diffuser Experiments and Theory Revisited." Journal of Physics: Conference Series 75 (2007)012010.
[10] Oman, R. A., Foreman, K. M., and Gilbert, B. L., "Investigation of Diffuser Augmented Wind Turbines". ERDA Rept. COO-2616-2, Parts I and II, Jan. 1977.
[11] Moeller, M. M., and Visser, K.D., "Experimental and Numerical Studies of a High Solidity, Low Tip Speed Ratio DAWT," AIAA- AIAA-2010-1585, 48th AIAA Aerospace Sciences Meeting and Exhibit, Orlando, FL., January 2010.
[12] Jedamski, D., and Visser, K., "Computational Analysis of a Diffuser using USM3D for Diffuser Augmented Wind Turbines". AIAA 2013-2933, 31st AIAA Applied Aerodynamics Conference, San Diego, CA, June 2013.
[13] Venters, R. (2014). "A Computational Investigation of Wind Acceleration in Relation to Turbine Performance and Design." Potsdam, New York: Clarkson University. 2000

Evaluation of a New Parameterization for Surface Stresses in Marine Atmospheric Boundary Layers Accounting for Non-Equilibrium Waves

Branko Kosović
National Center for Atmospheric Research, Boulder, Colorado, USA

Ned Patton
National Center for Atmospheric Research, Boulder, Colorado, USA

Mark Žagar
Vestas, Aarhus, Denmark

Peter Sullivan
National Center for Atmospheric Research, Boulder, Colorado, USA

Jimy Dudhia
National Center for Atmospheric Research, Boulder, Colorado, USA

Introduction

Flows in the marine atmospheric boundary layer (MABL) are affected by the interaction between surface waves and the atmosphere. Current parameterizations of surface stresses and fluxes in MABL are based on the assumption of wave-wind equilibrium and do not account for the effects of swell [1, 2]. Recent large-eddy simulations (LES) of the atmospheric boundary layer, coupled with an imposed wave field characterized by a realistic spectrum, have shown that non-equilibrium waves can significantly affect boundary layer winds [3]. This finding is of particular significance for offshore wind power development. It indicates that, when estimating the wind resource, it is important to accurately represent the effects of waves on hub-height winds. Based on LES of a MABL affected by non-equilibrium waves, we have extended the empirical surface stress parameterization developed by Andreas et al. to account for the effects of swell. The new parameterization was implemented in the Weather Research and Forecasting (WRF) model and tested using data from the FINO1 platform in the North Sea collected during 2006.

Body

Offshore wind power development requires accurately representation of the effects of waves on hub-height winds in estimating the wind resource or wind power forecasting. The results of our extension of the Andreas et al. [4] parameterization to account for the effects of swell show a small but potentially important improvement in predicting hub-height winds.

We first tested the new parameterization of the surface stress using the WRF Single Column Model (WRF-SCM). Following the successful test of our new surface layer formulation accounting for the effects of swell implemented within WRF-SCM, we used a three-dimensional, limited area version of WRF V3.6.1 to simulate an entire year (2006) over the North Sea. The numerical simulations were set up following industry standard practices for wind resource assessment. Each simulation was conducted daily for 30 hours starting at 00h UTC. The first 6 hours were used as a spin-up period. The output was saved every 20 minutes for the 24 hours between 06h UTC on the first day and 06h UTC on the second day. The computational domain covered the North Sea and North-Eastern Europe centered on the FINO1 tower and was discretized using nested computational domains with grid cell sizes of 9 km, 3 km, and 1 km. The innermost domain covered an area of 100 km × 100 km. In the vertical direction, we used a stretched grid with 37 levels. Initial and boundary conditions were derived from NCEP's Final Operational Global Analysis.

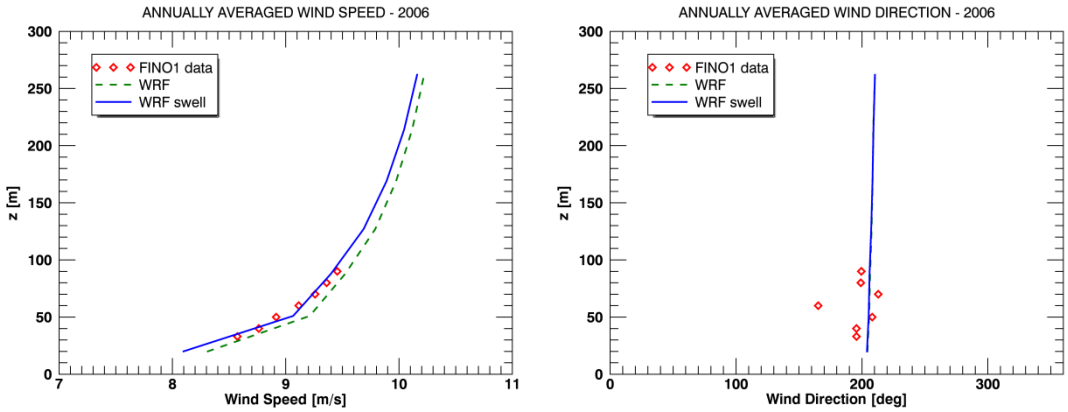

Fig. 1 Vertical profiles of annually averaged: (a) wind speed, and (b) wind direction at the FINO1 tower for 2006. Red diamonds depict the FINO1 tower observations, the green dashed line depicts results from a 3D WRF simulation using WRF's traditional Charnock formulation for surface roughness, z0 (Charnock, 1955), and the solid blue line depicts results from a 3D WRF simulation where the surface friction velocity is determined using Eq. 8 using the observed hourly wave data at FINO1

To assess the influence of the new parameterization, we conducted two simulations. A baseline simulation used WRF's standard Charnock [1] parameterization of wave effects on all domains, while the second simulation includes our new surface layer parameterization on the innermost domain only and used the Charnock parameterization on the outer domains. The assumption is that the wave state in the broad area surrounding the FINO1 tower can be represented by the measurements at the tower. For the simulation considering swell, observed wave-state information from FINO1 was updated hourly and held constant for the subsequent hour.

As can be seen from Fig. 1, reductions in annually averaged hub height wind speed error using the new wave-state-aware surface layer parameterization are modest. However, since wind turbine power production depends on the wind speed cubed, the error in estimated power production is reduced by almost 5%, which can substantially impact wind resource assessment and decision making with regards to the viability of particular location for a wind plant location. Furthermore, for a single 30-hour forecast, significant reductions in wind speed prediction errors can yield substantially improved wind power forecast skill, thereby mitigating costs and/or increasing revenue through improved: 1) forecasting for maintenance operations and planning, 2) day-ahead forecasting for power trading and resource allocation, and 3) short-term forecasting for dispatch and grid balancing.

Acknowledgments

This work was supported by the Department of Energy, Energy Efficiency and Renewable Energy Program, award DE-EE0005373.

References

[1] Charnock, H., 1955: Wind stress on a water surface. Quart. J. Roy. Meteorol. Soc., 81, 639–640, doi:10.1002/qj.49708135027.
[2] Drennan, W. M., P. K. Taylor, and M. J. Yelland, 2005: Parameterizing the sea surface roughness. J. Phys. Ocean., 35, 835–848, doi:10.1175/JPO2704.1.
[3] Sullivan, P. P., J. C. McWilliams, and E. G. Patton, 2014: Large-eddy simulation of marine atmospheric boundary layers above a spectrum of moving waves. J. Atmos. Sci., 71 (11), 4001–4027, doi:10.1175/JAS-D-14-0095.1.
[4] Andreas, E. L., L. Mahrt, and D. Vickers, 2012: A new drag relation for aerodynamically rough flow over the ocean. J. Atmos. Sci., 69 (8), 2520–2537, doi:10.1175/JAS-D-11-0312.1.

Small Wind Turbine Performance Evaluation Using Field Test Data and a Coupled Aero-Electro-Mechanical Model

Brian Wallace
Pennsylvania State University, University Park, USA

Dennis K. McLaughlin
Pennsylvania State University, University Park, USA

Susan W. Stewart
Pennsylvania State University, University Park, USA

Introduction

In small wind turbine applications, the electro-mechanical characteristics of the wind electric system can have a significant impact on the power production of the machine. Small wind turbines are almost always configured with a 2- or 3-bladed rotor directly coupled to a permanent-magnet synchronous generator (PMSG) which generates 3-phase AC power. The electro-mechanics of the system comprises of the drive efficiencies of the PMSG, efficiencies of the power electronics, and effective impedance of the load sink. Modern small wind turbines are moving towards maximum power point tracking (MPPT) algorithms which allow the wind turbine rotor to more consistently track its on-design performance points. It is the coupling of the electro-mechanics to the aerodynamics of the rotor that facilitates the MPPT approaches being developed. Without MPPT, as is common in not-so old wind-electric systems like the Whisper 175, small wind turbines typically spin at higher rotational speeds than they were designed for aerodynamically, producing less power and more noise. It is the coupling between aerodynamics and electro-mechanics that causes these high rotational speeds. The back-emf of the power system on the PMSG is not enough to operate the turbine rotor at the designed rotational speed. Little published research is available on this topic. Due to the competitiveness of the small wind industry, any developmental data produced by manufacturers is usually kept out of the public forum.

Body

A series of field tests and theoretical analyses was performed on various wind turbine rotor designs at two Penn State residential-scale wind-electric facilities. This work involved the prediction and experimental measurement of the electrical and aerodynamic performance of three wind turbines; a 3 kW rated Whisper 175, 2.4 kW rated Skystream 3.7, and the Penn State designed Carolus wind turbine. Both the Skystream and Whisper 175 wind turbines are OEM blades which were originally installed at the facilities. The Carolus rotor is a carbon-fiber composite 2-bladed machine, designed and assembled at Penn State, with the intent of replacing the Whisper 175 rotor at the off-grid system. Rotor aerodynamic performance is modeled using WT_Perf, a National Renewable Energy Laboratory developed Blade Element Momentum theory based performance prediction code. Steady-state power curves are predicted by coupling experimentally determined electrical characteristics with the aerodynamic performance of the rotor simulated with WT_Perf. A dynamometer test stand is used to establish the electromechanical efficiencies of the wind-electric system generator. Through the coupling of WT_Perf and dynamometer test results, an aero-electro-mechanical analysis procedure is developed and provides accurate predictions of wind system performance. The analysis of three different wind turbines gives a comprehensive assessment of the capability of the field test facilities and the accuracy of aero-electro-mechanical analysis procedures. Results from this study show that the Carolus and Whisper 175 rotors are running at higher tip-speed ratios than are optimum for power production. The aero-electro-mechanical analysis predicted the high operating tip-speed ratios of the rotors and was accurate at predicting output power for the systems. It is shown that the wind turbines operate at high tip-speeds because of a miss-match between the aerodynamic drive torque and the

operating torque of the wind-system generator. Through the change of load impedance on the wind generator, the research facility has the ability to modify the rotational speed of the wind turbines, allowing the rotors to perform closer to their optimum tip-speed. Comparisons between field test data and performance predictions show that the aero-electro-mechanical analysis was able to predict differences in power production and rotational speed which result from changes in the system load impedance.

Results in this study fill a void left in existing research in the field of small wind-electric systems. A complete set of dynamometer test results are presented for the Whisper 175 PMSG. This information has been used to develop an electro-mechanical model of the PMSG and is coupled with WT_Perf BEM rotor performance predictions to produce overall system power production predictions. Predictions are directly compared to results from the field-test campaigns. The additional capability to interchange rotor designs at the facility and change the root pitch angle to more closely match the aerodynamic and electro-mechanical properties of the generator and control system will soon be exploited in the next month of operation. This will also be reported in the presented paper.

Wind Turbine Nacelle Transfer Functions (NTFs) Calculated from Upwind Lidar and Tower Measurements

Clara St. Martin
Department of Atmospheric and Oceanic Sciences, University of Colorado, Boulder, CO, USA

Julie K Lundquist
Department of Atmospheric and Oceanic Sciences, University of Colorado, Boulder, CO, USA

National Renewable Energy Laboratory, Golden, CO, USA

Andrew Clifton
National Renewable Energy Laboratory, Golden, CO, USA

Scott J Schreck
National Renewable Energy Laboratory, Golden, CO, USA

Abstract

Despite their potential as a valuable source of individual turbine power performance information and turbine array energy production optimization information, nacelle-mounted anemometers have often been neglected because complex flows around the blades and nacelle interfere with their measurements. This work quantitatively explores the accuracy of and potential corrections to nacelle anemometer measurements to determine the degree to which they may be useful when corrected for these complex flows, particularly for calculating power curves in the absence of other meteorological data. Using 2.5 months of detailed upwind and nacelle-based measurements from a utility-scale wind turbine (a General Electric GE 1.5sle model with a 77-m rotor diameter), we calculate nacelle transfer functions (NTFs) and explore their sensitivity to atmospheric and turbine operational parameters to provide guidelines for the use of NTFs and to derive useful wind measurements from nacelle-mounted anemometers.

The wind measurement equipment upwind of the turbine includes meteorological tower anemometers on a 135-m tower and LIDAR vertical wind profiles. We compare hub-height inflow tower and LIDAR measurements to the wind profile across the entire swept rotor area (SRA) defined as the rotor-equivalent wind speed (REWS). To our knowledge, this is the first effort applying REWS to NTFs. We calculate unique empirical transfer functions for different atmospheric conditions defined by temperature stratification and turbulence intensity. The NTFs calculated for this site do not vary with atmospheric stability, though the NTFs do vary with inflow turbulence and blade pitch angle, which suggests careful investigation into turbine design, control and operation may be required for calculating NTFs for other sites.

High Intensity Wind Effect on Full-Scale PV Solar Panels

Derek Eden
University of Ottawa, Ottawa, ON, Canada

Elena Dragomirescu
University of Ottawa, Ottawa, ON, Canada

Shayan Mehranfar
University of Ottawa, Ottawa, ON, Canada

Introduction

The increase in use of photovoltaic (PV) solar panel systems for renewable energy production has generated extensive research into their aerodynamic behavior and structural effects, in an effort to update the current design guidelines with comprehensive recommendations based on field measurements and numerical simulations of wind-induced potential failures. The current study presents the design details of a wind-damage simulator which can re-produce high intensity drag, lift and shear wind forces on full-scale solar panels. In addition field measurements were performed on PV panels installed on a medium-rise flat roof and the results were used for calibrating the wind-damage simulator.

Wind Effect on PV Solar Panels

This paper outlines the CFD analyses performed for a 5 m x 5 m x 3 m high hollow structure large enough to house full-scale PV panels, with a 750 mm outlet on the roof extracting air through the enclosure and one 300 mm inlet on the bottom right corner of each side-wall which can open for releasing the internal pressure inside the box. Laminar CFD analyses were performed on the system, both with and without PV solar panels in the structure, for outlet wind speeds ranging from 10 m/s to 40m/s. Three solar panels analyzed were of dimensions 2 m x 1 m and inclined at 20° from the horizontal (Fig. 1). The results obtained were analyzed to characterize the wind speed profile of the flow in the domain as a whole and around the solar panels, in an effort to reproduce accurate test conditions for the PV panels with predictable wind streamline patterns and pressures.

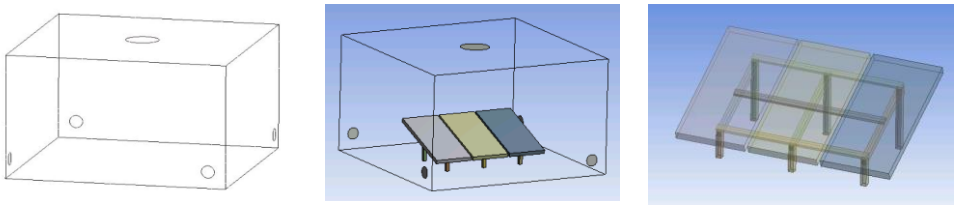

Fig. 1 CFD Simulation Details (a) Without panels, (b) With panels, (c) Panel geometry

The results of the CFD analyses showed a large variation in uplift pressure across the domain floor with a strong relation to the roof outlet velocity, reaching a maximum value of 4.3 kPa. A similar variation was noticed when solar panels were used, with maximum uplift of up to 3.8 kPa (Fig. 2), and was consistently found to be between 0.86-0.90 of the floor uplift before the panels.

The directional vector field of the wind within the domain was found to be similar in nature and increasing in velocity magnitude through increasing the roof outlet velocity. The introduction of the solar panel array into the enclosure was found to alter the flow for all the outlet wind speeds investigated; measurements taken from key locations within the domain show that the initial velocity distributions were reduced by an average of 32%. The simulated PV solar panels that were tested experienced large uplift forces of up to 3.8 kPa, with a widely ranged distribution of pressure throughout the panels' surface. Because these pressures were produced by wind currents

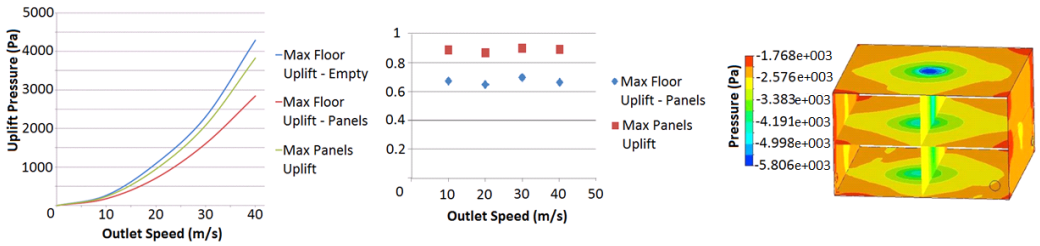

Fig. 2 (a) Maximum Pressure Distribution, (b) Ratio to Max Floor Pressure, (c) Typical Pressure Distribution (40m/s Outlet)

induced from the lateral inlet flows, it represents a more realistic simulation of the fluctuating behaviour of wind uplift phenomenon in nature. The time history plot of the lift force measured on the PV solar panels installed on the flat roof of the Mann Parking building over the month of October 2014 (Fig. 3), show the maximum forces exerted on the panel that were analyzed to calibrate the simulator to achieve appropriate pressures. It was found through the CFD analyses that through the increasing of the outlet speed from 10 m/s to 40 m/s, uplift pressure and pressure time lapse patterns of the simulation remained similar with increasing magnitude.

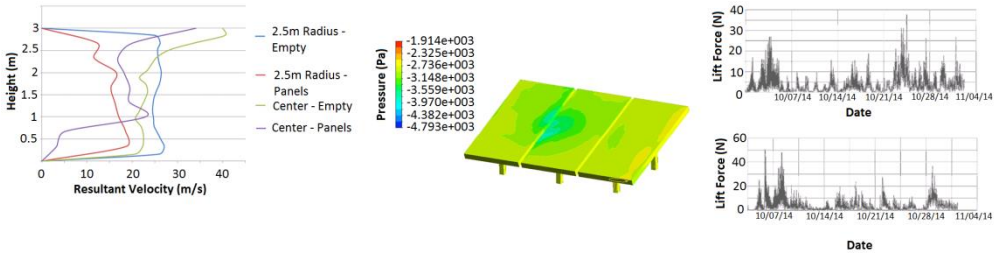

Fig. 3 (a) Wind speed profile with Panels, (b) Uplift Pressure Distribution on PV Panels (40m/s Outlet), (c) Panel Uplift Force (Location 1), (d) Panel Uplift Force (Location 2)

The CFD analyses prove that through minor design iterations, from materials readily available, a similar structure can be constructed for simulating very high wind-induced pressures on PV solar panels, which can reproduce the field conditions at the solar panels` site, and cause potential failure. Further CFD simulations of such a device would provide data necessary to analyze the failure of the PV panels in realistic wind speed scenarios, and to classify their failure mechanisms in a systematic approach based on the flow field and streamlines that would be generated.

References

[1] Baskaran, S. and Dragomirescu E., Wind Effect on Photovoltaic Solar Systems in single and cluster arrangements, in Proceedings of the 3rd American Association for Wind Engineering Workshop, Hyannis, Massachusetts, USA, August 12-14th, 2012.

[2] Ayodeji, A., Experimental Investigation of wind effect on Solar Panels, Paper 1177, The University of Western Ontario Electronic Thesis and Dissertation Repository, 2013.

Control of Static VAR Compensator for Prevention of Subsynchronous Resonance in Wind Farm Connected to Series Compensated Line

Diwash Koirala
The University of Western Ontario, London, Canada

Rajiv K. Varma
The University of Western Ontario, London, Canada

Introduction

Wind power is growing at a faster pace as compared to other forms of renewable energy sources across the globe. Many of these wind farms, in operation and under construction, use induction generator (IG) based wind turbines [1]. This additional wind power needs to be transferred in a stable manner to the load centres through transmission corridors having adequate capacity. Due to the high costs associated with upgrading existing lines or constructing new transmission lines, series compensation is considered to be an economic and effective means to enhance the power flow capacity of existing transmission lines [2]. However series compensation in a transmission line may result in subsynchronous resonance (SSR) in the generating power plants during transients and faults [2-4]. In 1971, a growing mechanical strain due to SSR caused the breakdown of shaft span between synchronous generator and exciter at Mohave power plant in US [4]. It was shown that self-excited induction generator wind farms connected to series compensated lines are prone to SSR [5,6]. Recently in 2009, the circuits of the double fed induction generator (DFIG) based wind farm in Texas were damaged due to overvoltage resulting from subsynchronous interaction between the DFIG and series compensated transmission line [7]. This paper presents a new control technique of a dynamic reactive power compensator known as Static Var Compensator (SVC) for mitigating the potential of SSR in a double-cage induction generator (DCIG) based wind farm connected to a series compensated transmission line. A nonlinear time domain analysis is performed in EMTDC/PSCAD software to demonstrate the effectiveness of the proposed controller.

System Study

The study system, considered for this paper is a modified version of the IEEE First SSR benchmark system [3]. The synchronous generator in IEEE First SSR benchmark system is replaced by 50-MW and 100-MW, realistic sized wind farms. A shunt capacitor is connected at the wind farm terminal to provide the reactive power requirement of the double cage induction generators and to maintain system power factor close to unity. A series compensation of X_c = 50% with respect to the total transmission line reactance is considered in this study. A 100 MVAR inductive and 100 MVAR capacitive thyristor controlled reactor -thyristor controlled capacitor type SVC is connected at the terminal of the wind farm. A proportional integral (PI) control scheme is employed in SVC for SSR mitigation. The measured bus voltage is compared with the reference voltage and the error is provided to the PI controller. The parameters of the PI controllers are tuned by step response analysis. A step change is applied to the reference voltage from 1 p.u. to 1.05 p.u. The PI parameters that provide the smallest rise time with an overshoot less than 10%, and a minimum settling time are chosen.

A six cycle, three phase to ground fault is applied at the terminals of a 100 MW wind farm connected with a line which is series compensated at a realistic level of 50%. The results of this study are depicted in Fig 1. The terminal voltage rises up to 4 p.u., shaft torque rises up to 20 p.u. and the electric torque rise up to 200 p.u. (in absence of generator saturation). These values are far beyond those under normal operating conditions and may cause significant damage to the shaft of wind turbine. There is further a substantial drop in the speed of generator resulting in the destabilization of the wind generator. However, as shown in Fig. 2, by placing an SVC at the wind farm terminal with the proposed controller, the bus voltage is limited to 1.4 p.u., shaft torque is restricted to 1.7

p.u., the electric torque is constrained to 5 p.u. and the speed of generator does not decline below 0.9 p.u. The subsynchronous resonance phenomenon is damped down quickly.

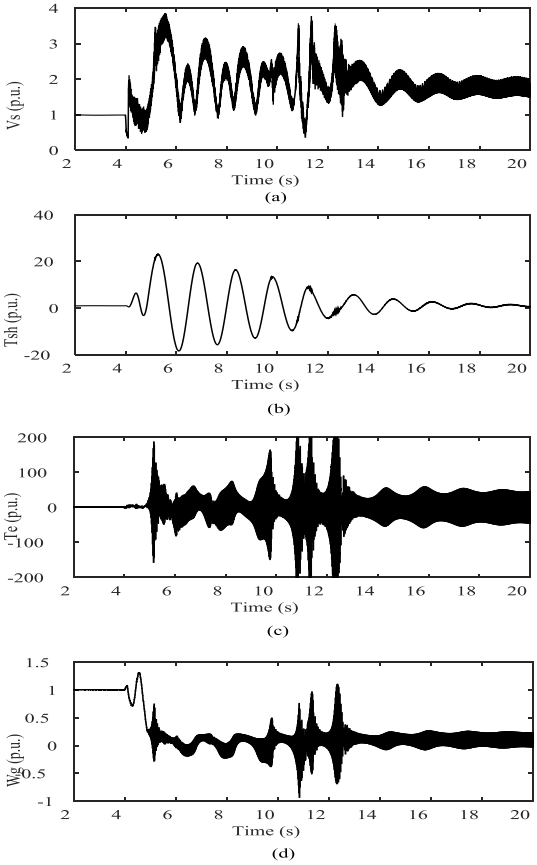

Fig. 1 Fault response of 100 MW wind farm with 50% series compensation, without SVC. (a) PCC Voltage. (b) Shaft Torque (c) Electromagnetic Torque. (d) Speed

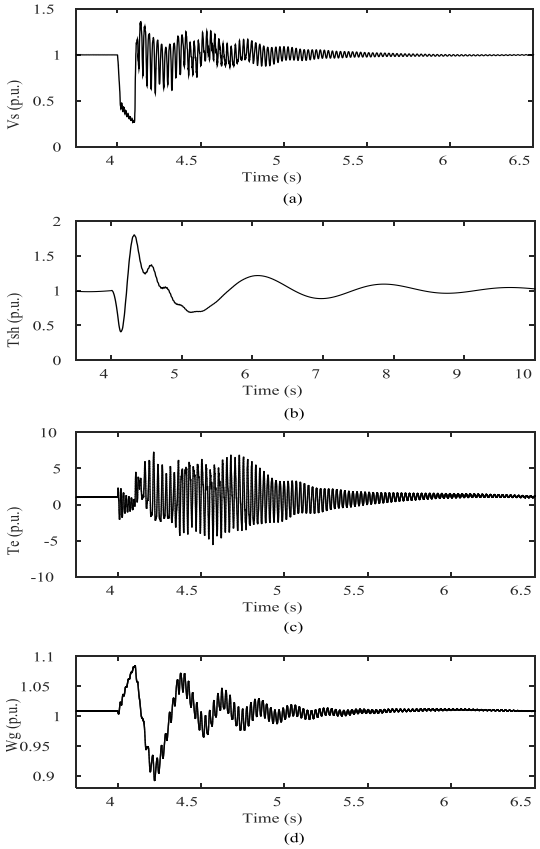

Fig. 2 Fault response of 100 MW wind farm with 50% series compensation and with SVC. (a) PCC Voltage. (b) Shaft Torque (c) Electromagnetic Torque. (d) Speed

It is therefore concluded that the SSR phenomenon can occur on a DCIG based wind farm even at a realistic level of series compensation. This can result in the amplification of shaft torque to unacceptable levels and potentially result in shaft failure due to cyclic fatigue. However, the proposed SVC controller can successfully alleviate this potential of SSR.

References

[1] "Global wind energy outlook," 2010 [Online]. Available: www.gwec.net.
[2] K.R. Padiyar, Analysis of Subsynchronous Resonance in Power System, Kluwer Academic Publisher, 1999.
[3] IEEE Committee Report, "First benchmark model for computer simulation of subsynchronous resonance," *IEEE Trans. Power App. Syst.*, vol. PAS-96, no. 5, pp. 1565–1572, Sep. 1977.
[4] D.N. Walker, C.E.J. Bowler, R.L. Jackson, and D.A. Hodges, "Results of subsynchronous resonance test at Mohave," *IEEE Trans. Power App. Syst.*, vol. PAS-94, no. 5, pp. 1878–1889, Sep./Oct. 1975.
[5] P. Pourbeik, R. J. Koessler, D. L. Dickmander, W. Wong, "Integration of large wind farms into utility grids (Part 2 - performance issues)," *Proc. IEEE PES General Meeting*, 2003, vol. 3, pp. 1520-1525, Jul. 2003.
[6] R. K. Varma, S. Auddy, and Y. Semsedini, "Mitigation of subsynchronous resonance in a series-compensated wind farm using FACTS controllers", *IEEE Trans. Power Delivery*, vol. 23, no. 3, pp. 1645–1654, Jul. 2008
[7] G.D. Irwin, A.K. Jindal, A.L. Isaacs, Subsynchronous control interactions between type 3 wind turbines and series compensated AC transmission systems. *Proceedings 2011 IEEE PES General Meeting*, pp 1–6, 2011

Shear Layer Effects of Cliff Edge: PEIWEE Experiment 2015

Dan Parvu, Julien LoTufo, Horia Hangan
WindEEE Research Institute, Western University, London, ON, Canada

Introduction

A full scale field measurement campaign using a WindScanner scanning wind LiDAR was undertaken during the month of May 2015 at the Wind Energy Institute of Canada (WEICan) PEI site, titled the Prince Edward Island Wind Energy Experiment (PEIWEE). The campaign was collaboration between the WEICan, Cornell University, York University and WindEEEE Research Institute (Western). An overview of the entire campaign is presented separately. The WindEEE part of the campaign had two main objectives. The primary objective was the evaluation of the newly acquired WindScanner system, which involved the generation of scanning patterns from a geometrical point of view and the performance assessment of the WindScanner under different meteorological conditions. The secondary objective was the characterization of different flows, such as shear layer effects of cliff edges, wind turbine wake analysis and flow over forest canopies. This paper discusses the wind velocity measurements obtained over a cliff edge situated at PEI's North Cape and some comparison is provided to the data acquired from the Bolund escarpment campaign [1].

Remote Sensing

LiDARs (Light Detection and Ranging) are currently being used in a wide variety of applications, from laser altimetry for high-resolution terrain mapping to atmospheric remote sensing and meteorology. Typically, for atmospheric flows, LiDARs are used to measure wind speeds and wind turbulence. Doppler LiDARs measure the movement of aerosols, such as minute dust and other particles in the air, which is then used to estimate wind speed [2]. The measurement technique is based on Doppler shift, therefore the LiDAR can only provide information about the component of velocity along the line of sight of the emitted beam, called the radial velocity. WindScanner LiDARs have been developed as part of the windscanner.dk project at DTU [3]. The instruments are similar to other commercially available wind LiDARS [4], [5] with a major difference: the laser beam is steered using two independent prisms [6]. WindScanner systems have previously been successfully used to determine various characteristics of wind flows such as the assessment of upwind conditions of a wind turbine [7], two-dimensional mean wind fields estimation under a hovering helicopter [8]and vertical wind profile measurement over a small escarpment of the Bolund peninsula [1].

Fig. 1 a) map cutout showing general location with respect to Canadian provinces;
b) precise location on the North Cape of PEI.

The Experiment

A shear flow over a cliff edge was investigated using the WindScanner system. The experiment was set up in a location on the North Cape of PEI (see Fig. 1). Several vertical wind profile measurements have been performed at different distances from the LiDAR (see Fig. 2). Maintaining the same scanning pattern, the measurements were

subsequently repeated for three LiDAR positions (5m increments inland). For each scanning pattern, the measurement is represented by line-of-sight velocity which is then corrected during the data analysis stage.

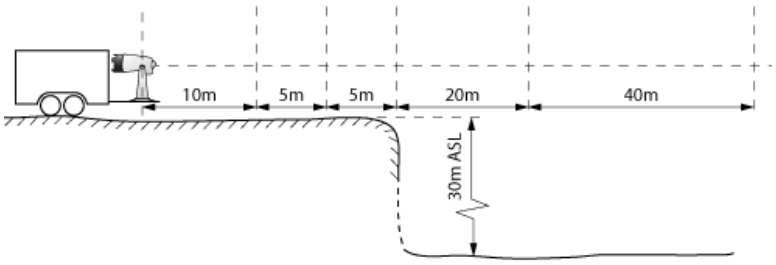

Fig. 2 Vertical wind profile measurement locations with respect to LiDAR and cliff edge.

Data Analysis and Comparison and Discussion

Line-of-sight velocity data is logged at a sampling rate of 250Hz using a procedure presented in [9]. Vertical profiles situated at distances of 10m, 15m, 20m, 40m, and 80m from the measurement system were investigated. This was accomplished by changing the focus of the laser beam. The WindScanner LiDAR gives raw spectra and wind speed estimates for each sample. Wind profiles are obtained through filtering and manipulation of the raw laser Doppler spectra. The spectral signal is then converted directly into wind speed based on the a priori calibration of the system. The resulting vertical wind profiles will be compared to the experimental results obtained from the Bolund escarpment campaign.

Acknowledgments

Technical University of Denmark, Wind Energy Institute of Canada

References

[1] J. Mann, N. Angelou, M. Sjöholm, T. Mikkelsen, K. H. Hansen, D. Cavar, and J. Berg, Laser scanning of arecirculation zone on the Bolund escarpment, in *Journal of Physics: Conference Series*, 2014, vol. 555, p. 012066.
[2] L. Kristensen, P. Kirkegaard, and T. Mikkelsen, Determining the velocity fine structure by a laser anemometer with fixed orientation. Danmarks Tekniske Universitet, Risø, 2011.
[3] T. Mikkelsen, Lidar-based Research and Innovation at DTU Wind Energy? a Review, in *Journal of Physics: Conference Series*, 2014, vol. 524, p. 012007.
[4] N. Angelou, J. Mann, M. Sjöholm, and M. Courtney, Direct measurement of the spectral transfer function of a laser based anemometer, Rev. Sci. Instrum., vol. 83, no. 3, p. 033111, 2012.
[5] D. A. Smith, M. Harris, A. S. Coffey, T. Mikkelsen, H. E. Jørgensen, J. Mann, and R. Danielian, Wind lidar evaluation at the Danish wind test site in Høvsøre, Wind Energy, vol. 9, no. 1–2, pp. 87–93, 2006.
[6] T. Mikkelsen, J. M. Sorensen, and M. Nielsen, Rotating prism scanning device and method for scanning. Google Patents, 2013.
[7] T. Mikkelsen, N. Angelou, K. Hansen, M. Sjöholm, M. Harris, C. Slinger, P. Hadley, R. Scullion, G. Ellis, and G. Vives, A spinner-integrated wind lidar for enhanced wind turbine control, Wind Energy, vol. 16, no. 4, pp. 625–643, 2013.
[8] M. Sjöholm, N. Angelou, P. Hansen, K. H. Hansen, T. Mikkelsen, S. Haga, J. A. Silgjerd, and N. Starsmore, Two-Dimensional Rotorcraft Downwash Flow Field Measurements by Lidar-Based Wind Scanners with Agile Beam Steering, J. Atmospheric Ocean. Technol., vol. 31, no. 4, pp. 930–937, 2014.
[9] N. Angelou, F. Foroughi Abari, J. Mann, T. Mikkelsen, and M. Sjöholm, Challenges in noise removal from Doppler spectra acquired by a continuous-wave lidar, in *26th International Laser Radar Conference*, 2012.

Visualization of Boundary Layer and Flow Separation Using Thermography

Farid Samara
University of Waterloo, Waterloo, Canada

Professor David A. Johnson
University of Waterloo, Waterloo, Canada

Introduction

Predicting the locations of laminar to turbulent transition and complete flow separation due to stall is crucial to the design and performance of wind turbine blades. Recent measurement techniques have focused on visualization for its high spatial resolution and accurate estimation of the performance of different blades. Swytink-Binnema [1] successfully calculated the fraction of the blade which was stalled on an operating 30 KW wind turbine using tufts installed along the blade. Other visual techniques that have been developed to determine the transition location include: temperature-sensitive paint, pressure-sensitive paint, thermography, and oil film interferometry [2]. Lang *et. al.* [2] successfully located the boundary layer on a rotating blade using an infrared camera [2][3].

In this study, an infrared camera is used to visualize stall because it is less intrusive than attaching tufts or applying a layer of sensitive paint. There is no need to modify the blade for the infrared camera to detect stall and the boundary layer. Infrared thermography has advanced over the years to have a temperature resolution as precise as 0.02 K [2]. With such resolution the different flow behaviors can be detected. When the airfoil is placed in a wind tunnel, the flow is laminar at the leading edge of the airfoil. As the flow develops along the chord it turns turbulent. As the angle of attack increases, the airfoil becomes stalled and complete flow separation occurs as seen in Fig. 1. The heat transfer rates between the free stream and the surface of the airfoil is dependent on the flow happening at that specific region. Thus the regions of laminar flow, turbulent flow, separation bubble, and stall can be found via the differential temperature across the airfoil.

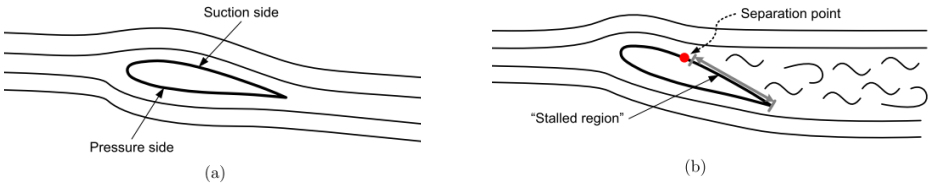

Fig. 1 Shows the difference between (a) attached flow and stalled flow (b) Reprinted from [1] with authors permission

Body

For experimental purposes, the airfoil profile NREL S833 is used because that profile was used in the design of a wind turbine blade by Abdelrahman and Johnson

[4] and is readily available. The coefficient of lift, coefficient of drag, and stall are well documented [5]. The chord length of the airfoil is 178 mm

[4].The airfoil is placed at the outlet of a 2 ft. by 2 ft. low-speed open circuit wind tunnel at the University of Waterloo. An infrared heater is placed at an angle facing the top of the airfoil. The infrared camera is placed perpendicular to the suction side of the airfoil.

In the first experiment the airfoil is at an angle of attack of 6 degrees such that the airfoil is not stalled. The infrared heater heats the surface to steady state temperature. Since the temperature of the airfoil is hotter than free steam, the attached flow cools the surface of the airfoil, starting at the leading edge. As the laminar layer develops and thickens, the rate of heat transfer decreases, thus increasing the airfoil surface temperature relative to the leading edge. During the transition between laminar and turbulent, the rate of heat transfer would be at its

minimum. This makes the surface temperature reach its highest peak. As the flow turns turbulent, the rate of heat transfer increases cooling on the blade. An example is provided in Fig. 2, which shows an infrared image of a helicopter blade as well as the intensity profile along the chord of the airfoil. I_{ref} and I_{run} are the intensity profiles before and after heating the blade respectively. Tripping dots are placed at the leading edge to promote early transition to turbulent flow.

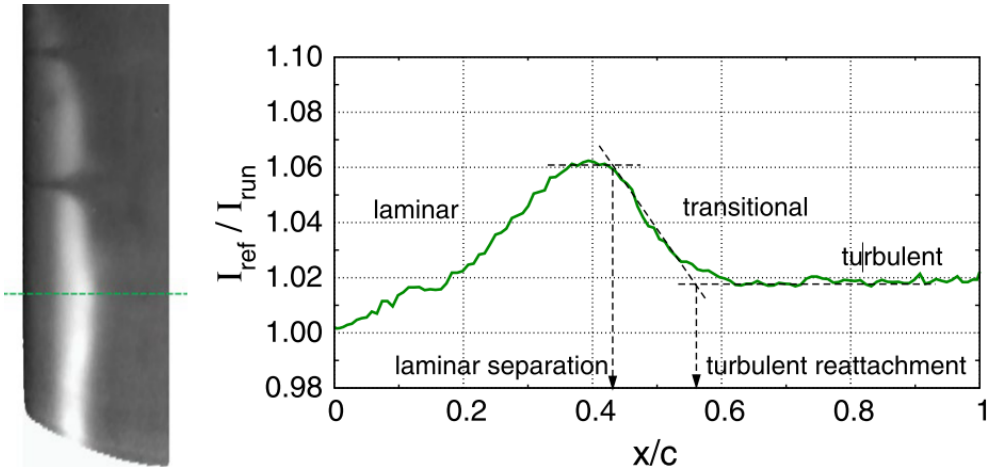

Fig. 2 An infrared image of the blade (Flow: left to right) and Temperature intensity versus distance along the cord of the blade. Reprinted from [2] with authors permission

In the second experiment, the setup is the same as the first except the angle is attack is 20 degrees and the airfoil is stalled. A similar heat pattern is seen in this setup but when the laminar flow turns turbulent it detaches from the airfoil. From the separation point forward, the temperature increases. Given the temperature differential between the flow states, the infrared image is able to show where along the airfoil stall is occurring. The infrared images are compared to oil surface visualization techniques to confirm the results.

Future work may include using infrared thermography to study a dynamic rotating wind turbine to study the stall along the blade. An important advantage of using thermography to study the performance of the blade is that there is no need to modify the blade.

Acknowledgments

The authors are grateful for support from National Science and Engineering Research Council of Canada (NSERC)

References

[1] Swytink-Binnema, N., "Digital Tuft Flow Visualization of Wind Turbine Blade Stall", MASc thesis, University of Waterloo, Canada 2014
[2] Lang, W., Gardner, A. D., Mariappan, S., Klein, C., and Raffel, M., 2015," Boundary‐layer transition on a rotor blade measured by temperature‐sensitive paint, thermal imaging and image derotation". *Exp Fluids*, DOI 10.1007/s00348-015-1988-5
[3] Richter, K., Schulein, E., 2014," Boundary-layer transition measurements on hovering helicopter rotors by infrared thermography" Exp Fluids DOI 10.1007/s00348-014-1755-z
[4] Abdelrahman, A, and Johnson, D.A. 2014, " Development of a Wind Turbine Test Rig and Rotor for Trailing Edge Flap Investigation: Static Flap Angles Case", 2014 J. Phys.: Conf. Ser. 524 012059
[5] Airfoiltools.com, 'NREL's S833 Airfoil (s833-nr)', 2015. [Online]. Available: http://airfoiltools.com/airfoil/details?airfoil=s833-nr. [Accessed: 28- Jul- 2015].

Interaction between the Atmospheric Boundary Layer and Wind Turbines: Assessment of Multiple-Lidar Scanning Strategies and Wake Measurements

Giacomo Valerio Iungo, Armita Hamidi, Mithu Debnath, Ryan Ashton
University of Texas at Dallas, Richardson, TX

Julie K. Lundquist
University of Colorado, Boulder, CO

James Wilczak, W. Alan Brewer, Aditya Choukulkar, Daniel Wolfe
National Oceanic and Atmospheric Administration, Boulder, CO

Ruben Delgado
University of Maryland Baltimore County, Baltimore, MD

William Shaw
Pacific Northwest National Laboratory, Richland, WA

Introduction

Predictions of wind turbine performance and reliability are strictly connected to the accuracy in the characterization of the atmospheric boundary layer and its interactions with wind turbines. Wind field is a highly turbulent and heterogeneous flow, and its morphology becomes even more complex by flowing across wind turbine arrays, indeed characterized by large velocity deficits, enhanced turbulent fluxes, coherent vorticity structures (such as tip and hub vortices), flow dynamics and instabilities. Therefore, the experimental characterization of such complex fluid dynamic system requires measurement techniques with high accuracy in sensing wind velocity, adequate spatial and spectral resolution, flexibility in designing different scanning strategies, and a relatively large sensing volume comparable at least to the downstream extent of a typical wind turbine wake. One of the most promising technologies currently available fulfilling these requirements is the scanning Doppler wind LiDAR. In this work tests to assess different multiple-LiDAR scanning strategies are presented, which were carried out during the XPIA (eXperimental Planetary boundary layer Instrument Assessment) experiment. Then, different LiDAR scanning strategies developed by the UTD team to measure wakes produced by utility-scale wind turbines are described. Particular attention is paid to the variability of wind turbine wakes under different thermal stability regimes of the atmospheric boundary layer.

Validation and Measurements with Scanning Doppler Wind LiDARS

For the XPIA experiment, six scanning Doppler wind LiDARs were deployed at the Boulder Atmospheric Observatory, four Leosphere 200S, one Halo Photonics Streamline, and the NOAA HRDL (Fig. 1). Different scanning strategies performed with multiple and simultaneous scanning wind LiDARs were tested, by varying the size of the measurement volume and temporal resolution. The experiment included 3D fixed-location high frequency tests, virtual towers, sector and volumetric scans, and 3D simultaneous point-wise measurements over large volumes. The general approach for data-analysis consists in comparing wind velocity data retrieved from simultaneous scanning wind LiDARs with the respective one obtained from the 300 m meteorological tower and wind profiling LiDARs. Preliminary results show that a high level of accuracy can be achieved through multiple simultaneous LiDAR measurements. However, a certain level of uncertainty can be introduced as a function of the specific setup adopted or accordingly to the accuracy on time overlapping of different LiDAR signals.

Subsequently, wakes produced by utility-scale wind turbines are measured through different LiDAR scanning techniques. Specifically, planar, volumetric and 1D high-frequency measurements were performed in order to

characterize effects of atmospheric stability on wake recovery (Iungo *et. al.* 2013, 2014). It is observed that wind turbine wakes recover faster under convective regimes than for neutral or stable conditions.

Fig. 1 Scanning Doppler wind LiDARs deployed for the XPIA experiment.

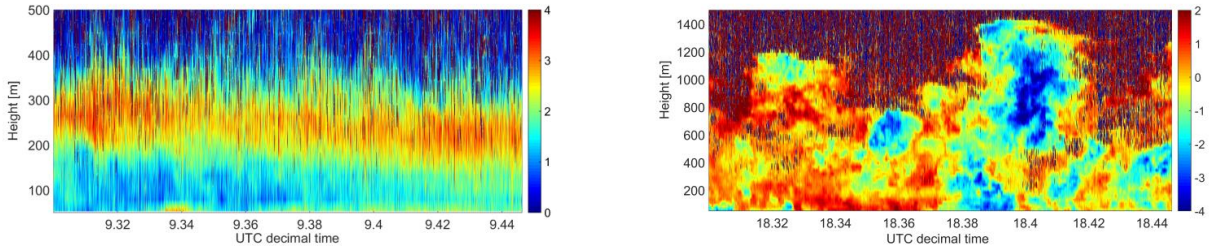

Fig. 2 Measurements of a Low Level Jet (a) and convective cells (b) through a scanning LiDAR.

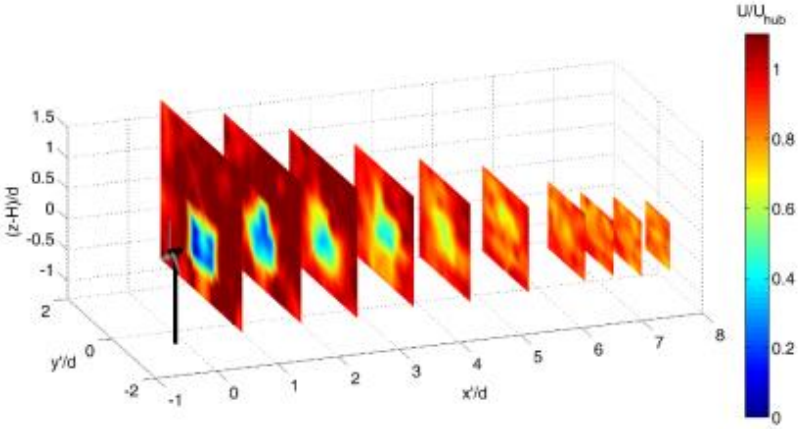

Fig. 3 Volumetric scan of a wind turbine wake carried out with scanning Doppler wind LiDARs.

References

[1] Iungo, G.V., Y-T. Wu and F. Porté-Agel 2013, *J. Atmos. Ocean. Technol.* 30 (2) 274-287
[2] Iungo, G.V. and F. Porté-Agel 2014, *J. Atmos. Ocean. Technol.* 31 (10) 2035-2048

Pressure and Velocity Characterization of a Blunt Trailing Edge Airfoil Wake with Three-Dimensional Forcing

Heather Clark
University of Toronto Institute for Aerospace Studies, Toronto, Canada

Philippe Lavoie
University of Toronto Institute for Aerospace Studies, Toronto, Canada

Introduction

The use of thick airfoil sections at the root of wind turbine blades may be required to ensure the structural integrity of large, high-load designs. However, airfoils that meet the demand for physical strength typically exhibit reduced aerodynamic performance due to premature boundary layer separation [1]. For the thick profiles of interest, implementation of a blunt trailing edge has been shown to increase the maximum lift coefficient and lift curve slope, relative to those obtained with a sharp trailing edge [2]. These benefits are accompanied by increased base drag and the onset of vortex shedding in the wake, as a result of flow separation at the blunt trailing edge. Mitigation of these adverse phenomena is therefore of interest for the optimization of turbine blades under constraints of both structural loading and aerodynamic performance.

The present work addresses the development of flow control strategies for the wake of a simplified bluff body, with the primary objective of the reduction of mean and fluctuating drag through the suppression of the von Karman vortex street. The geometry of focus is a blunt trailing edge profiled body with a chord of 12.5 times the thickness, which is denoted by d. The nominally two-dimensional separated wake is characterized by the emergence, above a critical Reynolds number, of three-dimensional secondary instabilities of varying spatial scale [3]. Active distributed (three-dimensional) forcing [4] of the wake was found to result in a maximum decrease of 18% in mean drag and 94% in fluctuating drag in the recent experimental study of Naghib-Lahouti *et al*. [5], where it was additionally shown that the activity of the primary vortices was reduced relative to features of smaller scale. The demonstrated success of the chosen control method motivates the continued investigation of distributed forcing of the blunt trailing edge wake with increasingly complex schemes. Closed-loop control is expected to increase robustness and may improve performance in terms of drag reduction or other objectives, relative to the open-loop case. The current study contributes to the development of a closed-loop controller by examining the ability to characterize the time-dependent state of the wake from surface pressure measurements. While stochastic estimation of the evolution of the von Karman vortices at a single spanwise location has been performed [6], the present experimental investigation incorporates three-dimensional pressure information for a more complete representation of the intrinsic flow features.

Experiments

Experiments were performed in the closed-return wind tunnel at the University of Toronto Institute for Aerospace Studies. A schematic illustration of the blunt trailing edge model is displayed in Fig. 1 with the coordinate system that is used in this work. Three-dimensional passive forcing of the wake is implemented with an array of vortex generators that are distributed according to the characteristic spanwise wavelength of the dominant secondary instability. Experiments were conducted at Reynolds numbers of 5000 and 8000, based on model thickness and freestream speed. An array of 24 Knowles miniature electret condenser microphones was used to measure the fluctuating pressure on the base of the model, with two-component velocity measurements acquired simultaneously using a LaVision FlowMaster PIV system. For the baseline and controlled flows, PIV measurements were obtained in a horizontal (x-z) plane in the lower shear layer, as well as in vertical (x-y) planes at multiple spanwise positions.

Results

In the baseline flow, the interaction of primary and secondary instabilities yields a three-dimensional wake structure that is unsteady in time. Large-scale instabilities are evident in the distortion of the primary vortices, as displayed by the instantaneous contours of streamwise velocity in Fig. 2a. The corresponding instantaneous measurement of the fluctuating pressure is shown in Fig. 2b, where the observed quasi-sinusoidal distribution is consistent with the spatial organization of the velocity field. The control strategy is found to increase the base pressure while globally reducing the amplitude of base pressure fluctuations. Additionally, amplitude modulation of the pressure signals that is observed in the natural wake decreases in strength with distributed forcing as a result of the modified three-dimensional flow structure. A comparison of the mean and instantaneous properties of the velocity and pressure for the baseline and forced wakes will be presented.

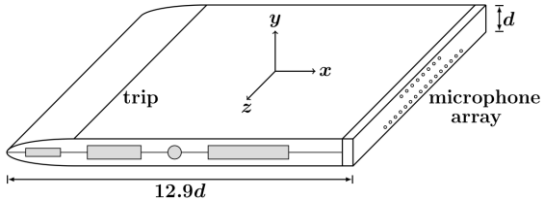

Fig. 1 Schematic illustration of the blunt trailing edge wind tunnel model and coordinate system.

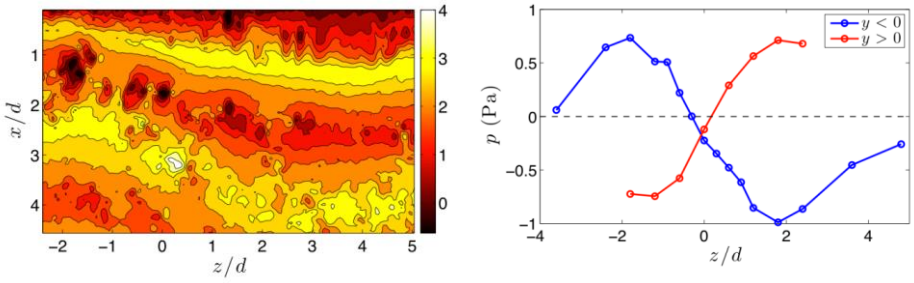

(a) (b)

Fig. 2 Instantaneous contours of the streamwise velocity component, in units of m/s, are shown in (a), with the simultaneously acquired fluctuating pressure in (b)

References

[1] Baker, J. P. and van Dam, C. P., "Drag Reduction of Blunt Trailing-Edge Airfoils," BBAA International Colloquium on Bluff Bodies Aerodynamics & Applications, 2008.

[2] Standish, K. J. and van Dam, C. P., "Aerodynamic Analysis of Blunt Trailing Edge Airfoils," *Journal of Solar Energy Engineering*, Vol. 125, 2003, pp. 479-487.

[3] Ryan, K., Thompson, M. C., and Hourigan, K., "Three-dimensional transition in the wake of bluff elongated cylinders," *J. Fluid Mech.*, Vol. 538, 2005, pp. 1-29.

[4] Choi, H., Jeon, W.-P., and Kim, J., "Control of Flow Over a Bluff Body," *Annu. Rev. Fluid Mech.*, Vol. 40, 2008, pp. 113-139.

[5] Naghib-Lahouti, A., Lavoie, P., and Hangan, H., "Distributed forcing flow control in the wake of a blunt trailing edge profiled body using plasma actuators," *Phys. Fluids*, Vol. 27, No. 3, 2015, 035110.

[6] Clark, H., Naghib-Lahouti, A., and Lavoie, P., "General perspectives on model construction and evaluation for stochastic estimation, with application to the blunt trailing edge wake," *Exp. Fluids*, Vol. 55, No. 7, 2014, 1756.

New multi-scale physical simulations for Wind Energy in the WindEEE Dome

Horia Hangan
WindEEE Research Institute, Western University, Canada

Introduction

While physical simulations constitute an important basis of investigation in many fluid mechanics applications spanning from transportation (aerospace, automotive and rail), civil engineering design (wind engineering) or pollution dispersion, the wind energy sector has not yet made full use of the capacity offered by physical experiments. Experimental fluid mechanics and its applications relies on wind tunnels and have therefore lagged behind the newer Computational Fluid Dynamics (CFD) advances with applications to multiscale, multi-physics fluid phenomena closer to real life complexities. Recently novel facilities and novel techniques have emerged that can bring experimentation closer to real life phenomena. One of the most recent developments in this area is the WindEEE Dome facility at the University of Western Ontario in Canada and accompanying measurement techniques.

The WindEEE Dome

The WindEEE Dome at the Western University, Canada is a novel three dimensional and time dependent wind testing chamber. It is conceived as a hexagonal chamber of 25 meters in diameter surrounded by a "return circuit" of the same hexagonal shape of 40 meters in diameter, see Fig. 1. Its aim is to create a wide variety of wind systems (e.g. tornadoes, downburst, all kind of gusts and currents, shear winds and boundary layers, etc.) at large scales and Reynolds numbers.

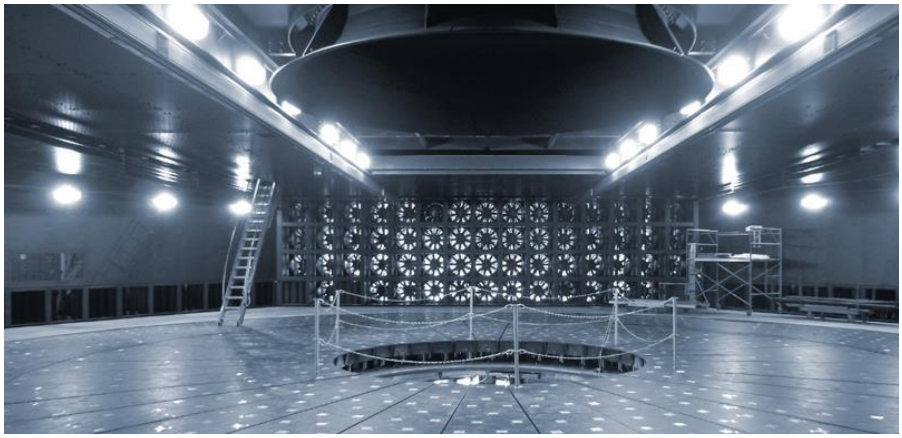

Fig. 1 Photograph of the inner chamber of the WindEEE Dome

WindEEE does that by varying the configuration, wind speed and direction of 106 fans in the dome. 100 of them are situated on the peripheral walls of the inner testing chamber distributed as follows: 8 fans situated on 5 of the 6 sides of the dome and 60 fans arranged in a matrix of 15 fans per row x 4 rows on the 6th wall. The other 6 fans are larger and are situated above the testing chamber ceiling. WindEEE operates in two distinct modes: (i) multi-fan wind tunnel with the 60 fan wall (14 meters wide x 4 meters high) pushing air inside the chamber and with the air recirculating above the chamber. In this mode any type of spatial and/or time correlations may be produced. In this mode WindEEE can generate multi-scale ABL flows, gusts, currents or vertically/horizontally sheared winds; (ii) axisymmetric mode in which 8 fans on each of the 6 walls are coupled with the larger 6 fans situated above the ceiling. In this mode WindEEE can produce for instance tornadoes and downbursts of up to 5 meters in diameter and translating at 2 m/s over 5 meters.

Multi-scale flows for wind energy applications

Boundary layer flows can be generated at various scale ranging from 1/2000 to 1/1 over various rough walls. This is possible by using a combination of a contraction, passive flow conditioning elements such as spires and roughness elements, as well as active flow conditioning by manipulating the fans on the wall in a spatial and time-dependent manner.

Fig. 2 is showing results in terms of mean and turbulence intensity profiles matched with ESDU standard profiles (ESDU 1982, 1983) for two scales 1/50 and 1/300. A variety of topographic flows for scales between 1/2000 to 1/20 can also be obtained. For instance, Fig. 3 shows inflows obtained for a complex topographic terrain for speed-up mean and turbulence intensity flow profiles matched with numerical simulation of a larger site area.

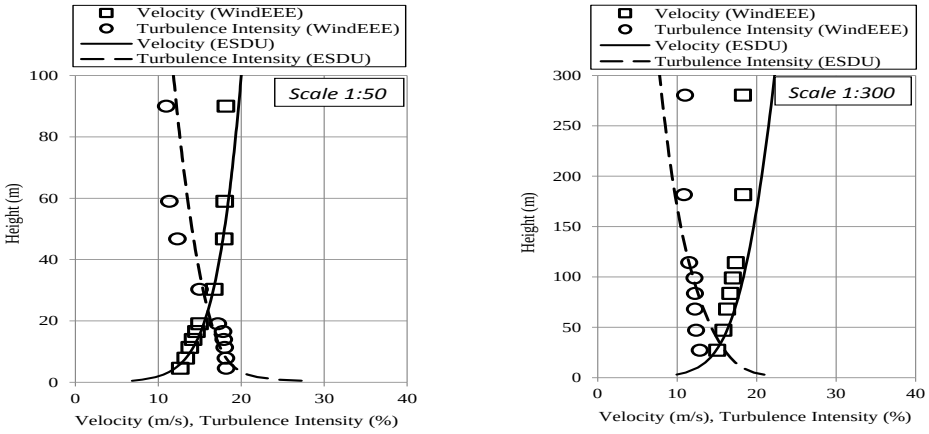

Fig. 2 Mean and Longitudinal Turbulence Intensity profiles at scales 1/50 and 1/300

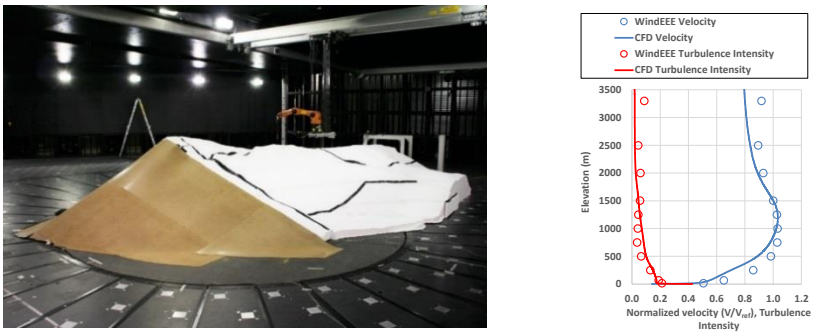

Fig. 3 Mean and Turbulence Intensity profiles for speed-up flow over complex topography

Large Scale Measurement Techniques

Given the complexity both in time and space of these type of flows, as well as the large measurement volumes involved, it is envisaged that even multi-camera, large scale PIV systems will not be suited to characterize these type of flows. Therefore a new type of particle tracking technique, the Large Scale Particle Streak Velocimetry (LSPSV) method is under development at WindEEE RI aiming at measurement areas of the order of 10 sq.m. Particle streaks are captured using a stroboscopic lamp. The velocity and position of the tracked particle are determined and pixel values are then converted into length units using camera calibration values. Vectors are then plotted and the procedure is repeated for each streak identified in the images in order to obtain a vector field. The Large Scale PSV setup proposed and tested herein shows the potential to be a less costly, fast, easy to use alternative to large scale PIV.

Uncertainty in Doppler Lidar Radial Velocity Variance Measurements

H. Wang, R.J. Barthelmie, P. Doubrawa
Sibley School of Mechanical and Aerospace Engineering, Cornell University, Ithaca NY, USA

S. C. Pryor
Department of Earth and Atmospheric Sciences, Cornell University, Ithaca NY, USA

Introduction

Wide spread adoption of lidar in the wind energy community requires not only proven accuracy for the mean wind speed but also skill for variance (the second-moment of the wind components, i.e. turbulence). While lidars can provide mean wind speed measurements with high accuracy, "their use in measuring atmospheric turbulence has not yet been established" [1]. Scan geometries optimized to minimize errors in the mean wind components are not sufficient to ensure minimization of the systematic error in the second moments of a wind field [2]. The correct method to estimate flux and variance of turbulence should include three steps [1]: (1) radial velocity variance measurements; (2) correction for the volumetric averaging effect on the radial velocity variance; (3) flux and variance estimation of a wind field with an inverse method. Each step mentioned above produces and contributes uncertainties to the final flux and variance estimates. This presentation will focus on the evaluation of the uncertainty in the first step, that is, how the uncertainty in radial velocity variance measurements is related to the sampling interval and the total sampling length.

Body

Radial velocity variance estimated from a time series is subject to both systematic and random errors. With the assumption of a homogeneous and stationary wind field, it can be shown that both the systematic and random errors are functions of the turbulence integral time scale, the averaging length and the sampling interval. While the systematic error approaches zero as the averaging length increases, the random error reaches an asymptotic non-zero value which is determined by the turbulence integral time scale and the sampling interval.

A field experiment was designed to evaluate the uncertainty in radial velocity variance estimate mentioned above (Fig. 1). Three sonic anemometers with 10 Hz sampling frequency were used to estimate the "true" wind field, while a pulsed Doppler lidar was configured to probe the wind field at locations nearby the three sonic anemometers consecutively with the sampling interval of about 7.5 seconds at each location. The experiment lasted for two days at the Wind Energy Institute of Canada. The sonic anemometer measurements are converted to radial velocities using the scan geometries of the lidar measurements to provide a reference. The turbulence integral time scale is also estimated from the sonic anemometers. Initial analysis has shown that the hourly mean and variance from the sonic anemometers and the lidar match very well (Fig. 2).

The following analyses will be conducted and presented. The effect of sampling interval on radial velocity variance uncertainty will be evaluated by resampling the original time series with increased sampling intervals. The effect of averaging length will be assessed by sampling subsets of the original time series. A comparison will be conducted between the sonic radial velocity variance uncertainty and the lidar radial velocity variance uncertainty to exam the effect low frequency sampling of lidar radial velocity on the uncertainty in variance estimate. The final analysis will focus on, given a scan geometry and a turbulence integral time scale, the minimum averaging length and maximum sampling interval needed to reach an uncertainty level and how they are related to designing a scan geometry for measuring atmospheric turbulence.

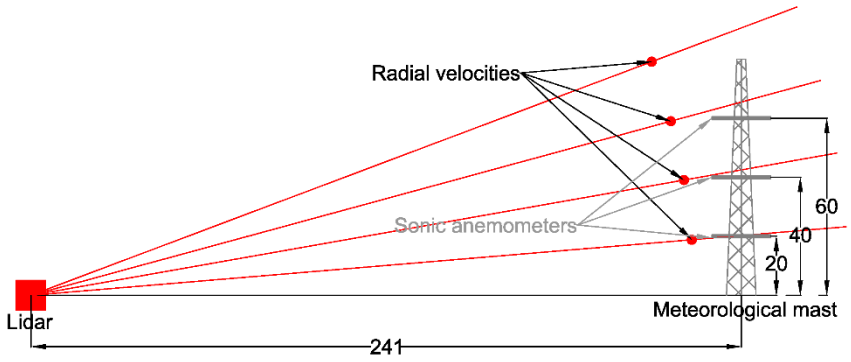

Fig. 1 Schematics of the locations of Doppler lidar radial velocity measurements and the sonic anemometers

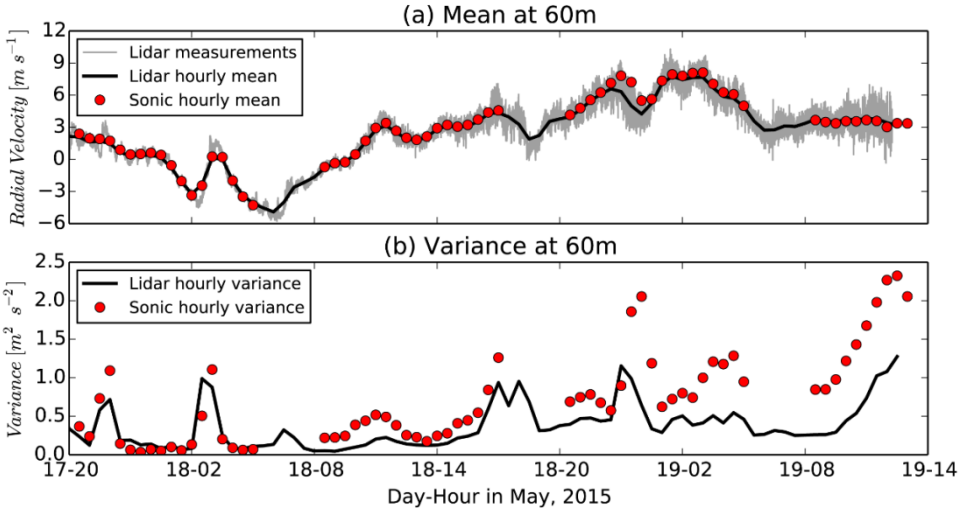

Fig. 2 Time series of the hourly mean and variance of radial velocities from the lidar and the sonic anemometer at 60 m above the ground

Acknowledgments

This work is funded by the U.S. National Science Foundation under the award No. 1464383 and the U.S. Department of Energy under the Award No. DE-EE0005379. We thank the Wind Energy Institute of Canada for giving the access to the test site and providing assistance.

References

[1] Sathe, A., Mann, J., Vasiljevic, N., and Lea, G.: A six-beam method to measure turbulence statistics using ground-based wind lidars, Atmos. Meas. Tech., 8, 729-740, 10.5194/amt-8-729-2015, 2015.
[2] Sathe, A., Mann, J., Gottschall, J., and Courtney, M. S.: Can Wind Lidars Measure Turbulence?, Journal of Atmospheric and Oceanic Technology, 28, 853-868, 10.1175/JTECH-D-10-05004.1, 2011.

Experimental Investigation of Dynamic Delamination in Curved Woven and Unidirectional Composite Laminates

İmren Uyar
METU Center for Wind Energy, Middle East Technical University, Ankara, Turkey

Burcu Taşdemir
METU Center for Wind Energy, Middle East Technical University, Ankara, Turkey

Demirkan Coker
METU Center for Wind Energy, Middle East Technical University, Ankara, Turkey

Introduction

In the wind energy industry, new advances in composite manufacturing technology and high demand for lightweight structures are fostering the use of composite laminates in a wide variety of shapes as primary load carrying elements. However, once a moderately thick laminate takes highly curved shape, such as corners of spars, Interlaminar Normal Stresses (ILNS) are induced together with typical Interlaminar Shear Stresses (ILSS) on the interfaces between the laminas. The development of ILNS promotes mode-I type of delamination propagation in the curved part of the L-shaped structure, which is a problem that has recently raised to the forefront in in-service new composite wind turbines.

Body

This paper discusses the results of an experimental investigation of the failure of highly curved CFRP composite laminates under the quasi-static shear loading. An experimental setup is designed to apply the quasi-static shear loading. Three lay-up configurations are investigated: the [0/90] fabric, the uni-directional [0] and the cross-ply [90/0] composite laminates. The effects of material lay-up, inner radius and thickness on the failure process are studied. It is observed that the delamination propagation in L-shaped laminates is highly dynamic even though the loading is quasi-static. The load displacement curves are recorded and the subsequent dynamic delamination is captured with a million fps high speed camera (Fig. 1).

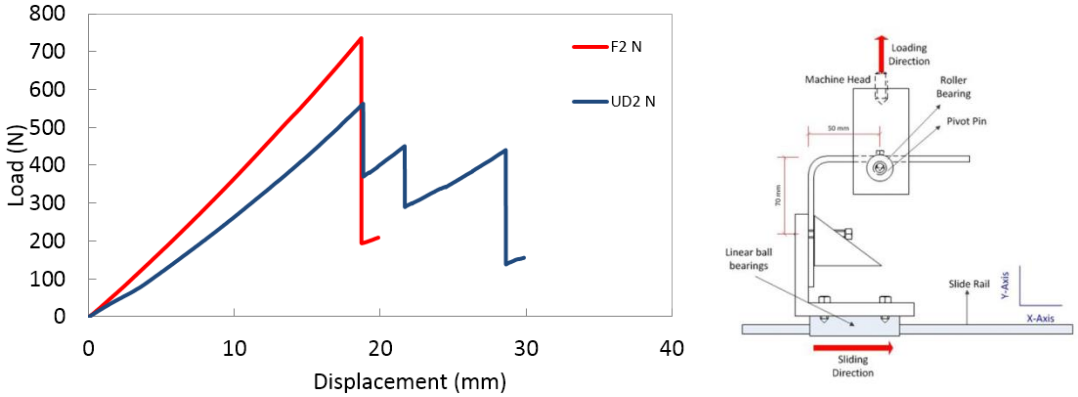

(a) (b)

Fig. 1 (a) The load-displacement curves of the fabric and cross-ply specimens. (b) Schematic of the loading fixture for perpendicular loading of the arm

Multiple delaminations in a single load drop are observed in the failure of the woven fabric laminate (Fig. 2a) whereas a sequential delamination at each discrete load drop is seen in the cross ply laminates (Fig. 2b). When the fracture surface of woven fabric specimen is investigated with the microscope, it is seen that the crack follow the 5HS weave structure. Because of this, the crack is not seen as a clear interface in the high speed camera pictures.

Although it is observed as a single crack, the crack appears to be branched and multiple cracks are seen in the micrographs. In the cross-ply laminate, the high speed camera pictures show sequential delamination growth. The crack growth starts at the inner part of the curved region, at the 3rd interface. The cracked specimen continues to carry the load and a second delamination initiates at the 5th interface. The subsequent delaminations propagate in the 3rd load drop, at the 7th and the 9th interface (Fig. 2b). The stiffness of the specimen decreases after each load drop but the specimen still carries load as far as its capacity. After the experiment, the failure surface was investigated with the microscope and the locations of the delaminations were obtained. Also the crack types are classified. An example of the micrographs is shown in Fig. 2b. Three types of cracks are monitored. The first one shows the delamination while propagating, induced with the matrix cracking in the 90° ply. The second delamination propagates in the 0° layers and the final delamination grows straight between the 90° and 0° layers, which is called the interlaminar. It is concluded that the weave of the fiber bundles can change the delamination mechanism, even though the loading, boundary conditions, dimensions, orientation and the material are kept intact. The weave fabric texture prevents the complex failure types when it is compared with the cross-ply material. But the cross-ply material is more damage tolerant in the 90/0 orientation.

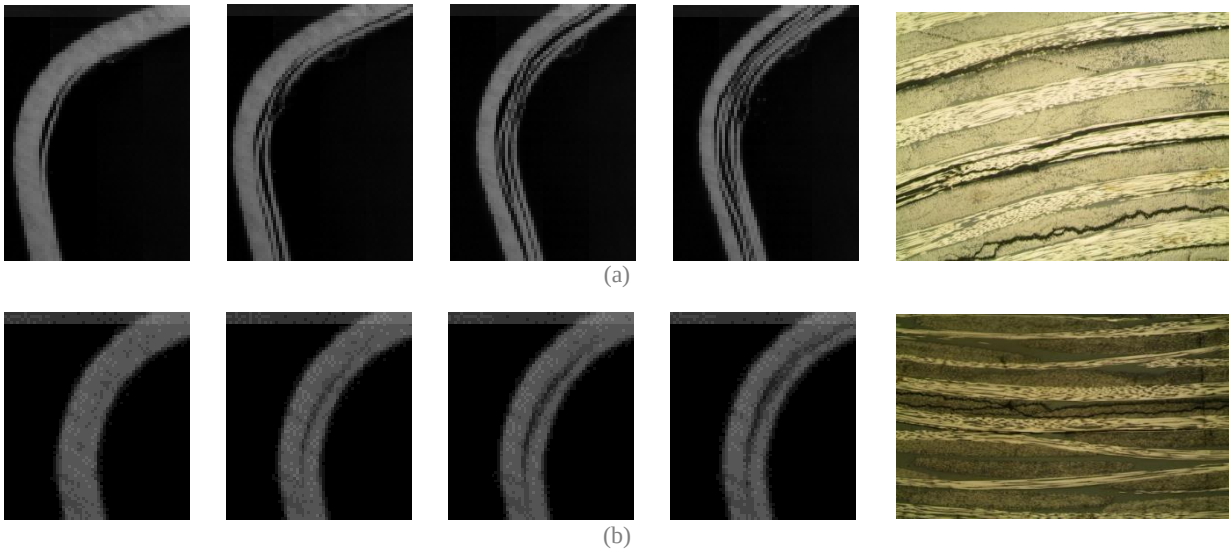

Fig. 2 (a) The high speed images of the UD [0/90] laminate with the micrograph of the curved region. (b)The high speed images of the Fabric [0/90] laminate with the micrograph of the curved region.

The delamination is then observed to be propagating to the arms at the intersonic speed of 2200 m/s. this is the first known experimental evidence showing intersonic delamination.

Acknowledgments

This work was supported by METUWIND, METU Center for Wind Energy. The authors would also like to acknowledge the contribution of Denizhan Yavas and Burak Gözlüklü.

References

[1] Experimental investigation of dynamic delamınation in curved composite laminates ,Uyar İ. MSc Thesis, September 2014.

Design of a Micro Wind Farm Model for Wind Tunnel Measurements of Power Output Variability and Unsteady Loading

Juliaan Bossuyt
KU Leuven, Leuven, Belgium

Michael Howland
Johns Hopkins University, Baltimore, USA

Charles Meneveau
Johns Hopkins University, Baltimore, USA

Johan Meyers
KU Leuven, Leuven, Belgium

Introduction

In this study we describe the design and instrumentation of a porous disc wind turbine model which can measure the power output, thrust force and incoming velocity with a high temporal resolution. The small size and compact instrumentation make it possible to perform wind tunnel studies of very large wind farms with detailed temporal information from every turbine making it possible to study power output variability and unsteady loading of the turbines for different wind farm layouts.

Body

Wind tunnel studies of large wind farms are typically able to measure the average power output of the tested wind farm[3]. However, to optimize the wind farm lay-out for a maximum power output and wind turbine lifetime, mean power output measurements are not sufficient. Instead, detailed temporal information about the power output and unsteady loading from every single wind turbine in the wind farm is needed. This information is further useful to study the power output intermittency which is crucial for the integration of large wind farms in electric power grids.[1] Scaling issues also tend to limit the number of turbines and the turbine spacing of tested wind farms. A very small porous disc model which can reproduce the far wake flow characteristics of a rotating wind turbine and with a realistic thrust coefficient of 0.75 - 0.85, was designed. With a diameter of 3cm the model makes it possible to do wind tunnel studies of wind farms with 100 wind turbines or more.

The porous disc model is instrumented with two strain gages in a half bridge configuration for higher accuracy strain measurements. With a simple structural model the strain is related to the integral thrust force on the porous disc. Increased vibrations at the natural frequency are corrected by the structural model, improving the frequency response of this measurement technique up to the natural frequency of the porous disc model. With the known thrust coefficient and a correction for the spatial filtering of the porous disc, it is possible to reconstruct the time signal of the incoming velocity and to calculate the equivalent power output of the porous disc model assuming a power coefficient.

The designed porous disc model can thus be used for measurements of the thrust force, incoming velocity and power output up to the natural frequency of the model. This is shown by reproducing the -5/3 spectrum from the incoming flow. Fig. 1 compares the time signal of the reconstructed velocity and the simultaneously measured velocity of a hot-wire probe. A good agreement is found confirming the capabilities of the model. Small discrepancies can be mainly explained by a difference in location between the hot-wire probe and the porous disc model and the amount of spatial filtering associated with the latter. Thanks to its small size and compact instrumentation, the model allows wind tunnel studies of large wind turbine arrays with detailed temporal

information from every wind turbine. Translating to field conditions with a length-scale ratio of 1:3,000 the frequencies studied from the data reach from 10^{-4} Hz up to about 6.10^{-2} Hz. The models capabilities are further demonstrated with a large wind farm measurement consisting of around 100 instrumented wind turbine models. A modular wind farm set-up was designed to easily measure different wind farm lay-outs. The electrical connection for the strain gages and the mounting of the porous disc models is done with audio jack connections. Fig. 2 shows the correlation between the thrust force of stream wise aligned wind turbine models in the wind farm. The result shows a clear correlation, which is in good agreement with LES simulations in Ref. [2] and confirming the model's capabilities for measuring fluctuating quantities of interest to wind farm designers and operators.

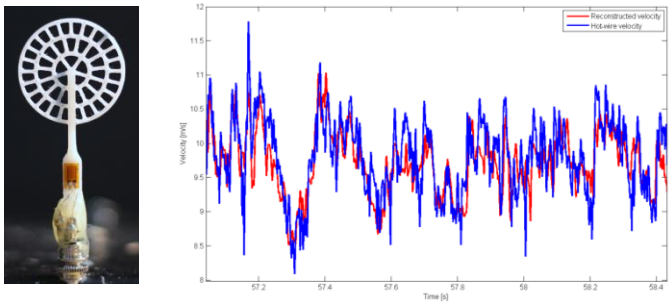

Fig. 1 Porous disc model (Left). Time signal of the reconstructed velocity from the porous disc model compared to the simultaneously measured velocity from a hot-wire probe (right).

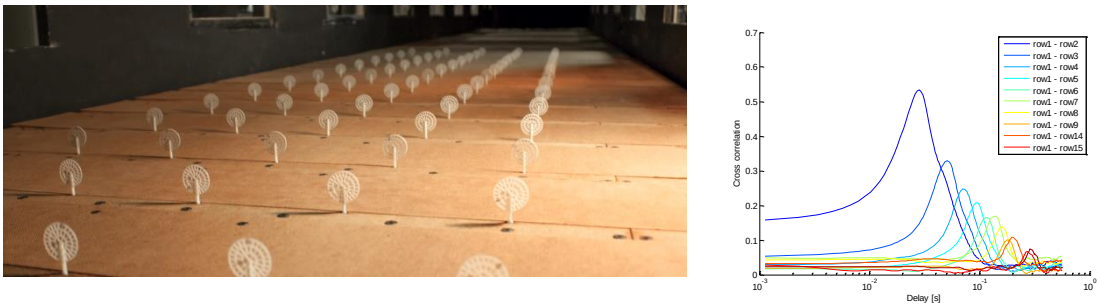

Fig. 2 Micro wind farm set-up (Left). Cross correlation between the thrust force of stream wise aligned wind turbine models (right).

Acknowledgments

Work supported by ERC (ActiveWindFarms, grant no. 306471) and by NSF (grants CBET-113380 and IIA-1243482, the WINDINSPIRE project).

References

[1] J. Apt, "The spectrum of power from wind turbines", *Journal of Power Sources*, 169, 369-374 (2007).
[2] R. J. A. M. Stevens and C. Meneveau, "Temporal structure of aggregate power fluctuations in large-eddy simulations of extended wind-farms", *Journal of Renewable and Sustainable Energy 6*, 043102 (2014).
[3] R. Theunissen, P. Housley, C. B. Allen and C. Carey, "Experimental verification of computational predictions in power generation variation with layout of offshore wind farms", *Wind Energy* (2014)

The Wind-Structure Interaction of a Shallow Wind Turbine Foundation

Jordan Kiss, Tim Newson
Geotechnical Research Centre, Department of Civil and Environmental Engineering, Western University, London, Ontario, Canada.

Craig Miller
Boundary Layer Wind Tunnel Laboratory, Geotechnical Research Centre, Department of Civil and Environmental Engineering, Western University, London, Ontario, Canada.

Introduction

Wind turbines are subjected to millions of load cycles from the wind during their design lives. Potential performance issues are related to fatigue experienced in various components from this long-term loading. Unfortunately there is a paucity of appropriate field-scale datasets, suitable for calibration and validation of design approaches and for foundation design in particular. A multi-disciplinary research project is underway to integrate laboratory element testing, scaled physical laboratory testing, full scale field monitoring and numerical modeling of a wind turbine founded on a shallow foundation in Southern Ontario. A significant component of the project is to provide understanding of the full 'wind-chain' from the incoming wind field to the underlying soil and its effects on the performance of the wind turbine. The turbine tower and its foundation have been instrumented with various sensors. Typical data from this monitoring is presented and the implications for soil strength-stiffness degradation due to the associated loading cycles during operation of the wind turbine are examined.

Body

A 2.3 MW wind turbine located in South-Western Ontario is the object of this field study. The turbine has a rotor diameter and hub height of 93 m and 80 m respectively. The turbine is founded on a shallow octagonal foundation with a diameter of 19 m. The foundation is 3 m deep at its thickest and tapers out towards the edges. A detailed site investigation involving laboratory tests and *in-situ* tests has been performed previously, [1]. The site is underlain by carbonate clayey silt tills and has a heavily weathered upper crust. The wind farm is classified as an IEC 61400-1, Class IIb site.

The foundation has been instrumented with four uniaxial MEMS tiltmeters able to determine the angle of inclination from the horizontal down to +/- 5 arc sec. Readings of the tiltmeters are sampled at 20 Hz. The tiltmeters are installed at each of the cardinal directions to measure the rotation of the foundation. Wind speed and direction is collected and averaged at 1 sec intervals from 5 cup anemometers installed on a meteorological (MET) tower located 150 m to the North West. Wind speed and direction is also recorded at the nacelle of the turbine. A Fiber Bragg Grating sensor array of strain gauges has also been installed at the four cardinal directions at six elevations up the turbine tower to measure longitudinal deformation and is sampled at 100 Hz.

At the end of this project, a long-term database of the wind environment and turbine system response will be compiled. This will allow the analysis of extreme events, as well as typical operating conditions. For the purposes of brevity, only a typical 2 hour operating data period will be presented herein, with the responses from one tiltmeter (TM3). The fluctuation of the wind speed over the 2 hour duration (in a direction coincident with the axis of rotation of the tiltmeter) had an average value of 12.25 m/s and a standard deviation of 1.62 m/s, giving a turbulence intensity of 13.2%. The associated response of the foundation was then analyzed. The angle of rotation for the tiltmeter is plotted for the same 2 hour period in Fig. 1. The mean rotations (θ_m) were 0.0330 and -0.0318 degrees, with standard deviations of 0.0251 and -0.0248 degrees respectively. It is evident that the angles of rotation were fluctuating about the neutral point, indicating that the foundation is rocking back and forth, and not about a point with a positive bias, which has implications for the instantaneous moments.

Rain-flow counting techniques were then employed to group similar amplitude rotational cycles into bins, to categorize levels of strain on the underlying soil and enable fatigue estimates to be made. Fig. 2, depicts a histogram for the tiltmeter. A Rayleigh distribution was fitted to the histogram and the statistics are shown. [2] presented an empirical relation to find the expected maximum values in a Rayleigh distribution for a given number of cycles as shown in equation (1).

$$\theta_{max}/\theta_s=[\ln(N)/2]^{1/2} \quad [1]$$

Where θ_{max}/θ_s is the ratio of the maximum rotation to the significant rotation (value of the highest 1/3 of the rotations) and N is the number of cycles. For the 2 hour period and approximate cycle frequency, the maximum response rotation was found to be 0.1204 and this matches well with the extreme values shown in the histogram. Assuming proportional responses of the moments and rotations to the applied wind speeds, the 50-year gust wind speed (59.5 m/s) would give maximum rotations of 0.16 degrees and soil strains in the range of 10^{-2} to 10^{-3}, with reductions of soil shear modulus G/G_o to 0.2-0.3. This has been confirmed using the design maximum moments using 3D elasto-plastic finite element analysis and is generally in the same strain range as assumed by the design codes. For typical fatigue calculations, it is assumed that up to 1000 strain cycles of this approximate magnitude may occur in a 20 year design life of a turbine. Further cyclic stress-strain laboratory testing is being conducted on the soils to determine the accumulated strain damage due to applied strain cycles over a typical turbine life-cycle. This aspect and others will be discussed further in the presentation.

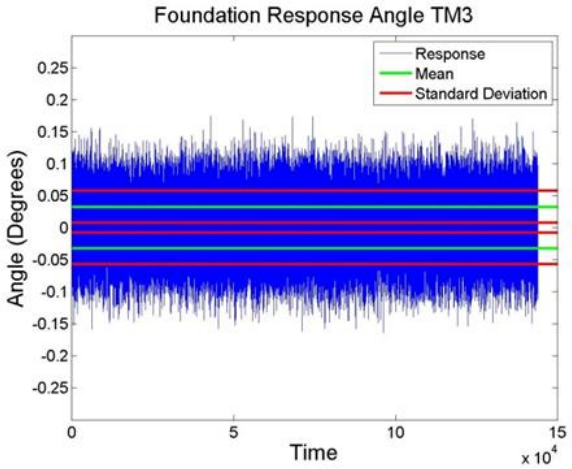

Fig 1. Foundation rotation time record

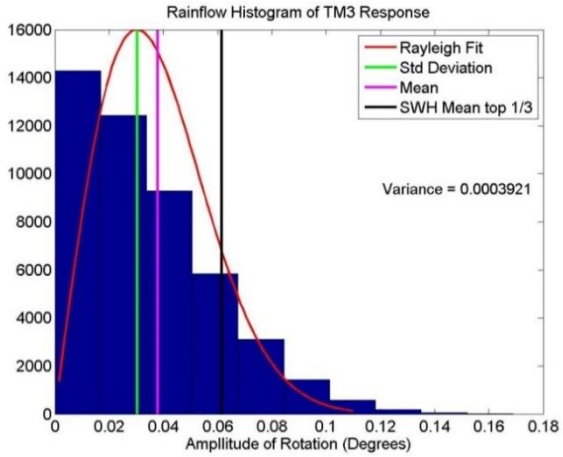

Fig 2. Rainflow histogram rotation cycles

References

[1] Tyldesley, M., Newson, T., Boone, S., and Carriveau, R. 2013. Characterization of the geotechnical properties of a carbonate clayey silt till for a shallow wind turbine foundation, *18th International Conference on Soil Mechanics and Geotechnical Engineering*, CFMS, Paris, France, 1: 2407-2410.

[2] Liu, P.C. and Pinho, U.F. 2012. Extreme Waves and Rayleigh Distribution in the South Atlantic Ocean Nar the Northeast Coast of Brazil, *The Open Oceanography Journal*, 6: 1-4.

Overview of the DOE A2E Experimental Planetary Boundary Layer Instrumentation Assessment (XPIA)

Julie K. Lundquist, Katja Friedrich, Joseph C.-Y. Lee, Paul T. Quelet, Clara St. Martin, Ken Tay, Brian J. Vanderwende, Rochelle Worsnop
Department of Atmospheric and Oceanic Sciences, University of Colorado Boulder, Boulder, Colorado, United States

William J. Shaw, Robert Newsom
Pacific Northwest National Laboratory, Richland, Washington, United States

James Wilczak, Laura Bianco, W. Alan Brewer, Aditya Choukulkar, Robert Banta, Scott P. Sandberg, Ann Weickmann, Dan Wolfe
National Atmospheric and Oceanic Administration, Boulder, Colorado, United States

Ruben Delgado, Lynn Sparling, Alexandra St. Pe, Patrick Langan, Adam Lass, Evan Lavin, Edward Strobach
University of Maryland Baltimore County, Baltimore, Maryland, United States

Andrew J. Clifton
National Renewable Energy Laboratory, Golden, Colorado, United States

John Schroeder, Scott Gunter
Texas Tech University, Lubbock, Texas, United States

Giacomo Valerio Iungo, Ryan Ashton, Mithu Debnath, Armita Hamidi
University of Texas at Dallas, Richardson, Texas, United States

Steven P. Oncley, Branko Kosovic
National Center for Atmospheric Research, Boulder, Colorado, United States

Introduction

Wind energy now provides 20% of the electricity in some parts of the United States, with potential to provide far more. Large wind farms interact with the atmospheric boundary layer, responding to the diurnal heating cycle as well as mesoscale flow features. In turn, wind farms generate complex local wind flows characterized by increased turbulence mixing and modified wind profiles of turbine wakes. To optimize wind energy deployment and production, and to assess wind farms impacts, accurate measurements of the complex flows within and around wind farms are required.

Body

To assess current capabilities for quantifying features of the complex flow, atmospheric turbulence, and atmospheric stability within wind farms, the US Dept of Energy sponsored the eXperimental Planetary boundary layer Instrumentation Assessment (XPIA) campaign at the Boulder Atmospheric Observatory in spring 2015. In addition to deploying state-of-the-art wind scanning remote sensing technology, such as Ka-band radars and scanning lidars, the XPIA team developed and tested new multi-Doppler scanning techniques. To quantify the uncertainty of these new types of measurements, results of these scans and retrievals are compared to traditional

measurements from 12 sonic anemometers mounted on the BAO's 300-m tower, as well as to profiles from profiling lidars (Fig. 1). Radiosonde launches, and temperature and moisture profiles from the tower provide data for similar assessment of multiple microwave radiometers.

The field campaign and preliminary results will be presented, focusing on observations of complicated wind profiles such as nocturnal low-level jets, cases of strong wind veer, and rapid increases and decreases in wind speed indicative of ramping events.

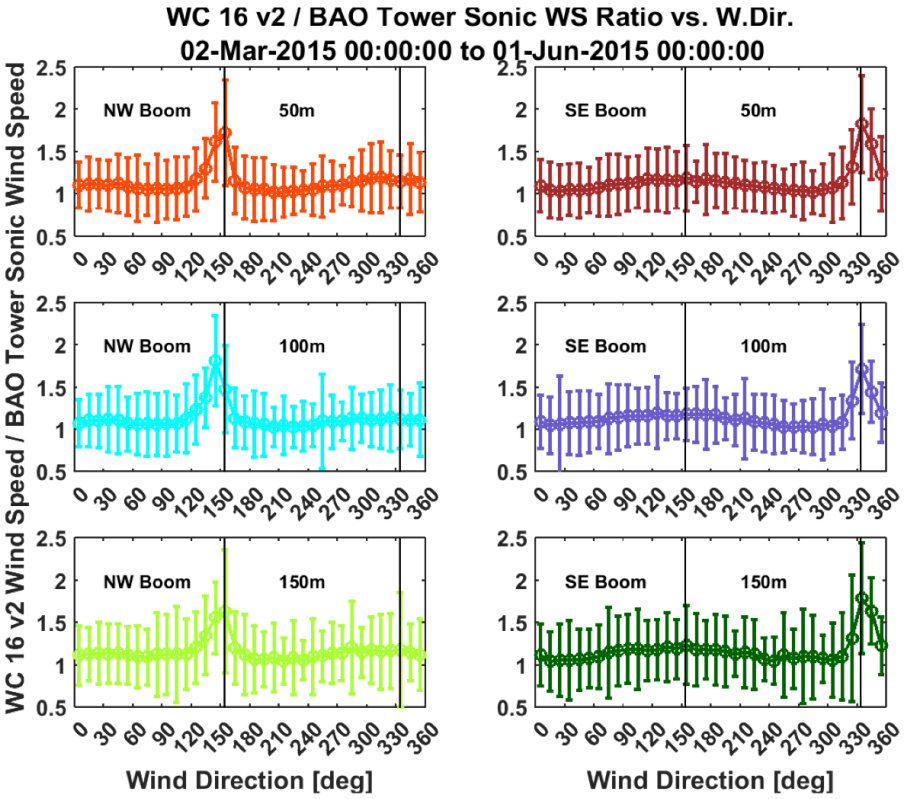

Fig. 1 Ratios of WindCube v2 horizontal wind speeds to sonic anemometers horizontal wind speeds for the NW boom sonics (left column) and SE boom sonics (right column) at 50 m (top row), 100 m (middle row), and 150 m (bottom row) altitudes. Mean ratios are represented in circles with standard deviations represented as bars. Vertical lines indicate boom directions.

Acknowledgments

We would like to acknowledge operational, technical and scientific support provided by NCAR's Earth Observing Laboratory, sponsored by the National Science Foundation, as well as field support from NOAA staff Bruce Bartram and Duane Hazen. Erie High School, the St. Vrain School District, and Lefthand Water District all cooperated generously with access to their sites for field deployments.

Methodology to Quantify Efficiency of Land-Based Wind farm

Kiran Bhaganagar
Associate Professor, Department of Mechanical Engineering, University of Texas, San Antonio, TX.

Rolando Vega
University of Texas, San Antonio

Mohammad Sazzad
University of Texas, San Antonop

Introduction

Annual energy production (AEP), an estimate of the total energy production of a wind farm during a period of one-year is calculated by applying the manufacture power curve to reference wind speed frequency distribution approximated as a Rayleigh distribution at hub-height, assuming 100% availability, and applying expected energy losses. AEP is the important metric used to assess profitability for the wind farm owner to negotiate with utility company. Energy-losses in a wind farm that arise due to wake interference between the wind turbines are not accurately accounted in AEP predictions. Wake deficit conditions exist when the wind entering a downstream turbine is affected, partially or fully, by the wake of an upstream turbine, and can lead to lower energy production from the downstream turbine. Turbine wake-wake interactions are influenced by many conditions including atmospheric boundary layer (ABL) velocity profile, stability, turbulence intensity, and rotor vortices. Wind turbine wakes significantly deteriorate the operational characteristics of a wind plant. To-date the lack of complete knowledge of power deficits in a wind farm due to wake interferences significantly effects predictive power of a performance of a wind plant.

Objective

The objective of the present work is to develop metrics to quantify wake-effects using field data of a major on-shore wind farm in conjunction with large-eddy simulation numerical tools. We focus on quantifying the wake effects in terms of atmospheric stability effects and ABL conditions, such as wind velocity and wind direction, and thus provide an accurate estimation of AEP of the wind farm. This is the first study for an on-shore wind farm and is an important direction in improving the economic predictability of a wind farm. We propose a methodology using an energy-based approach to quantify wake-effects. The results have clearly demonstrated that atmospheric stability plays a role in calculating the wake-interference corrected AEP. The specific site under consideration showed near neutral to unstable dominating the ABL for the 67.5% of the year with stable conditions only occurring 32.5%. Presence of stable events increase wake-effects up to 10-D, and wake-effects in unstable events dominate up to 5-D. Wind direction and wind speed also is linked to the atmospheric stability. Unstable events are characterized by constant well-mixed turbulence in the ABL, whereas, high-shear region are the characteristic features during the stable events.

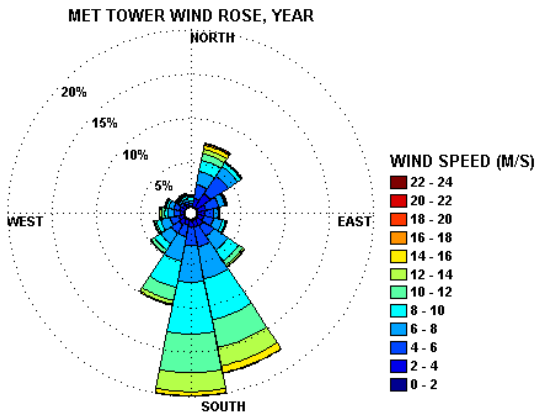

Fig. 1 Wind rose plot for a year showing the winds are primarily from the South.

AEP

Wind farm AEP is calculated from filtered 10 minute average power data sets. Energy is calculated for each power data point and summed across each turbine, ($AEP_{turbine}$), and summed across the farm (AEP_{farm}).

$$AEP_{turbine} = \sum_{i=1}^{n} \frac{P_i}{6}$$

$$AEP_{farm} = \sum_{i=1}^{T} AEP_{turbine,i}$$

Where , n is the number of filtered data points, P_i is the filtered power at n, and is divided by 6 to convert from 10 minute kW to kWh.

Large-eddy simulations

Large-eddy simulations (LES) are conducted at different instances of the diurnal cycle using the NREL SOWFA tool, which solves the 3-D filtered Navier-Stokes equations. For this purpose, precursor ABL simulations are first conducted to obtain quasi-equilibrium ABL solution. The ABL simulations are then coupled to the wind-plant solver. The simulations have been performed for 12 different Richardson number representing different instance of the diurnal cycle. LES database is used to estimate the AEP.

Conclusions

As it has been well noted that one of the largest difficulties in wind farm wake evaluations is that wind turbine and local MET tower data is very difficult to obtain from producers due to the overly confidential nature of the data. Hence, we use combination of numerical simulations and SCADA data to evaluate the wake deficits and thus improve the AEP calculations. Atmospheric stability is an important metric that will dictate the AEP at that location. This is one of the first studies for a land-based wind farm that quantifies the wake interferences effects in the calculation of AEP.

Acknowledgments

Kb Acknowledges the support from NSF division for sustainable energy for financial support and TACC for providing with computational resources

Curved Beam Strength and Toughness of Thin Ply CFRP Non-Crimp Fabric Laminates

M A Arca
METUWIND, Middle East Technical University, Ankara, Turkey

M Papila
METUWIND, Middle East Technical University, Ankara, Turkey

D Coker
METUWIND, Middle East Technical University, Ankara, Turkey

Introduction

Generally, the substantial part of the wind turbines are the blades, since its performance and properties directly affect the performance of the turbine [1]. Demand for composites in wind turbine industries emerges from the need of light weight structures without any loss of strength and stiffness Wind turbine blades are usually made of fiber composite structures, generally glass fiber structures. Although, Superior properties make carbons fibers preferable to glass fibers, properties of CFRP composites highly depend on manufacturing quality [2]. Development of the novel spread tow-thin ply technique eventuated in new class of material called thin ply non-crimp fabric, which are fabric type layers formed by stitching the tow spread thin (ply thicknesses as low as 0.02 mm) UD layers. They provide reduced waviness and increased mechanical properties in the out-of-plane and impact performance over fabric type composites and also they are more flexible, easy to store and handle [3].

Method and Results

In this study, Failure behavior and Mode-I, Mode-II fracture toughness of TPNCF laminates are determined by fracture toughness and curved beam strength tests and compared with equivalent UD laminates. High speed camera system (Photron AS4 1.000.000 fps) is used in the experiments in order to gain better understanding of the effect of thin ply non-crimp fabric materials on failure process and the dynamic crack growth process. TPNCFs are composed of 24 plies and each having 2 thin plies tied together by stitching in the [0/45] configuration, stacked in the order of [0/45/-45/0]12T. Equivalent UD laminates are composed of 24 plies stacked in the order of [0/45/-45/0]6T.

(a) (b) (c)

Fig. 1 Experimental Setup for (a) DCB test (b) ENF test, (c) curved beam strength test

Both UD and TPNCF laminates are composed of same epoxy and 0°/0° interface. Although, FT values of UD laminates are nearly same, TPNCF laminates have high FT values. Since stitching causes rough and uneven fracture surface, leading to incnrease on fracture resistance, Both Mode I and Mode II fracture toughness values of TPNCF laminate are higher than the UD laminate.

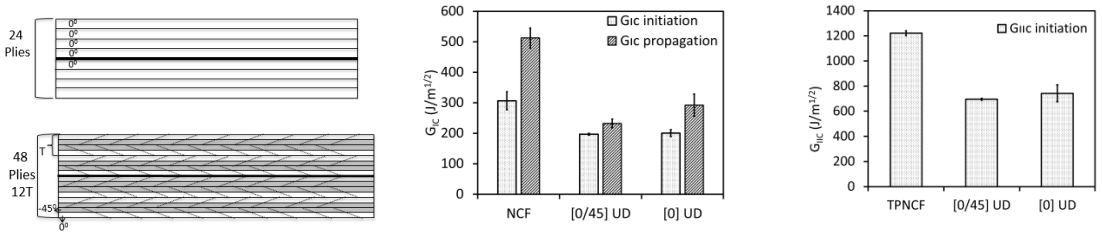

(a) (b) (c)

Fig. 2 (a) laminate sketch, (b) and (c) are the bar graph of Mode-I and Mode-II fracture toughness values, respectively

UD laminates can resist up to 700N and two load drops occur (Fig. 3a). After the first load drop specimen carries load without changing the slope, indicating that cracks do not extend all through the width of the specimen and specimen does not loss its load carrying capacity completely. TPNCF laminates can carry load up to 1800N and one load drop occurs (Fig. 3a). After the load drop load carry in capacity decreases to 500N, indicating that the failure occurs throughout the width direction and specimen loses its stiffness.

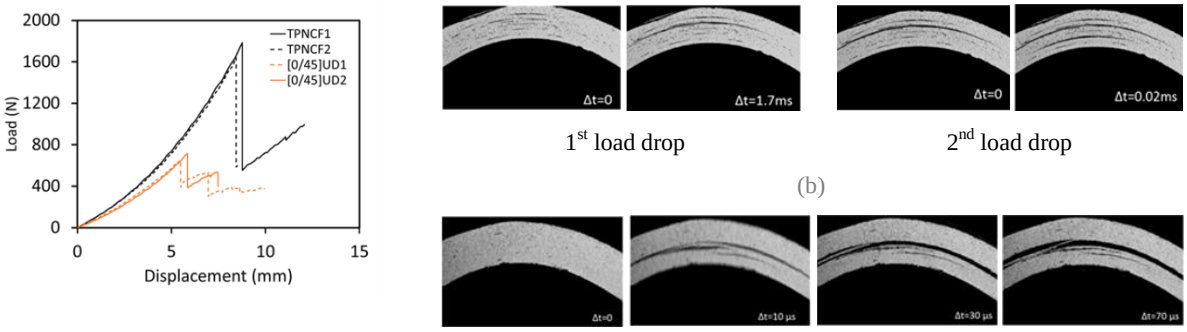

(a) (b) (c)

Fig. 3 (a) 4-Pt bending load displacement curves of UD and TPNCF laminates, High speed photos taken at 100,000 fps (b) UD laminate (c) TPNCF laminate

Photos of UD laminate (Fig. 3b) shows that delamination nucleates from the initial defects. At the second load drop third delamination nucleates from the initial defect below middle part close to inner radius. Whole process ends in 1.7ms and 0.02ms which are very stable. Failure process of TPNCF laminate (Fig. 3c) takes 70 µs which is highly unstable. Stitching prevents 0°/45° microcraks, preventing the delamination, stiffening the laminate and increasing the failure load. For all of the tests two major delamination observed at the mid part.

Acknowledgments

This work was supported by METUWIND, METU Center for Wind Energy.

References

[1] Mishnaevsky Jr. P.L., Encyclopedia of Life Support Systems thermal to mechanical energy conversion: engines and requirements - Composite Materials In Wind Energy Technology.
[2] Sørensen B.F., Jørgensen E., Debel C.P., Jensen F.M., Henrik H.M., Jacobsen T.K., Halling K.M., Improved design of large wind turbine blade of fibre comp. based on studies of scale effects (Phase 1)-Summary Report, Risø National Laboratory, Risø-R-1390(EN), 2004.
[3] Shin S., Kim R.Y., Kawabe K., Tsai S.W. (2007), Exp. studies of thin-ply laminated composites. Comp. Scn. and Tech.; 67: 996-1008.

The Customizable Tool for Creation of Structured Mesh and CAD Geometry of an Vertical Axis Wind Turbine Rotor

Marlen Balbekov
ForWind - Center for Wind Energy Research, University of Oldenburg, Oldenburg, Germany

Viktor Dmitriyev
Business Information Systems / VLBA, Universities of Oldenburg, Oldenburg, Germany

Bernhard Stoevesandt
Fraunhofer-Institut für Windenergie und Energiesystemtechnik IWES Nordwest, Universities of Oldenburg, Oldenburg, Germany

Joachim Peinke
ForWind - Center for Wind Energy Research, Universities of Oldenburg, Oldenburg, Germany

Introduction

The methods in the Computational Fluid Dynamics (CFD) are dedicated to solve and analyze problems in domain of *fluid flows analysis* by means of numerical analysis. As long as the numerical methods mainly consists out of algorithms which require significant computation power, it's very crucial to pay attention to the software tools and packages, which are used in computations. One of the examples of the freely available tools for performing numerical computations is the OpenFoam project. It is mainly dedicated to address CFD challenges. It's a quite popular and rapidly evolving software tool, which is used in scientific and industrial projects. For instance, OpenFoam is adapted and used by our research group with focus on developing a software that helps in designing wind turbines and blades. The process of a CFD simulation can be subdivided in three different categories: (1) a pre-processing, (2) a solving and (3) a post-processing. Current work focuses primary on the tools and techniques, which are important for the "pre-processing".

Body

According to the work of H.Versteeg and W. Malalasekera [1], over 50% of the time spent in industry projects, which work primary on a CFD, is devoted to the definition of the "object" geometry and its supporting "grid" construction and generation. The overall numeric solution to a flow problem can be derived from a combination of small solutions provided by a single grid's cells, which make ups the whole grid at the end. It means that the accuracy of a CFD solution is heavily relies on the total amount of cells available in inside single grid. Thus, having larger number of cells will lead to the better accuracy of the final result. On the other side, increasing number of cells means higher demand in the computational resources. However, the quality of a particular mesh is another factor to be considered. Having a good formed grid has a strong impact of efficiency and accuracy of computation while solving for a CFD problem.

The development of algorithms and utilities (e.g. programs or sculpts) for automatic meshing and geometry with minimal input information still remains a challenging tasks without unique approach. In this work we consider a method for constructing block-structured curvilinear grids in three-dimensional space with complex geometry, but using only a simple topology. The creation of a valid multi-block grid to be processed later on in the OpenFOAM by the blockMesh [2] utility requires a significant amount of time and a lot of manual work. Usually manual routines in constructing a mesh for the OpenFOAM should be repeated again and again for each particular experiment. This process includes manually division of the main working region into sub-regions with less complex configurations. Such division simplifies setting the shape of the curves, boundary conditions for the faces of the block and simplifies organization of the connection between the blocks. Current work is dedicated to

minimize amount of manual work required in the construction of grids for the vertical axis class wind turbine projects.

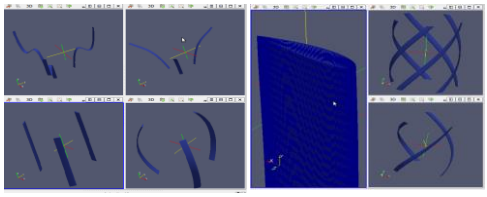

Fig. 1 The possible types of geometry obtained in STL format

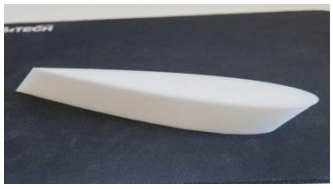

Fig. 2 Airfoil's blade produced on 3D printed with precision of 0.3mm (layer height)

The method relies on the functionality of the blockMesh utility provided within OpenFOAM for grid construction routines. The input file for the blockMesh utility is a special type of dictionary of a file that contains set of blocks, vertices, edges and boundary conditions. The task is to automatically fill in this set of parameters. Basically, one single block consist out of 4 edges located on a single plane and connection reprecented by curves. Automation can speed up the construction of such grid and provide a control over a size of particular set of cells inside the block, which is one of the main factors to obtain required values of the "y plus" (dimensionless wall distance). Whether "y plus" condition is very critical for the accuracy of the results of different models of turbulence. The number of blocks depend on the selected type geometry. The initial (baseline) data used as a construction parameters are: The type of airfoil (specified by standard dimensionless coordinates or the equation of an airfoil), the pitch angle of the blades, the airfoil chord, twist angle of the blade relative to the axis of a rotation, the number of blades, the blade shape and step height of a blade. For the pre-visualization of the blade, the geometry construction can be saved to the stereolithography (STL) format (see Fig.1), which can be interpreted by almost any CAD system. The accuracy of the STL format is controlled by the number of points on the curve of the airfoil. One of the significant advantages of the STL format is that file with STL data is considerably smaller in comparison with its analogs from proprietary software. The resulting highly accurate STL geometry can be used to obtain unstructured grid in OpenFOAM via the snappyHexMesh utility. A high accuracy of the geometry significantly increases the speed of obtaining unstructured grids. All calculations and settings for the template header of a blockMesh are generated by the Octave script.

A distinctive feature of the method is that the geometry construction is performed in a layer by layer fashion. This approach has several advantages such as speed, versatility, flexibility and adaptability. This allows modifications of the geometry depending on specified configuration parameters. It opens the possibility to use in the design various blade modifications, profile types, forms and factors (e.g., arm type, foundations type, "close/open", etc.). This method allows to configure (change) many parameters and automatically build grids and geometry for the construction with different types of vertical wind turbines including traverses. Thus, besides getting multiple numbers of different wind turbines shapes with modifications very fast and error-prone, the method also creates a high-quality mesh, which allows to perform numerical experiments with high precision and speed. Layering can be successfully used for rapidly prototyping solid-state patterns of the blades. These master models have sufficient accuracy and strength to be later on used as a templates for the production of high-tech composite blades of the wind turbines of desired format. The rapid prototyping uses 3D printing, where one of the printing parameters is the height of the material layer, to obtain the solid blade of the designed wind turbine (see Fig.2).

Acknowledgments

Authors would like to thank ForWind - Center for Wind Energy Research from University of Oldenburg for the support in current work.

References

[1] H.K. Versteeg and W. Malalasekera, An Introduction to Computational Fluid Dynamics, 2007 (pp. 15, 17, 23)
[2] "OpenFOAM finite volume programming environment for CFD". http://www.openfoam.com/. Accessed on 06.08.2015.

Experimental Study of Turbulent Swirling Wakes with Stereoscopic Particle Image Velocimetry

Marlin Holmes, Pourya Nikoueeyan, Jonathan W. Naughton
University of Wyoming, Laramie, WY, USA

Introduction

The operation of wind turbines in the wakes of other turbines can lead to an appreciable decrease in power production. There is evidence that swirl modifies wake behavior, in particular wake strength, growth rates, and decay rates [1]. Extensive work has been performed on the classical case of the axisymmetric wake [2,3], but only a few studies have been performed on swirling wakes in wind tunnels and in the field [4,5]. To date, little attention has been focused on the swirling axisymmetric wake examining fundamental flow physics with minimal artifacts. It is studies such as this that are needed to not only understand how swirl specifically modifies wake behavior but also to aid validation efforts of wake flow simulations. The overall goal of this project is to study the swirling axisymmetric wake with minimal flow artifacts to better understand how swirl modifies turbulent structure. The objective of the work presented in this here is to utilize stereoscopic Particle Image Velocimetry (PIV) to gain deeper understanding of how changes in swirl relates to changes wake deficit, decay and growth.

Experimental Approach

All work for this study will be carried out in the University of Wyoming open return wind tunnel. The swirling wake will be produced using a custom designed wake generator consisting of an enclosed servomotor that will be wire mounted in the test section to minimize flow artifacts. The wake will be produced by rotating a honey comb 3.8 cm (1.496 in) in diameter with cell diameters of 0.3 cm (0.125 in). The rotational rate will be controlled by a Faulhaber speed controller operated via LabView. PIV data will be obtained using a LaVision PIV system with 2 cameras to capture stream wise velocity profiles (~10 x/D). Vector fields will be obtained by processing the raw images with LaVision's DaVis processing software from which all relevant data can be extracted. The data presented here is derived processing three hundred images to produce axial and radial velocity fields. All three cases presented were performed at a wind tunnel velocity of 25 m/s. Earlier studies performed in similar conditions resulted in an approximate wake Reynolds number of Re_D=45,000 [1].

Current Results

As shown in Fig. 1, mean axial velocity contours have been obtained for three cases: ω=0 rpm, ω=3000 rpm, and ω=4000 rpm. As the rate of rotation is increased it can be seen that the wake strength grows larger as represented by larger regions of blue contours. In (c) velocities of approximately 10 m/s can still be found at nearly six diameters (x/D) downstream. In comparison in (a) the wake has risen to nearly free stream velocity of 25 m/s at approximately five diameters downstream. From these preliminary results it can be shown that increased rotation rates impact the strength of wake deficits. It should be noted that the intensity peaks at 2.5 and 5 diameters downstream are not indicative of actual flow behavior and are artifacts of the measurement.

Conclusions and Future Work

Preliminary data shows that increased rotation rates affects wake behavior specifically wake strength or the persistence of the wake deficit. It should be noted that wake strength is a complex function of wake generator porosity and rotation rate, which makes conclusions hard to draw from a limited number of cases. However, future work will utilize Laser Doppler Anemometry to quantify the swirl produced by the wake generator. Additional stereoscopic PIV measurements will be used to obtain 3 component velocity fields as well as information related to turbulent statistics. As this flow contains a relevant out of plane velocity component Stereoscopic PIV should yield valuable information pertaining to how swirl modifies wake behavior which cannot be obtained from two

component velocity fields alone. To capture the changes in the turbulence structure in the wake flow that occur as the swirl changes, Proper Orthogonal Decomposition will be used.

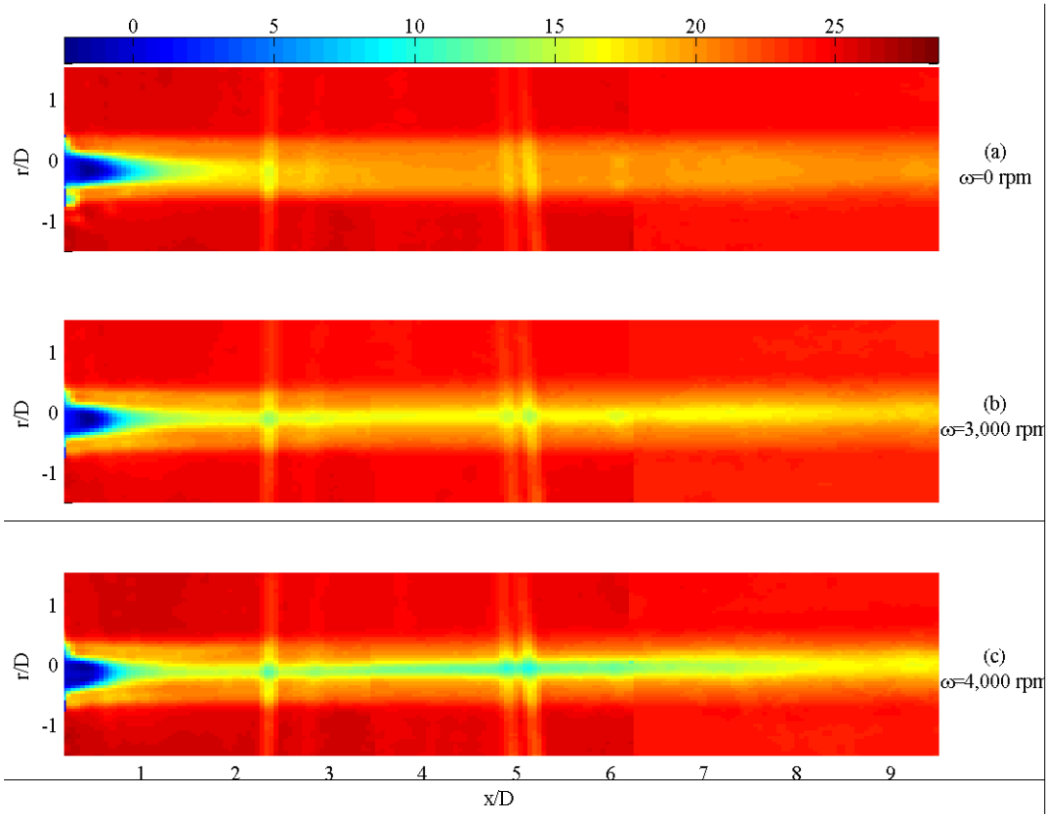

Fig. 1 Axial velocity for three different wakes: one non-rotating and two rotating wakes

Acknowledgments

This work was supported by the U.S. Department of Energy, Office of Science, Basic Energy Sciences under Award # DE-SC0012671. This project is partially support by funding from an NSF GK-12 grant, project number 0948027. Marlin Holmes would also like to thank Eric DeMillard for his assistance with the experiments.

References

[1] Hind, M., Holmes, M., and Naughton, J. W., "Experimental Investigation of Turbulent Swirling Wakes (AIAA)," *52nd Aerospace Sciences Meeting*, 2014.
[2] Johansson, P. B. V., and George, W. K., "The far downstream evolution of the high-Reynolds-number axisymmetric wake behind a disk. Part 1. Single-point statistics," *Journal of Fluid Mechanics*, vol. 555, May 2006, p. 363.
[3] Johansson, P., George, W., and Gourlay, M., "Equilibrium similarity, effects of initial conditions and local Reynolds number on the axisymmetric wake," *Physics of Fluids*, vol. 15, 2003, p. 603.
[4] Iungo, G., Wu, Y., and Porté-Agel, F., "Field Measurements of Wind Turbine Wakes with Lidars," *Journal of Atmospheric and Oceanic Technology*, vol. 30, Feb. 2013, p. 120921142126008.
[5] Wosnik, M., and Dufresne, N., "Experimental investigation and similarity solution of the axisymmetric turbulent wake with rotation," *ASME 2013 Fluids Engineering Division Summer Meeting*, Nevada: 2013.

Research Activities on an Operating Wind Farm

Marianne Rodgers
Wind Energy Institute of Canada, North Cape, Canada

David Watson
Wind Energy Institute of Canada, North Cape, Canada

Gerald Giroux
Wind Energy Institute of Canada, North Cape, Canada

Introduction

The Wind Energy Institute of Canada (Institute) is a not for profit research institute, located in Prince Edward Island, Canada, whose mission is to advance wind energy across Canada. The Institute owns and operates a 10 MW Wind R&D Park with a 1 MW/2 MWh battery energy storage system. Utilizing the Wind R&D Park as a large lab, the Institute, in partnership with several universities and other research institutes, has a variety of ongoing research.

Body

A major research stream at the Institute includes service life estimation of the turbines. This is important for long term planning and has implications for the Institute and industry. Research includes data collection from the wind park's supervisory control and data acquisition system, from system monitoring tools, and from lidars and anemometers on the site. Research by three universities and the WindEEE Institute, which involved strategic placement of anemometers and lidars throughout the site, will improve understanding of optimal turbine placement and operation as well as the influence of cliffs on the wind resource. When this information is combined with blade and gearbox condition monitoring, ice detection, and strain gauges on the tower, increased understanding of the stresses on wind turbines will be realized, especially during extreme events such as high winds and ice storms.

The Institute is also active in research in wind energy integration. The 1 MW/2 MWh storage system is being used in a variety of month long test scenarios to understand the impact that storage can have in integrating wind energy into the network. This research includes collaboration from the local utility, General Electric (the battery manufacturer), as well as international collaborators and academia.

The Institute, with a world-class wind resource, a utility scale wind park and storage system, and unique geographical features in the form of a 14 m cliff and 300 degree exposure to the ocean, makes it an ideal place for research. The Institute's one second data along with their IEC standard 80 m meteorological mast ensures that high quality data is available for any type of experiment. The Wind R&D Park and Storage system serve as a unique research infrastructure that is available for collaborative projects with universities, industry, utilities, and system operators.

Acknowledgments

The Wind R&D Park and Storage System for Innovation in Grid Integration was made possible when the Natural Resources Canada Clean Energy Fund awarded the Institute $12 million federal contribution, to demonstrate the economic and technical feasibility of wind energy storage in Canada. The project has also been supported through a $12.6 million loan with the Government of PEI, which is being repaid from the sale of power produced by the Wind R&D Park.

3D Measurements and Modelling of Wake Flow Around a Full-Scale Vertical Axis Wind Turbine (Nenuphar)

Mikael Sjöholm, Nikolas Angelou, Kasper Hjort Hansen, Torben Mikkelsen
Technical University of Denmark, Department of Wind Energy, Risø Campus, 4000 Roskilde, Denmark

Joanna Kluczewska-Bordier, Pascal Beneditti, Alexandre Immas, Nicolas Parneix, Frederic Silvert
Nenuphar, Campus de l'Institut Pasteur de Lille, 1, rue du Professeur Calmette, 59000 Lille, France

Introduction

During January-February 2015, Nenuphar and DTU collaborated in acquiring 3D wind field measurements around an onshore prototype of an offshore floating VAWT concept. The mobile 3D remote-sensing based WindScanner facility www.windscanner.dk provided 3D wake measurements around a 2 MW VAWT offshore prototype (NENUPHAR) operated at an onshore test site well-exposed to the strong Mistral winds near Fos-sur-Mer, Southern France. The WindScanners measured the mean and turbulence flow fields within and behind the 42 m tall and 51.5 m wide Vertical Axis Wind Turbine (VAWT). The campaign resulted in a total of 37 wind field runs. The paper presents the observed VAWT wake flow measurements and compare with the first vortex and CFD model predictions.

The WindScanner system [1][2], consisting of three space and time synchronized wind lidars, was operated at Fos-sur-Mer to measure wind and wake field around a Nenuphar prototype vertical axis wind turbine (VAWT). Three WindScanners are each equipped with a continuous-wave ZephIR lidar and a dual prism scanning system to steer the laser beams within a +/-60 degrees scan cone. Controlled focus stages set the line-of-sight measurement range between 10 m and 200 m. A wind speed sampling rate of 100 Hz per unit was used for this campaign. The WindScanners scanned the wind field along common predefined trajectories in 3D space and time, enabling measurements of all three velocity components of the wind field simultaneously.

A 54m meteorological mast, installed at a distance of approx. 200 m from the wind turbine provided standard meteorological data (wind speed at different heights, direction, temperature, air pressure). Also derived information such as wind shear and turbulence was registered.

The joint WindScanner-Nenuphar test measurements resulted in hitherto unprecedented information about the rotor zone and wake from a full scale operating VAWT, including measurements of the flow within the rotor itself. Mean wind and turbulence fields were measured inside the rotor while operating, and in its diffusing wake downwind to 2 Ø.

Furthermore, the 3D wake structures observed behind the operating VAWT have been modelled by vortex models (ARDEMA) and CFD models. ARDEMA is a set of a two dimensional (ARDEMA 2DS) and a three dimensional unsteady vortex code (ARDEMA 3DS) developed by AREVA, NENUPHAR with subcontracting to DELFT University and the CORIA inside the MADRILLET Technopole. CFD simulations are run following Nenuphar internal methodology with commercial software using URANS formulation. The main difference between the two types of calculation is the modelling of the viscous effects, which are inherently calculated in CFD but are calculated using a semi-empirical model in ARDEMA.

Comparisons between model representation of the near wake of the Nenuphar VAWT and the 3D WindScanner wind field measurements will be presented. To this end, measurements of the wake in a horizontal plane through the turbine and in a vertical plan behind it will be used. Comparisons with the measured induction field will also be carried out.

Fig. 1 Short-range WindScanners in operation around Nenuphar VAWT at Fos-sur-Mer, Fr.

The three space and time synchronized short-range WindScanners R2D1, R2D2 and R2D3 in operation at the Nenuphar test site at Fos-sur-Mer. The wake influences mean and turbulent wind fields were scanned in both horizontal and vertical planes through the running rotor and in the wake behind the 51.5 tall Ø 42 m tall Nenuphar VAWT.

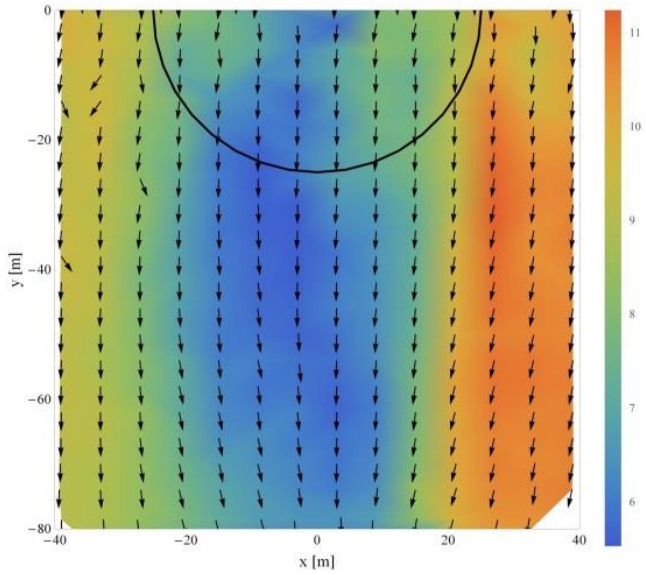

Fig. 2 Horizontal plane mean wind field at hub height 27 m (top view - Case 14).

Example of a WindScanner measured wake field within and behind the operating Nenuphar proto type (Case14: 5-min mean flow from 16:00 -16:05). A VAWT induced wind speed reduction is observed already within the rotor and the VAWT wake is observed to propagate downwind throughout the2D downwind scan area scanned. When top-viewed as the NenuPhar turbine is rotating anticlockwise, and to the right, where the blades are turning up against the wind, the wake exhibits wind speeds + 1 m/s higher than on the other side, where the blades are moving along the wind. This asymmetric flow behavior is also seen in the CFD model results.

Acknowledgments

EU MARINET is gratefully acknowledged for giving support to the WindScanner wake measurements on the Nenuphar test turbine at Fos-Sur-Mer; Southern France, cf. MARINET Grant application no. 317 [Jan. 2014].

References

[1] Mikkelsen T, Mann J and Courtney M 2008 Wind Scanner: A full-scale Laser Facility for Wind and Turbulence Measurements around large Wind Turbines *EWEC 2008* (Brussels: EWEA - The European Wind Energy Association) p 10
[2] Mikkelsen T 2014 Lidar-based Research and Innovation at DTU Wind Energy – a Review *J. Phys. Conf. Ser.* **524** 012007

Complex Terrain and Wind Farm Interactions

Matthew Welch, Jonathan Naughton
University of Wyoming, Laramie WY, USA

Ryan Jacobson
Power Company of Wyoming, Denver CO, USA

Introduction

Good wind resources are often found in areas with complex terrain. The complex terrain wind environment is not well understood, and, as a result, is not modeled well [1]. In addition, the performance of wind plants decreases with size as a result of wake interactions. To optimize wind farms in complex terrain, a better understanding of winds in complex terrain (inflow behavior), and turbine interaction with each other in complex terrain (wake behavior) is needed; however the issue of data availability arises. There simply are a limited number of wind data sets in complex terrain (for example, reference [2]). Those data sets that are available typically have limited spatial resolution and represent a limited view of complex terrain missing important characteristics of locations like the western United States [2]. A rare research opportunity to obtain raw wind data from the Chokecherry and Sierra Madre Wind Energy Project (CCSM) has been provided by the Power Company of Wyoming (PCW) where wind data over several years from many met towers across a large complex region were obtained in the development process. The objective of the present work is to characterize winds in the CCSM complex terrain under different atmospheric conditions. To accomplish this, data from multiple towers over several years will be considered.

Data

The CCSM project performed a comprehensive characterization of the winds at the wind farm site. Data were obtained from 38 met towers in a 320,000 acre region from periods of time ranging from 2 to 7 years as shown in Fig. 1. The current study provides data for 1 met tower per 13 square miles [3]. To ensure redundancy and to capture wind variation with height, each met tower consists of 2 anemometers at 40, 60, and 80 meter heights. The redundancy in the second anemometer is to address tower shadowing. The wind speeds are captured at 1 Hz, and then averaged over 10 minute intervals. Each met tower has three wind vanes; one for each anemometer height location. The data from these towers indicates a Class 6-7 wind resource at the best sites with Class 5 at some locations in the region.

Analysis

First, the data went through a quality control process to ensure good information for characterizing the winds and was then analyzed. Tower shadowing, sensor failure, and sensor icing as well as missing and bad data were identified in the quality control process. Winds that measured less than 0.5 m/s were also regarded as a zero wind speed. Using the resulting data, the flow will be characterized in several different ways using an approach similar to those of previous studies [5]. First, the data will be sorted by wind speed and direction to build typical flow patterns within the CCSM project area. In addition, the data will be further sorted by stability conditions to identify those effects on the wind patterns. Flow characterization will be looked at in three different areas: stability, wind direction, and wind speed.

Future Work

The eventual goal is to utilize this data to better understand wind in complex terrain (inflow behavior) and its interaction with the individual turbines (wake behavior). The present work will also provide experimental data necessary for validating Computational Fluid Dynamic (CFD) models and overall performances of wind farms [4]. Sorting the data to build data sets for specific conditions will enable identification of the sensitivity of the

flow patterns to the conditions, and will also allow for validation of simulations under the same atmospheric conditions. As the CCSM project is still under development, repeating the analysis before, during, and after wind farm construction is also planned. Using these results, understanding of the effects of the wind farm development on the local wind patterns as well as on turbine wake development and growth can be gained.

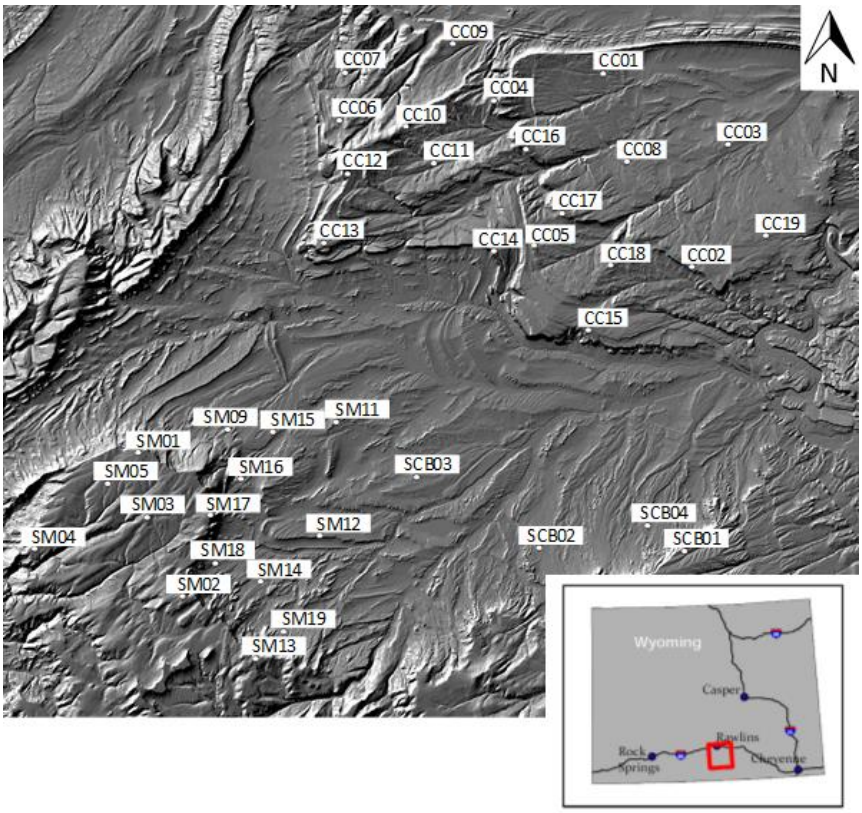

Fig. 1 Topography Map of Chokecherry and Sierra Madre Wind Energy Project with met tower locations shown.

Acknowledgments

This work was supported by the U.S. Department of Energy, Office of Science, Basic Energy Sciences, Under Award # DE-SC0012671.

References

[1] Complex Flow Workshop Report; DOE/GO-102012-3653, May 2012.
[2] Berg, J., Mann J., Bechmann, A., Courtney, M. S., and Jorgensen, H. E., " The Bolund Experiment, Part I: Flow Over a Steep, Three-dimensional Hill, *Boundary-Layer Meteorology*, 141, pp. 219-243, 2011.
[3] Lundquist, Katherine A., Fotini Katopodes Chow, and Julie K. Lundquist. 'An Immersed Boundary Method For The Weather Research And Forecasting Model'. *Mon. Wea. Rev.* 138.3, pp. 796-817, 2010.
[4] Politis, E. S. et al. 'Modeling Wake Effects In Large Wind Farms In Complex Terrain: The Problem, The Methods And The Issues'. *Wind Energ.* 15.1, pp. 161-182, 2011.
[5] Wharton, Sonia, and Julie K. Lundquist. 'Assessing Atmospheric Stability And Its Impacts On Rotor-Disk Wind Characteristics At An Onshore Wind Farm'. *Wind Energ.* 15.4, pp. 525-546, 2011.

Wind Turbine Wake Modeling Based on New Metrics for Wake Characterization

Paula Doubrawa
Cornell University, Ithaca, NY, USA

Rebecca J. Barthelmie
Cornell University, Ithaca, NY, USA

Mathew J. Churchfield
National Renewable Energy Laboratory, Golden, CO, USA

Introduction

Wind turbine wakes are significantly impacted by atmospheric conditions, such as ambient and wake-generated turbulence. Understanding the detailed dynamics of wakes is therefore critical to predicting plant performance and to maximizing the efficiency of wind farms, both directly (e.g., guiding the placement and spacing of generators within a wind farm) and indirectly (e.g., serving as a basis for the improvement of turbine design standards and control systems). However, this knowledge requires atmospheric data at a high spatial and temporal resolution, which are not easily obtained from direct measurements. As a consequence, wake dynamics research is often based on results obtained from numerical models, which vary in fidelity and computational cost. On one end of the spectrum, very simple two-dimensional models (e.g., [1] and [2]) reproduce a simplified idealized wake based on assumptions about the wake shape, deficit profile, and spreading rate, as well as some level of symmetry. On the opposite end and at a higher cost, the evolution of three-dimensional turbulent fields may be obtained from large-eddy simulations of the atmospheric boundary layer coupled to a turbine model. There is still the need for a compromise, in which unsteady wakes can be simulated in more detail but still at a low enough cost to allow for sets of experiments to be performed operationally. This work aims at filling this gap by developing spectral and statistical methods that are based on high-resolution large-eddy simulation (LES) results and that reproduce unsteady wakes with sufficient accuracy and detail without the need for high-performance computational power.

Body

The work presented here is based on a simulation of Egmond aan Zee, an offshore wind farm 14 km off the coast of the Netherlands. It was performed using NREL's SOWFA tool [3], which includes a second-order accurate finite-volume fluid solver based on the Open-FOAM toolbox coupled to a structural dynamics and system dynamics model (FAST). The Vestas V90-3MW turbines are modeled as rotating actuator lines. The spatial resolution is 10 m away from the turbine, and 1-2 m around the turbines and in the wake. A precursor simulation is initially run without turbines in order to generate the necessary initial and boundary conditions, in which the turbulence intensity is 4.1% and the wind speed 9 m/s at the hub height of 70 m. The analysis conducted for this work focuses on two-dimensional planes of wind data behind the first upwind turbine at the distances of two (2D), four (4D), and six (6D) rotor diameters downstream, for a period of 20 minutes and sampled at a 1 Hz frequency.

The method developed aims at reproducing the wake shape and intermittent edges, the deficit profile, and meandering. The work presented here focuses on the results from the wake shape generation. Since there are several ways of characterizing wind turbine wakes, the first part of this work explores different approaches at defining the wake width, height, center, and lateral and vertical meandering.

Three main methods were tested for defining wake width, height and center. It was found that maintaining a moving frame of reference is not critical to defining the wake length scales, and that simple approaches are able to capture the global metrics of the wake. At 4 and 6 rotor diameters downstream, the axial evolution of the mean

wake width and mean velocity deficit matched the values predicted by similarity theory at infinite Reynolds numbers. One of the wake center definition methods presented very noisy results, thus overestimating the magnitude of the meandering. The two other methods presented more stable results, with correlations of at least 0.6 for vertical and horizontal meandering at all downstream distances.

After defining the wake area on the lateral-vertical planes, the wake edge was identified and used to obtain series of wake radii as a function of azimuth angle r(θ) for each second, and at each downstream distance. For each azimuthal series, the power density spectrum was obtained and filtered to keep only the frequencies responsible for most of the variations in the wake shape. Spectral techniques were developed to recreate the wake shape (Fig. 1), taking into account temporal and spatial coherence. The wake shapes generated from the spectral-statistical methods developed successfully reproduce the global characteristics of the original wake, such as mean wake width and height, mean azimuthal radius, and azimuthal radii mean spectra, and first-order auto-correlation. Continuing work focuses on incorporating velocity deficit and meandering into the process.

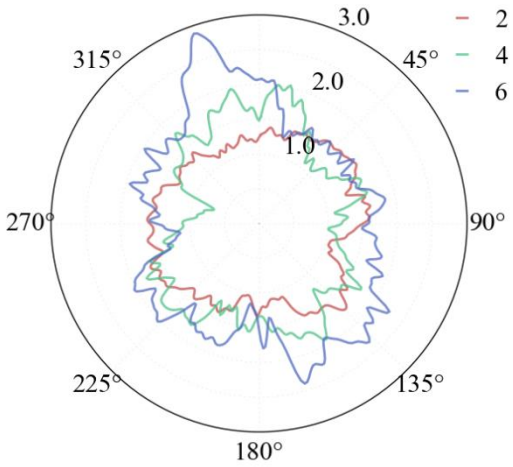

Fig. 1: Example of synthetic wakes produced with the spectral-statistical methods developed, for the downstream distances of 2 (red), 4 (green) and 6 (blue) rotor diameters, looking upstream. Radial axis goes from 0 to 3 rotor radii and origin is the wake center in the meandering frame of reference.

Acknowledgments

National Science Foundation 1464383, Department of Energy EE0005379, National Renewable Energy Laboratory XFC-5-42084-01, Indiana University High Performance Supercomputing Center.

References

[1] Jensen, N. O. “A Note on Wind Generator Interaction.” Risø National Laboratory, 1983.
[2] Ainslie, JF. “Development of an Eddy Viscosity Model for Wind Turbine Wakes.” In *Proceedings of the BWEA Conference*, 61–66, 1985.
[3] Churchfield, Matthew J., Sang Lee, John Michalakes, and Patrick J. Moriarty. “A Numerical Study of the Effects of Atmospheric and Wake Turbulence on Wind Turbine Dynamics.” *Journal of Turbulence*, January 1, 2012, N14. doi:10.1080/14685248.2012.668191.

WRF Simulations of a Pseudo Offshore Wind Farm: Validation against Field Measurements and Evaluation of Wind Turbine Drag Parameterization

Paula Doubrawa
Cornell University, Ithaca, NY, USA

Hui Wang
Cornell University, Ithaca, NY, USA

Sara C. Pryor
Cornell University, Ithaca, NY, USA

Rebecca J. Barthelmie
Cornell University, Ithaca, NY, USA

Introduction

A measurement campaign was undertaken in May 2015 at the Wind Energy Institute of Canada on Prince Edward Island. The site is located on the North Cape of the island, which spans approximately 1-2 km from coast to coast and presents abrupt roughness and terrain transitions from ocean to land, with coastal escarpments to the east and the west. The experiment aimed at measuring wakes behind 4 out of the 25 turbines on the site. This paper focuses on the integration and comparison of Weather Research and Forecasting (WRF) model simulations with the observations for the May 2015 period and addresses two key research questions: (i) how well WRF performs in terms of simulating phenomena responsible for non-logarithmic wind profiles (e.g. low level jets); and (ii) how the simulation results change when WRF is run the wind farm parameterization [1].

Body

The instruments deployed include a scanning lidar, three profiler lidars, and two meteorological masts with sonic anemometers measuring at several heights. The scanning lidar collected three-dimensional data in the form of discrete two-dimensional slices, with different scanning geometries depending on the prevailing wind direction. The profiler lidars and sonic anemometers provided point measurements at discrete heights. In order to provide a meteorological context for the measurements and to supplement the in situ data, the WRF model was run with two-way nesting down to a horizontal resolution of 1 km and with 10 vertical levels below 200 m.

The validation of the model results includes data from May 12 through May 26 at the instrument locations and across the rotor plane (20 m to 140 m). In comparison with the observed wind speeds, the model performed better at wind speeds higher than 7 m/s. The normalized errors relative to the lidar profiles were of similar magnitude, with wind speed over-estimations of ~33% and under-estimations of ~23% at the lidar closest to the coast. Over (under) estimations of the wind speed occurred on average 61% (39%) of the time. The model failed to reproduce subgrid-scale phenomena such as the development of pronounced internal boundary layers as offshore air flows past the escarpment onto the cape (due to the model resolution). However, it did capture a small change in the profile as it advected past the island. For onshore flow, the model produced a mean decrease in wind speed as the layer from 20 m to 200 m reached the cape. For easterly winds (direction between 30 and 150), the mean decrease was of ~1.2%. For westerly winds (direction between 230 and 350), the flow slowed down by ~2.2%. Moreover, the simulation reproduced the onset, location, and intensity of a low-level jet event observed on May 12 near 1200 UTC, from 200 m to 600 m, with an intensity of 16-19 m/s.

The comparison between the simulation with and without the turbine drag parameterization was conducted for a shorter period, including the first five days of the experiment (May 11 through May 15). The parameterization

uses the thrust coefficients of the turbines to convert kinetic energy in the atmosphere to non-productive drag, thus increasing the ambient turbulence and decreasing the mean momentum within the grid cells where the turbines are located. When the parameterization is used, the mean bias of the simulations is decreased especially for heights above 60 m (hub height for turbines closest to instrument locations is 80 m). The maximum decrease in bias is of 22% at 80 m when comparing the modeled winds against the profiler lidars. When the turbine drag parameterization was used, the change in turbulent kinetic energy was local and presented a temporal mean maximum of 0.5 m^2s^{-2} at 80 m, with increased values for the drag simulation. In terms of wind speed, there seems to be no clear distinction between the simulations. The differences in 80 m winds are on the order of 10^{-1} m/s but instead of being concentrated locally, are spread across the domain indicating that the 25 turbines on North Cape do not produce a coherent mesoscale wake.

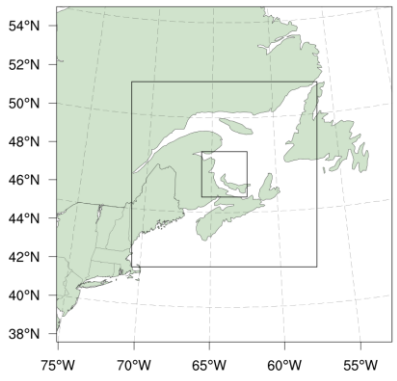

Fig 1: Domain configurations for WRF simulations, where horizontal resolutions are 9 km, 3 km and 1 km

.

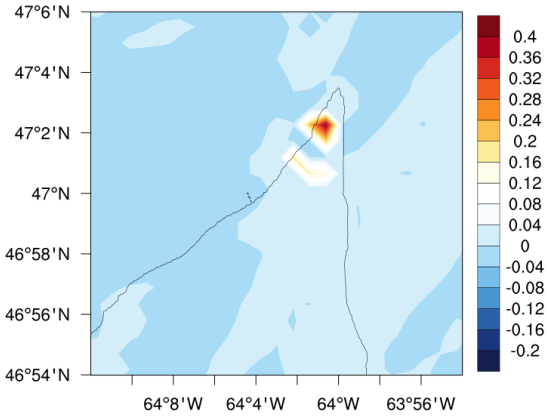

Fig. 2: Mean difference in turbulent kinetic energy [m2s-2] at 80 m (k_{drag}-k) at the wind farm location in North Cape, Prince Edward Island, Canada

Acknowledgments

National Science Foundation 1464383, Department of Energy EE0005379, National Renewable Energy Laboratory XFC-5-42084-01, Indiana University High Performance Supercomputing Center.

References

[1] Fitch, Anna C., Joseph B. Olson, Julie K. Lundquist, Jimy Dudhia, Alok K. Gupta, John Michalakes, and Idar Barstad. "Local and Mesoscale Impacts of Wind Farms as Parameterized in a Mesoscale NWP Model." *Monthly Weather Review* 140, no. 9 (March 6, 2012): 3017–38. doi:10.1175/MWR-D-11-00352.1.

Advanced Surface Pressure Measurement Techniques for Characterization of 3-D Wind Turbine Airfoil Stall

Pourya Nikoueeyan, Jonathan W. Naughton
University of Wyoming, Laramie, USA

Kevin J. Disotell, James W. Gregory
The Ohio State University, Columbus, USA

Introduction

Wind turbine blades experience highly unsteady inflow conditions. The resulting oscillatory variation in the relative wind speed and direction can lead to dynamic stall and complex flow reattachment cycles, the main source of unsteady loading on turbine components. This is an active area of study in terms of both dynamic stall aerodynamics and also control applications [1]. Besides understanding the physics of dynamic stall and flow mechanisms involved, accurate prediction of the aerodynamic coefficients is of great importance to the industry.

Due to the complexity and cost of using a force balance in pitch-plunge airfoil testing, conventional tap-tubing and electronic pressure transducers remain the most common sources of providing data for calculating aerodynamic coefficients. However, problems associated with the span wise distribution of the pressure ports and port placement near the trailing edge of the airfoils can cause significant uncertainties in load calculations. Such challenges can be overcome by employing more advanced flow measurement techniques. Fast-responding pressure-sensitive paint (PSP) is an optical surface pressure measurement technique capable of capturing global surface pressure distribution with an inherently fine spatial resolution. New developments in paint composition and the resulting increased frequency response have enabled unsteady PSP measurements [2]. The acquired global pressure distribution can be used to calculate loadings on the aerodynamic surfaces.

A recent collaboration between University of Wyoming and The Ohio State University has focused on demonstrating state-of-the-art PSP techniques on a low-Reynolds number airfoil at conditions relevant to wind turbine aerodynamics, including steady and unsteady stall. Beside the physical insights obtained from this work, this paper focuses on answering one main question: how much difference in span wise lift and moment coefficients occur due to three-dimensionalities induced by complex stall and reattachment flow structures?

Methods

The experimental campaign was conducted at the University of Wyoming low-speed wind tunnel facility. An in-house pitching mechanism was used to dynamically pitch a DU97-W-300 airfoil section of 10.2-cm chord about its quarter-chord axis at a chord-based Reynolds number of 2.25×10^5. A conventional tap-tubing system was used to acquire pressure profiles over the airfoil that were then used for in-situ calibration of PSP applied on the suction side of the airfoil. The PSP consisted of porous polymer/ceramic basecoat on the airfoil top surface that was over sprayed with platinum tetra porphyrin (PtTFPP) luminophore. Details regarding the test setup and instrumentation used in this study have been documented by Disotell et al. [3].

Lift and moment coefficients were calculated by integrating the pressure profile acquired from the tap-tubing system and also profiles extracted from PSP measurements. PSP data taken on the suction side shows two-dimensional flow organization before stall. Since flow does not separate on the pressure side of the airfoil for high positive angles of attack, the pressure distribution on the bottom side of the airfoil was assumed to be 2D along the span and data from pressure taps was used.

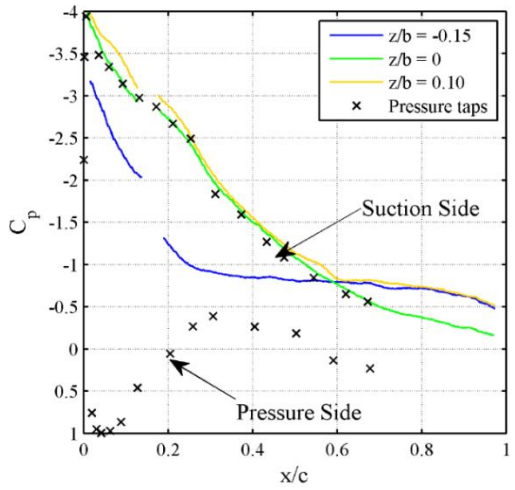

Fig. 1 Cp distribution from taps vs PSP data at several span-wise stations for α=17°

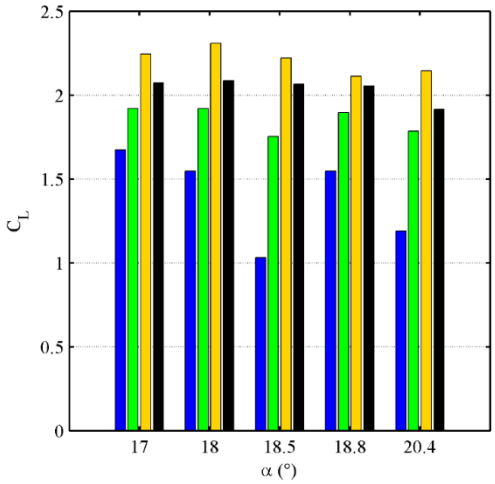

Fig. 2 Comparison of static lift calculated at different span-wise locations for different angles of attack (α) after static stall; colors follow legend in Fig. 1

Results and Discussion

For brevity, only one static stall case is presented in this abstract. Fig. 1 presents chord-wise (x/c) pressure coefficient profiles at several span-wise stations (represented by normalized span coordinate *z/b*, where *z/b=0* is at mid-span) extracted from the PSP and tap data. The suction-side pressure profile acquired by the surface taps agrees well with the PSP data; however, the lack of pressure taps on the trailing edge can cause loss of important information about the trailing edge flow organization. The flow three-dimensionality is also readily apparent from the chord-wise distributions extracted from the PSP results at several span-wise stations. Fig. 2 presents a comparison in sectional lift coefficients calculated based on the suction-side PSP data and compares them with the C_L calculated based on tap data for five different post stall angles of attack. High deviation in lift coefficients is observed across the span. It is also clear that the missing pressure measurements on the aft trailing edge section from pressure taps can result in 20% difference in the predicted lift coefficient.

Conclusions

The pressure signatures of static and dynamic stall over wind turbine blades are highly three dimensional and need measurement tools with fine spatial resolution and high frequency response to be captured completely. Capturing these three-dimensional flow structures is critically important for accurate prediction of aerodynamic loading on the blades. Considering the difficulties associated with using other measurement techniques, PSP is capable of measurements on airfoils and 3D blades under controlled conditions and can provide important physical insight about the aerodynamic loads when integrated to the test campaign.

References:

[1] J. Naughton, J. Strike, M. Hind, A. Babbitt, A. Magstadt, P. Nikoueeyan, P. Davidson and J. Sitaraman, 'Characterization and Control of Unsteady Aerodynamics on Wind Turbine Aerofoils', J. Phys.: Conf. Ser., vol. 524, p. 012025, 2014.
[2] J. Gregory, H. Sakaue, T. Liu, and J. Sullivan, 'Fast Pressure-Sensitive Paint for Flow and Acoustic Diagnostics', Annual Review of Fluid Mechanics, Vol. 46, pp. 303-330, 2014.
[3] K. Disotell, P. Nikoueeyan, J. Naughton, and J. Gregory, 'Single-Shot Pressure-Sensitive Paint Measurements of Static and Dynamic Stall on a Wind Turbine Airfoil', Presented at AHS Forum 71, Virginia Beach, VA, 2015.

Wind Turbine Wakes during PEIWEE

R.J. Barthelmie
Cornell University, Ithaca, NY 14853, USA

H. Wang
Cornell University, Ithaca, NY 14853, USA

P. Doubrawa
Cornell University, Ithaca, NY 14853, USA

G. Giroux
WEICan, North Cape, PEI C0B 2B0, Canada

S.C. Pryor
Cornell University, Ithaca, NY 14853, USA

Introduction

We present measurements of wind turbine wakes from five DeWind 2 MW turbines owned and operated by Wind Energy Institute for Canada (WEICan) during the May 2015, Prince Edward Island Wind Energy Experiment (PEIWEE) (Fig. 1). The objectives of the work are to; (i) develop optimized methods for detection and quantification of wakes from scanning lidar, (ii) examine the degree to which flow deformation at the escarpment leads to 'lifting' of the wake in the vertical, and (iii) to quantify and differentiate the roles of meander v. turbulent expansion of wakes.

Body

Existing WEICan measurements close to the wind turbines (rotor diameter (D) = 93 m, hub-height = 80 m) were supplemented by:

- A Galion scanning lidar deployed approx. 535 m from the western cliff close to T5, operated with both Plan Position Indicator (PPI) and Vertical Azimuth Display (VAD) scan geometries.
- Three Natural Power ZephIR lidars: Z447 deployed approximately 0.7 D from T4. Unit Z423 deployed 3.5 D to the northeast of T4. Z125 located 2 D east of T4.
- 3 × 3D Gill Windmaster Pro sonic anemometers deployed at 20, 40 and 60 m on the IEC compliant 80 m meteorological mast 2.5 D from T5.

Flow conditions during the experiment were dominated by weakly stable to neutral stability, westerly flow and relatively high wind speeds (Fig. 2). When flow was from 225-15° over north, individual and embedded wakes from T2, T3 and T4 were sampled by the Galion PPI scans (see Fig. 3, which shows scans of a multiple embedded wakes with flow along the row of turbines from the northeast to the southwest).

Work to be presented includes determining wake characteristics from scans from the scanning lidar, wind and turbulence profiles from measurements from the ZephIRs and analysis of the spectral characteristics of wakes using data from the Gill Sonics.

Acknowledgements

We gratefully acknowledge funding from NSF (#1464383) and DoE (EE0005379), and the use of WEICan facilities and staff time. RJB also acknowledges the Otto Mønsted Guest Professorship at the Danish Technical University.

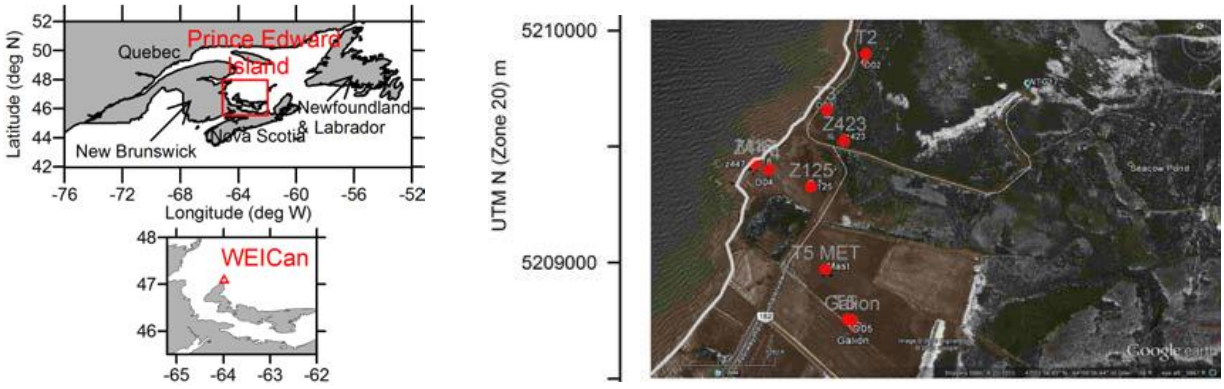

Fig. 1 Left: Location of Prince Edward Island and WEICan. Right: Overview of the measurement locations from Google Maps. The dimensions of the area are 1.5 km N to S and 2.25 km W to E.

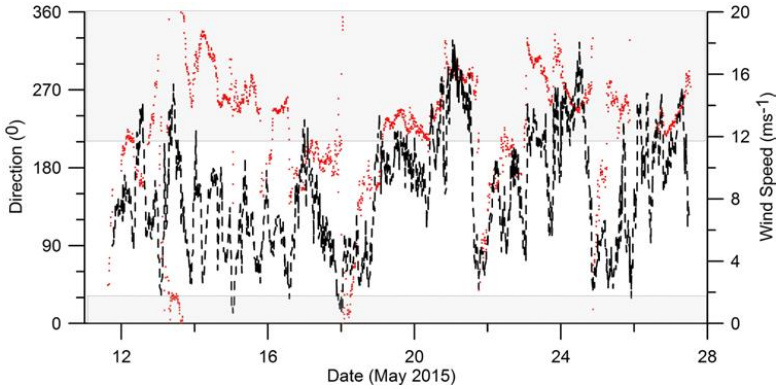

Fig. 2 Time series of wind speed and direction as measured with ZephIR lidar Z447. The boxes indicate directions for which there was potential to scan wakes from turbines T2-T4.

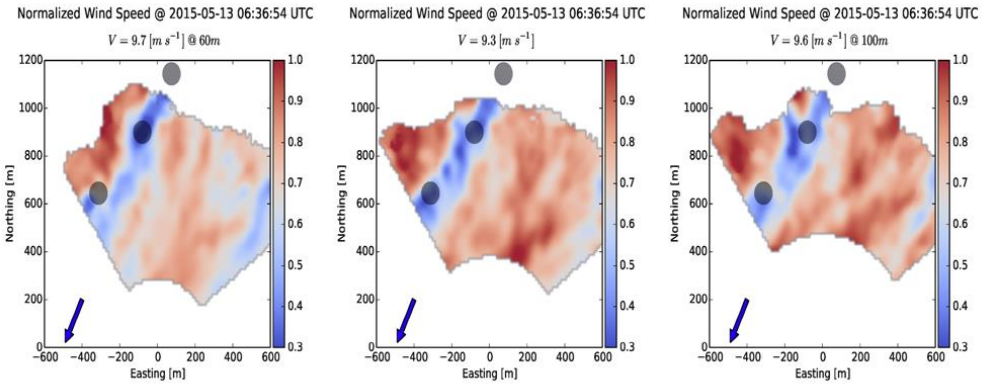

Fig. 3 Scanning lidar wind field retrieval for 60 (left), 80 (middle) and 100 m (right) height during northwesterly flow (direction indicated by the arrow). The black dots are turbines T2, T3 and T4 (north to south). The wind speeds are normalized to the 90th percentile value in the scan (which is used to represent the freestream velocity and is denoted by 1). Thus, a value of 0.5 indicates the flow at that point is 50% of the nominal freestream.

Large-Scale Physical Simulation of Flow over Complex Topography

R Kilpatrick
WindEEE Research Institute, London, ON, Canada

K Siddiqui
Department of Mechanical and Materials Engineering, Western University, London, ON, Canada

H Hangan
Department of Civil and Environmental Engineering, Western University, London, ON, Canada

Introduction

With wind turbines being increasingly situated in complex terrain, the ability to accurately predict wind conditions at these locations becomes paramount. To this end, an investigation of flow over complex topography was completed at the Wind Engineering, Energy and Environment Research Institute (WindEEE RI) test chamber, using a 1:25 scale Styrofoam model of Bolund hill, a 12 m high peninsula located near Roskilde, Denmark. Bolund Hill has been studied extensively in the wind energy community as it is topographically similar to a typical wind turbine site in complex terrain, albeit at smaller scale. Bolund is characterized by a long upstream fetch, a steep escarpment and a long flat section on top of the island (Bechmann [1]).

The principal objective of the present investigation was to investigate issues of scaling in topographic flows, with the eventual aim of gaining insight into the effects of surrounding complex topography on wind turbine flow dynamics. Measurements were taken using Cobra probes at key locations on the island as well as with particle image velocimetry (PIV) in vertical planes along Line A (239° wind direction) and Line B (270°). PIV in horizontal planes was conducted in the region of the escarpment.

Body

Fig. 1 shows upstream boundary layer profiles for nine different test cases, measured with three-component Cobra probes. By manipulating the fan speeds and roughness element heights, variations in Reynolds number, roughness and friction velocity were achieved. When compared to full-scale values for speed-up ratio and turbulent kinetic energy (TKE), Re_1 and Re_3 appear to the best-matched cases, however comparing the results across the entire range of Reynolds numbers may prove beneficial when investigating Reynolds dependency.

Fig. 2 presents Cobra probe measurements at three locations along the island, at heights of 2 m and 5 m above ground level, in the 270° wind direction (Line B) for speed-up ratio and change in TKE, along with comparative data from full-scale measurements and previous physical simulations. Data was normalized by upstream reference values in the manner laid out by Yeow (2013).

Cobra measurements of speed-up ratio generally match well with full-scale values and other physical models (Berg [2], Yeow [3]) at locations near the escarpment, but significantly under-predict near the centre of the model (M3) at both z = 2 m and z = 5 m heights. PIV results should help to verify this trend. Cobra predictions of TKE increase are more in line with results of other physical simulations, with generally good agreement at z = 5 m and severe under-prediction at z = 2 m at M6 and moderate under-prediction at M3 compared to full-scale results.

PIV measurements, conducted along Line A and Line B using four 12 megapixel cameras, should provide high resolution characterization of the flow, particularly in the highly turbulent shear layer located between M6 and M3. PIV measurements were also taken with the model cliff edge modified using clay to increase its sharpness and provide a more realistic proximity to the real escarpment edge of Bolund, which, according to Yeow [3] is expected to significantly affect speed-up and turbulence increase.

A thorough comparison of measurements at ~1:100 scale, 1:25 scale and full-scale is expected to provide insights on the specific issues presented by scaling of wind tunnel testing of complex topographic models, as well as to extend the understanding of potential effects of wind turbines situated amidst this topography.

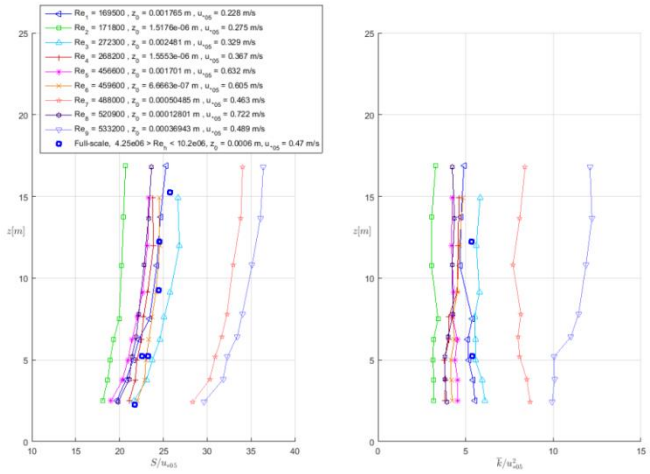

Fig. 1 Measured upstream profiles for Line B with comparison to full-scale values as per Bechmann [4] and Yeow [3]

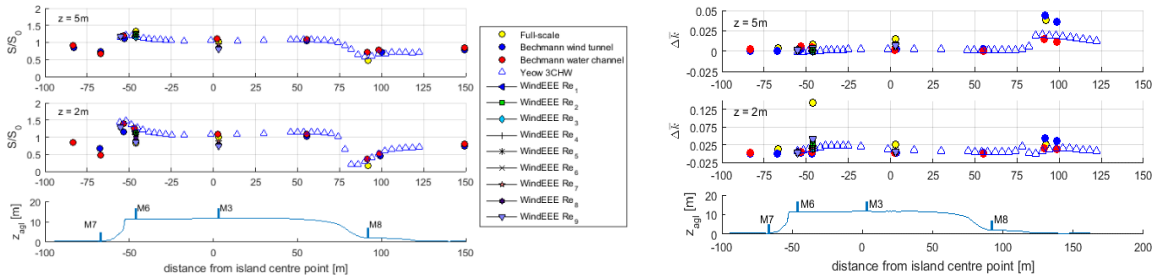

Fig. 2 Speed-up ratio and change in turbulent kinetic energy along line B

Acknowledgments

The authors would like to gratefully acknowledge the support of Natural Sciences and Engineering Research Council (NSERC) and Western University.

References

[1] Bechmann A., Berg J., Courtney M.S., Jørgensen H.E., Mann J., Sørensen N.N. (2009). The Bolund experiment: overview and background. Risø DTU report Risø-R-1658(EN), pp 1–50.
[2] Berg J., Mann J., Bechmann A., Courtney M.S., Jørgensen H.E. (2011). The Bolund experiment, part I: flow over a steep, three-dimensional hill. Boundary-Layer Meteorology, 141(2): 219–243. doi: 10.1007/s10546-011-9636-y.
[3] Yeow T.S., Cuerva-Tejero A., Perez-Alvarez J. "Reproducing the Bolund experiment in wind tunnel." Wind Energy 2013. doi: 10.1002/we.1688.
[4] Bechmann A., Sørensen N.N., Berg J., Mann J., Réthoré P.-E. (2011). The Bolund experiment, part II: blind comparison of microscale flow models. Boundary-Layer Meteorology. doi: 10.1007/s10546-011-9637-x

Using Large-Eddy Simulations to Estimate Spatial Coherence and Power Spectral Density of a Major Hurricane for Wind Turbine Design Applications

Rochelle Worsnop
University of Colorado-Boulder, Boulder, USA

George H. Bryan
National Center for Atmospheric Research, Boulder, USA

Julie K. Lundquist
University of Colorado-Boulder, Boulder, USA

National Renewable Energy Laboratory, Golden, USA

Introduction

Offshore wind development is being considered along the US East Coast, where hurricanes commonly occur. Characteristics of the hurricane boundary layer (HBL), especially in major hurricanes (≥ Category 3 on the Saffir-Simpson hurricane wind scale), are poorly understood due to a lack of observations. Large-eddy simulation (LES) can provide realistic wind profiles in hurricanes at low enough altitudes to determine how HBL characteristics may influence loads on potential offshore wind turbines. Even the most stringent wind turbine design (IEC Class I) are not rated to withstand winds greater than a weak Category 3 hurricane [1]. Since a cumulative average of 2.3 major hurricanes are expected to occur each year in the Atlantic Basin, it is important to understand how the extreme winds associated with these storms will affect offshore turbines [2].

Body

We use the LES model [Cloud Model Version 1 (CM1)] to simulate the wind characteristics for a theoretical offshore turbine during an idealized Category 5 hurricane, the strongest class of hurricanes and thus the "worst case" scenario for wind turbine designers. The model can create hurricane-like wind profiles at high spatial (< 10 m) and temporal resolution (< 1 s). We analyze power spectra and turbulence characteristics at elevations appropriate for wind turbines.

Given the need to understand conditions offshore during hurricanes, we assess power spectra and coherence from a modeled idealized hurricane using CM1. We compare the model to theoretical spectra and coherence to better understand the characteristics of the HBL as well as to determine the best theoretical models to represent wind velocities of an intense hurricane. The best theoretical power spectrum and coherence models can be used to simulate a full wind field using a stochastic wind simulator such as TurbSim. The full wind field can then be used in load simulators such as AeroDyn to calculate the turbine loads experienced during major hurricanes.

By comparison to the limited available observations, we find that a relatively "simple" and inexpensive configuration of the CM1 model accurately represents hurricane behavior in terms of mean wind speeds, wind speed variances, and power spectra. We then evaluate commonly-used spectra as compared to this "simple" CM1 model. The Kaimal and von Kármán power spectral models depict a peak in energy at lower frequencies than that in the HBL, suggesting that eddies containing the most power in a hurricane are smaller and occur at higher frequencies than represented in the commonly-used spectra. In addition, preliminary results show that the magnitude of the power spectrum produced using the theoretical models is at least 54% less than the magnitude of the power spectrum produced using the LES hurricane data. Modifications to the Kaimal model are suggested to better represent the HBL.

At a hurricane radius of 130 km, we analyze coherence of the flow at different horizontal separations. In the HBL, the flow is highly coherent (≥ 0.6) at all frequencies less than 0.2 Hz for the smallest horizontal separation

(15.6m). This means that flow is coherent across at least one-fourth the distance of a theoretical turbine blade (~63 m), assuming the standard NREL 5MW turbine with a hub height of 90 m and a rotor diameter of 126 m. As separation increases, coherence lessens at the highest frequencies in the flow as the eddy size becomes smaller than the separation length. Results also indicate that flow in the HBL remains highly coherent for much larger separations than that seen onshore and in a non-HBL atmosphere.

Acknowledgments

This material is based upon work supported by the National Science Foundation under Grant No. DGE-1144083. The authors also gratefully acknowledge Jun Zhang at the Hurricane Research Division (HRD) for providing observational hurricane time series. The authors also thank Branko Kosović for helping define the initial directions of this research.

References

[1] International Electrotechnical Commission. IEC 61400-1 Wind Turbines - Part 1: Design Requirements, Edition 3, 2007.
[2] NHC, 2013: National Hurricane Center. Available online at [http://www.nhc.noaa.gov/climo/].

Meso to Microscale Coupling Project

Sue Ellen Haupt
National Center for Atmospheric Research, Boulder, CO, USA

William Shaw
Pacific Northwest National Laboratory, USA

Branko Kosovic
National Center for Atmospheric Research, Boulder, CO, USA

Introduction

The development and validation of first-principles based, high-fidelity physics models within an open-source simulation environment has been identified as a crucial part of the Department of Energy's (DOE) Atmosphere to Electrons (A2e) program science goals and objectives. Furthermore, there has been an overwhelming consensus from the research community that these models must be developed and systematically validated using a formal verification and validation (V&V) process. There is a need to better understand basic physics process and how to parameterize them in models, including fluxes, boundary layer turbulence and their parameterizations, and issues related to blending different types of models across scales, including the terra incognita. Therefore, DOE has initiated a project focusing on a comparison between models in order to demonstrate the V&V-guided approach to model development specifically applied to the mesoscale-microscale coupling problem. This is a joint collaborative project between DOE labs and builds on prior efforts [1-6].

Initial Efforts

The DOE Meso Microscale Coupling Project seeks to develop and validate a set of first-principles based, high-fidelity physics models within an open-source simulation environment using formal verification and validation processes (Fig 1). Six DOE laboratories are working collaboratively to exercise various mesoscale and microscale models that can be coupled for a chosen set of cases based on field data from the Scaled Wind Farm Test (SWiFT) facility that display a range of atmospheric behavior. These cases have been validated and compared to determine the current state of atmospheric modeling and directions for the future of coupling mesoscale to microscale simulations.

The team identified test cases from 2012 that represent neutral, stable, and convective conditions, then exercised a variety of mesoscale (Weather Research and Forecasting – WRF, and Model Prediction Across Scales – MPAS) and microscale (WRF-LES, OpenFOAM, and HIGRAD) models for these cases. Sensitivity studies have been used to determine differences in parameterizations, resolution, and more.

The modeling results are compared with the observations from the SWiFT tower and wind profiler, including velocity components $[u, v, w]$, potential temperature θ, and subgrid turbulent kinetic energy - SGS TKE. In addition, spectra and cospectra are assessed, as well as surface heat flux, boundary layer depth, and shear across levels commensurate with wind turbine swept area. The results of these comparisons and interpretation will be presented.

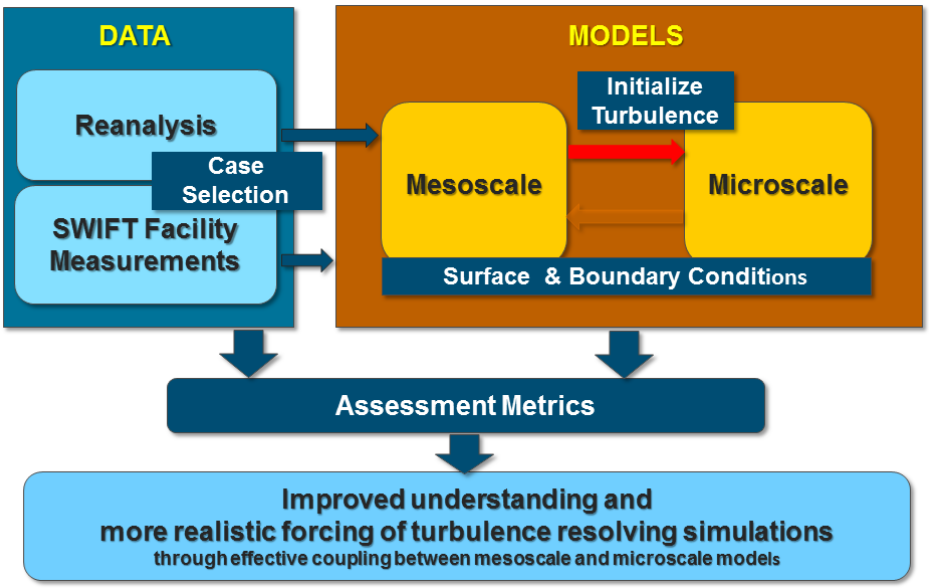

Fig. 1 Diagram of Meso to Microscale Coupling Project concept.

Acknowledgments

This work is funded by the US Department of Energy and is comprised of work being done at several DOE labs. Participants include Argonne National Laboratory, Los Alamos National Laboratory, Lawrence Livermore National Laboratory, National Center for Atmospheric Research, National Renewable Energy Laboratory, Pacific Northwest National Laboratory, and Sandia National Laboratory.

References

[1] M. Churchfield, C. Draxl and J. D. Mirocha, "A one-way meso-microscale coupling strategy for realistic wind plant aerodynamics large-eddy simulation," submitted to *J. Renewable and Sustainable Energy*, (2015).
[2] M. J. Churchfield, S. Lee, J. Michalakes, and P. J. Moriarty, "A numerical study of the effects of atmospheric and wake turbulence on wind turbine dynamics,: *J. Turbulence*, **13**, N14 (2012).
[3] B. Kosović, "Subgrid-scale modelling for the large-eddy simulation of high-Reynolds-number boundary layers," *J. Fluid. Mech*., **336**, 151–182 (1997).
[4] J. D. Mirocha, B. Kosović, M. L. Aitken, and J. K. Lundquist, "Implementation of a generalized actuator disk wind turbine model into the weather research and forecasting model for large-eddy simulation applications," *J. Renewable Sustainable Energy* **6**, 013104-1–013104-19 (2014).
[5] J. D. Mirocha, B. Kosović, and G. Kirkil, "Resolved turbulence characteristics in large-eddy simulations nested within mesoscale simulations using the Weather Research and Forecasting model," *Mon. Wea. Rev.* **142**, 806–831 (2014).
[6] Muñoz-Esparza, D., B., Kosović, J. D. Mirocha, and J. van Beek, "Bridging the transition from mesoscales to microscale turbulence in atmospheric models," *Bound-Layer Meteorol*. **153**(3), 409–440 (2014).

Sensing Skin for Large-Scale Surface Strain Measurements

Simon Laflamme
Dept. of Civil, Construction, and Environmental Engineering, Iowa State University, Ames, IA, USA

Austin Downey
Dept. of Civil, Construction, and Environmental Engineering, Iowa State University, Ames, IA, USA

Abstract

Existing sensing solutions facilitating continuous condition assessment of wind turbine blades are limited by a lack of scalability and difficulties in linking signals to structural conditions. With recent advances in conducting polymers, it is now possible to deploy network of thin film sensors over large areas, enabling low cost sensing of large-scale systems. We have developed a novel sensing skin consisting of a network of soft elastomeric capacitors (SECs). A single SEC, as shown in Fig. 1, acts as a large-scale surface strain gage transducing local strain into measurable changes in capacitance. Using surface strain data facilitates the extraction of physics-based features from the signals that can be used to conduct condition assessment. The technology may also be used during testing to overcome limitations of conventional foil gauges that measure very localized strain. In this presentation, we present the novel sensor and demonstrate its performance, in particular for utilizations in a network configuration. These demonstrations include laboratory experiments on a small network of sensors used for reconstructing strain maps and deflections shapes of cantilever plates, and numerical simulations of a dense network of sensors for damage detection, localization, and prognosis on wind turbine blades.

Fig. 1 A single SEC (3 x 3 in2)

Wind and Turbulent Intensity Variations at the WEICan North Cape Site

Stefan Miller, Peter Taylor and Soudeh Afsharian
CRESS, York University, Toronto, Canada

Gerald Giroux
Wind Energy Institute of Canada (WEICan), North Cape, Prince Edward Island, Canada

Introduction

As a part of the PEIWEE 2015 field program, six 10-m meteorological masts were installed on the main WEICan site (Fig 1). Measurements were made for the three month summer period (mid-May to mid-August). All masts measured wind speed and direction at 10m plus temperature at 2m. Tipping bucket rain gauges were added at two masts and surface pressure at one. On one mast close to a 12m cliff we added cup anemometers at three levels and additional temperature measurements were made on a second mast to assess stratification. For onshore flow the data are being used to investigate the wake caused by the cliff plus the impact of the roughness change from sea to land while in other cases we are looking at wakes behind the V47 turbines surrounding the area in which the masts were deployed.

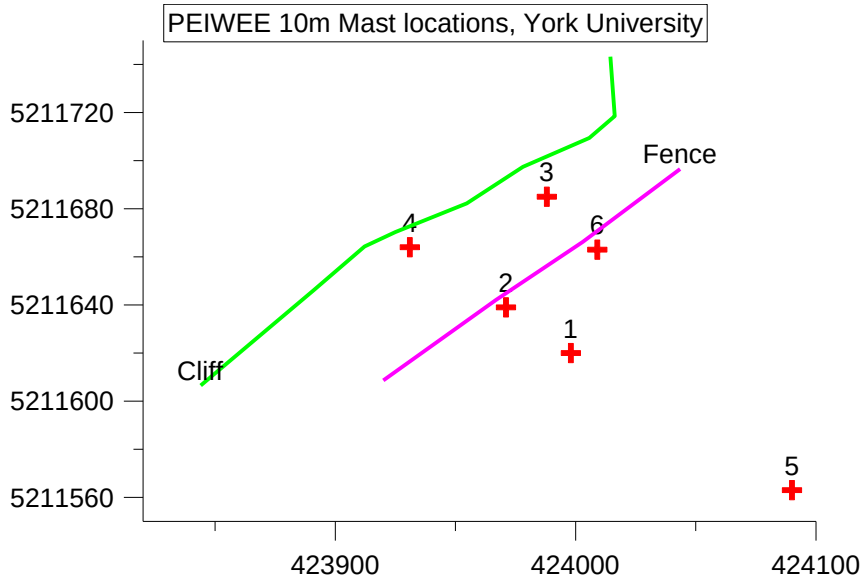

Fig. 1 Locations of the 10-m masts relative to the shoreline cliff and a low fence, Axes are UTM coordinates (m)

Preliminary Results

Analysis of the data is continuing but some sample early results can be seen in Fig.s 2 and 3. Fig. 2 shows the variation in 10-m wind speed (normalized by the 6-mast average) with distance inland from the cliff for wind directions greater than 3 m/s and averaged in 20° bins. For onshore flow (wind directions 225° to 45°) there is speed-up at the near shore masts while winds are relatively uniform for offshore flows, although there is a slight increase as the winds respond to a reduction in surface roughness within the WEICan site compared to trees and wind turbines to the SE.

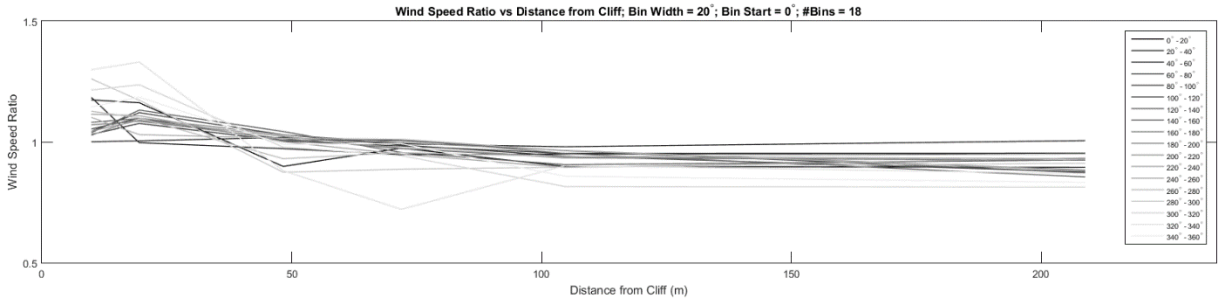

Fig. 2 Wind speed ratios (May-July 2015) for winds > 3m/s in 20° direction bins.

In Fig. 3 we cannot see much evidence of turbulence intensity (TI) variations in the wakes behind the V47 turbines although there is some evidence of wind speed reductions (not shown). The interesting features are for onshore flows. At mast 4 close to the shoreline we see increases in TI for flows parallel to the shorelines (winds from 55° and 210°) and low TI for onshore, over water, flow (250° - 30°) where the cliff wake has not extended up to 10m. At mast 2 we see large spikes in TI for flow approximately normal to the shoreline cliff (at 290° and 330°) with a dip in between at 315°. At this stage (July 31) we are hoping for more data to confirm the robustness of these observations. We also have velocity and temperature profiles at the near shore masts which will provide additional information.

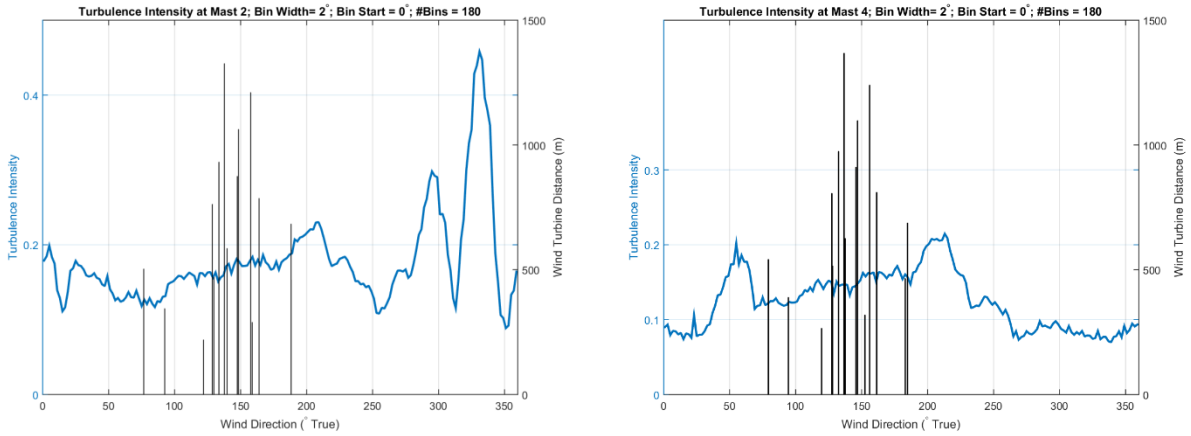

Fig. 3 Turbulence intensities at masts 2 and 4, averaged for all winds (may-july) > 3 m/s in 2° Direction bins. The vertical lines are bearings to the V47 turbines showing the distance away from the masts.

Acknowledgments

Funding for the York involvement in PEIWEE is through an NSERC Discovery grant to Peter Taylor plus IACPES support for Stefan Miller and Soudeh Afsharian. Local support from WEICan and the Cornell team was much appreciated.

Measurements and Modeling of Wind Turbine Relevant Flow Parameters at an Escarpment during PEIWEE

S.C. Pryor
Cornell University, Ithaca, NY 14853, USA

H. Wang
Cornell University, Ithaca, NY 14853, USA

P. Doubrawa
Cornell University, Ithaca, NY 14853, USA

G. Giroux
WEICan, North Cape, PEI C0B 2B0, Canada

R.J. Barthelmie
Cornell University, Ithaca, NY 14853, USA

Introduction

Although there are clear potential advantages to siting of wind turbines on escarpments due to speed-up of the flow, the potential for unbalanced loads across the wind turbine rotor from the associated large flow tilt angles, high shear and/or veer and for higher fatigue loading due to enhanced turbulence leads to enhanced uncertainty and the possibility for increased overall project costs. Thus, there is a need for improved understanding of flow conditions along and behind such terrain features. We present a combined observational and modeling analysis of flow parameters over an escarpment, and focus on heights and flow parameters of greatest relevance to the wind energy industry. We present measurements conducted during the Prince Edward Island Wind Energy Experiment (PEIWEE) at the Wind Energy Institute for Canada (WEICan) located on the Northern Cape of PEI during May 2015 (Fig. 1). The escarpment is 10-14 m high and extends for many kilometers. Behind the cliff edge the land gently slopes to the east (at slope angles of <3°). The over-water fetch to the west extends beyond 50 km making this an ideal location to study the impact of an abrupt terrain feature on flow (see example of the flow distortion in Fig. 2). To supplement the ongoing WEICan measurements, the following instrumentation was deployed: 3 3D Gill Windmaster Pro sonic anemometers at 20, 40 and 60 m on the IEC compliant 80 m meteorological mast (MM) located ~500 m east from the coast. Three Natural Power ZephIR lidars were deployed northwest of the MM. One (unit Z447) was deployed ~40 m from the cliff edge, co-located with an additional 3D Gill Windmaster Pro at 9 m height and a 18 m MM with cup anemometers and wind vanes at 18 and 10 m. A second lidar (unit Z423) was located 250 m to the eastsoutheast of this group (~235 m from the coast) and the third (Z125) to the east, ~280 m from the coast. To the south-east of the 80-m MM, a Galion scanning lidar was deployed ~535 m from the cliff and operated using a scan geometry that included both stacked arc-scans (approximate scan volume shown in Fig. 1) and VAD scans. In conjunction with these observations numerical simulations have been conducted with WRF (nested to 1 km), WAsP Engineering and WAsP-CFD.

Body

Flow conditions were dominated by weakly stable to neutral stability, westerly flow and relatively high wind speeds (Fig. 2). They were thus ideal to study the impact of the escarpment on flow parameters of relevance to the wind energy industry. Here we use the resulting observations to (i) quantify the impact of the escarpment on flow parameters, (ii) diagnose the height and longitudinal extent of the volume in which flow parameters exhibit evidence of the impact of the escarpment and (iii) evaluate simulations conducted using WAsP Engineering and

WAsP-CFD. Data from pseudo-RHI slices derived from stacked arc scans with the Galion indicate the speed up at 80-m a.g.l. extends 300-400 m inland. Data from the ZephIR lidar measurements at the cliff indicate shear exponent values >0.3 across a wide range of wind speed and TI values. Flow tilt angles 40-m from the cliff are generally below the recommended limit of 8°, and actually exhibit highest absolute values in (infrequently observed) southeasterly (i.e. offshore) flow. Simulations using WAsP-CFD reproduce the zone of preescarpment deceleration and at escarpment enhancement of wind speed, turbulence intensity and flow tilt angle well relative to the observations, but appear to under-estimate the flow tilt angle at the cliff and the longitudinal extent of the zone of enhanced turbulence intensity.

Fig. 1 Left: Overview of the site showing the 5 DeWind 2 MW turbines (cyan), ZephIR lidars (green), IEC compliant MM (green open circle) and the Galion (red dot). Center: Photograph from the 80-m MM looking northwest. T4 is shown in the center of the image. Z447, a Gill sonic and an 18-m MM were located west of T4 (towards the cliff). Photo: André Doucette. Right: Photograph of the escarpment looking south. Photo: Sara C Pryor.

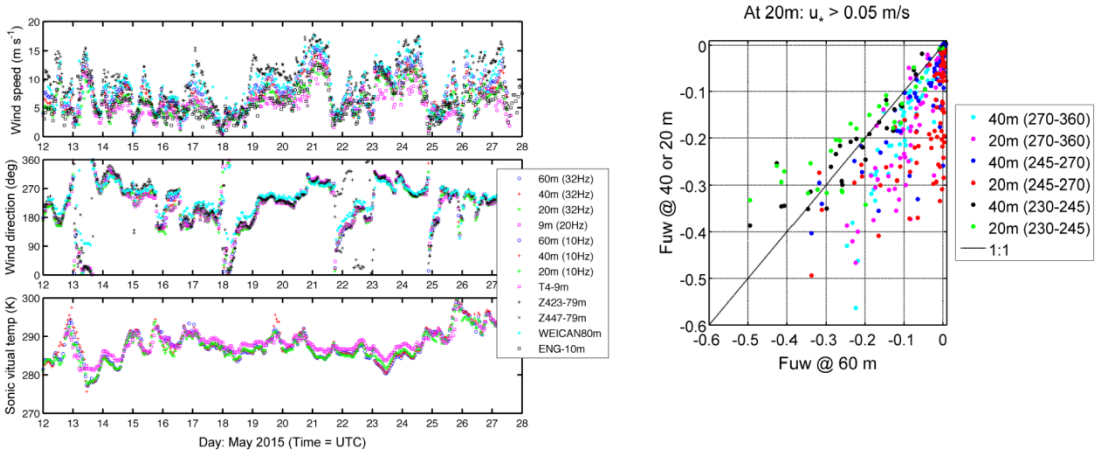

Fig. 2 Left: Hourly average mean wind speed, direction and temperature from the different instruments during the field experiment. Right: Profile of momentum flux at the 80 MM (400-m from the coast) conditionally sampled by wind direction. Note the presence of inverted flux profiles for flow along the cliff.

Acknowledgments

NSF (#1464383) and DoE (#DEE0005379.) Assistance from André Doucette and Carl Doucette.

'Breezy' Mysteries – Using a Combination of High-Fidelity Flow Simulation & Visualization to Extract Greater Understanding of Wind Turbine Wake Interactions

Sven Schmitz
Assistant Professor, Department of Aerospace Engineering, The Pennsylvania State University, University Park, PA 16802, USA

Earl P. N. Duque
Manager, Applied Research Group, Intelligent Light, Rutherford, NJ 07070, USA

Introduction

Over the past few years, significant progress has been made on understanding the wake recovery process downstream of utility-scale wind turbines in the atmospheric boundary layer (ABL); however, some 'mysteries' remain concerning i) Turbulent transport in the wakes of wind turbines, ii) Power distribution in an array of wind turbines, and iii) Vortex breakdown at the end of the turbine near wake and its effect on downward momentum transport into the rotor disk area. To date, field data are not acquired at sufficient spatial and temporal resolution to fully unravel the remaining 'mysteries' of wind turbine wakes. It is here that a combination of high-fidelity simulation and visualization has shown to provide some new insights that have the potential to impact future data measurement campaigns.

Numerical Methods

Wake Modeling: The actuator line method (ALM) has evolved to become the technology standard in the wind energy community to model the effects of wind turbine blades [1-3]. In the ALM, a blade is discretized as a series of (typically 25-40) actuator points. Sectional lift and drag forces are determined from the local flow velocity and angle of attack (AoA), which are then applied to an airfoil lookup table. In this work, the ALM is used in an OpenFOAM solver of the atmospheric boundary layer (ABL). – Flow Visualization: As for flow visualization of simulation data, the FieldView [4] tool was used to reduce the data by creating iso-surface and coordinate-surface extracts that were then used for flow-field visualizations and quantitative analyses in the turbine wakes.

Selected Results

Turbulent Transport and Power Distribution in Wind Turbine Arrays: Resolving the ABL using large-eddy simulation (LES) produces a wealth of raw volume data that is difficult to handle and to store for post-processing. This is greatly simplified using FieldView's portable data extracts (XDB) that can be used for both flow visualization and analyses. An example of dynamically clipped surfaces are shown in Fig. 1 where analyses of various flux integrals were performed separately for the upper-/lower halves of the rotor disk, thus providing new insights into turbulent transport and power distribution in wind turbine arrays.

Vortex Breakdown in Turbine Wakes: The breakdown process of root-/tip vortices is, to a large extent, dependent on the atmospheric stability state. A neutral ABL supports tip vortices for longer distances than an unstable ABL, which has additional implications on the recovery process of the wake momentum deficit. An example of the vortex breakdown process in a moderately-convective boundary layer (MCBL) is shown in Fig. 2 where the combined simulation/visualization methodology was able to correlate combinations of certain turbulent structures to tip vortex breakdown.

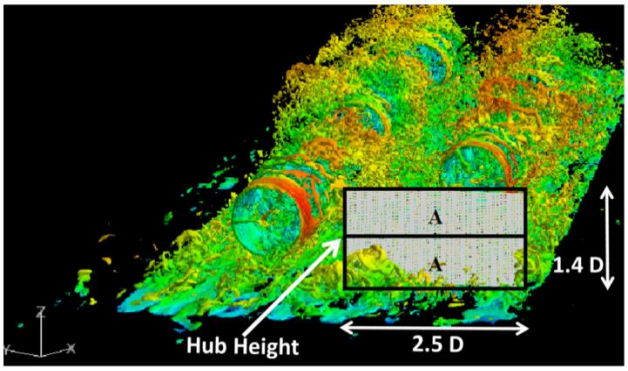

Fig. 1 Wake Integration Planes (created with 'dynamic surface clipping' in FieldView)

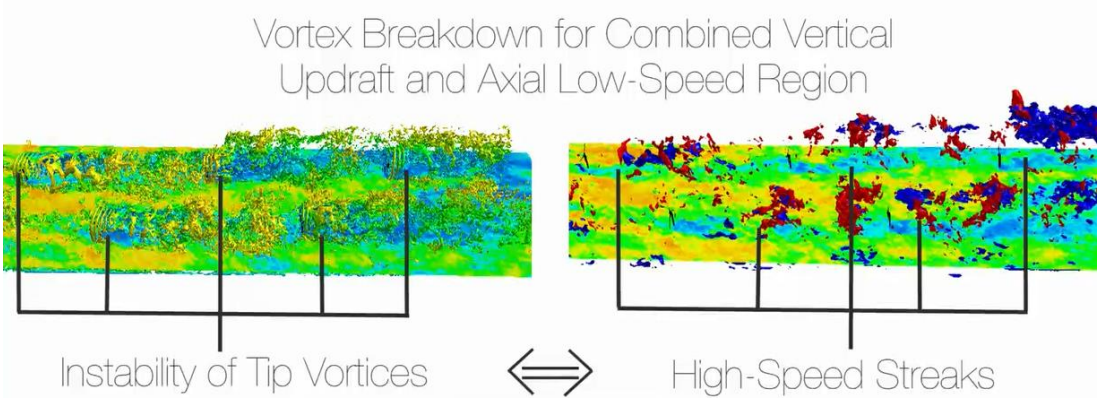

Fig. 2 Five NREL 5-MW Wind Turbines in Moderately-Convective Boundary-Layer Flow [5

The presentation will include a number of quantitative analyses of the combined simulation/visualization methodology and will provide a comprehensive discussion of the implications that results obtained thus far can have on future field testing.

Acknowledgments

The CFD images and post-processing were created using FieldView as provided by Intelligent Light through its University Partners Program. This work was supported by the Department of Energy (DE-EE0005481) as part of the "Cyber Wind Facility" project at the Pennsylvania State University.

References

[1] Sørensen, J.N., Shen, W.Z., 2002, Numerical modeling of Wind Turbine Wakes, ASME Journal of Fluids Engineering 124:393-399.
[2] Churchfield, M.J., 2011, Wind Energy / Atmospheric Boundary Layer Tools and Tutorials. Training Session at the 6th OpenFOAM Workshop, The Pennsylvania State University, June 2011.
[3] Jha, P.K., Churchfield, M.J., Moriarty, P.J., and Schmitz, S., 2014, Guidelines for Volume Force Distributions within Actuator Line Modeling of Wind Turbines on Large-Eddy Simulation-type Grids, ASME Journal of Solar Energy Engineering 136:0310014.
[4] Intelligent Light. URL http://www.ilight.com (accessed on July 30, 2015).
[5] Jha, P.K., Duque, E.P.N., Bashioum, J.L., and Schmitz, S., 2015, Unraveling the Mysteries of Turbulence Transport in a Wind Farm, Energies 8(7):6468-6496.

Measurements under Controlled Conditions for Wind Turbine and Plant Modeling and Validation

S. Schreck
NREL's National Wind Technology Center, Golden, Colorado, United States

L. Fingersh
NREL's National Wind Technology Center, Golden, Colorado, United States

S. Guntur
NREL's National Wind Technology Center, Golden, Colorado, United States

Introduction

Shortfalls in wind plant energy capture and elevated turbine fatigue loads, both associated with turbine-turbine interactions, are the principal causes of excessive cost of energy (COE) levels. Addressing these issues will require detailed knowledge of the complex fluid dynamic interactions throughout the wind plant. The ability to accurately predict wake initiation, evolution, and demise due to plant inflow conditions, plant layout, and turbine operating characteristics will facilitate optimizing plant energy capture, machine reliability, and COE.

Tight integration of wind turbine and plant modeling with focused, high quality experimental measurements is an effective strategy to thoroughly understand and accurately predict the physics of these phenomena. At present, wind plant scale fluid dynamics cannot be modeled with sufficient resolution to characterize individual turbine or full plant physics, even using today's most advanced high performance computers. Extensive research is required to establish how to accurately model these phenomena and to most reliably validate these models. A formal verification and validation (V&V) approach is being used to link targeted experimental activity to the modeling development and validation.

Accordingly, the current conference presentation will document closely coupled experiments/modeling for guiding model development and assessing model accuracy in predicting wind plant wake dynamics. Key facets of this approach will be coordinated wake measurement campaigns at the University of Milan ABL wind tunnel and at the SWiFT (Scaled Wind Farm Test) atmospheric facility. Also described will be opportunities for incorporating previous turbine rotor, blade, and airfoil measurements carried out in wind tunnels into this framework, to effectively support the capstone full rotor wake measurement experiments.

Summary of Content

Importantly, wind tunnel measurements enable resolution of detailed fluid dynamic phenomena. While these phenomena can be detected and characterized in the controlled inflow environment, most remain obscured by wind inflow variability in atmospheric testing. At present, resolved measurements of these detailed physical phenomena occupies central importance, because of compressed spatio-temporal scales crucial to the development, validation, and application of advanced high fidelity computational models.

To address these needs, the wind plant aerodynamics problem can be decomposed into five component physical interactions, which are listed below. Measurement campaigns under controlled conditions can be similarly partitioned, and pertinent data either already have been acquired in previous efforts or will be acquired in impending planned activities. The existing or planned measured data, measurement methodologies, and validation applications will be described in the conference work.

- **Inflow to rotor and blade loads.** Inflow states will include uniform/steady inflow, turbulence intensity, shear, and may encompass transient occurrences commonly referred to as "extreme events". Inflow velocity and turbulence distributions will be simultaneously measured along with rotor flow field to relate inflow structures to ensuing blade loads and to validate model predictions.
- **Formation of wake by rotor.** Interaction of inflow with the blades elicits responses in blade boundary layer state, flow field structure, and structural loads. Because boundary layer state and flow field, including rotational augmentation and dynamic stall, drive vorticity production and shedding, these are directly responsible for wake production and thus key measurements for physics comprehension and model

validation. Structural loads also will be measured as useful adjuncts to complement detailed flow field information.

- **Wake skew and meander**. Wake trajectory can deviate from center in steady (skewed) or dynamic (meander) fashion depending on rotor geometry, operating state, and wind inflow. These are important to measure, because wake skew and meander simultaneously affect induction on the associated upstream rotor and define where the wake impinges downstream. They also govern the authority of proposed wind farm control approaches to affect the flow through a turbine array.
- **Wake advection, instability, and dissipation.** As the aggregate wake travels downwind in a skewed/meandering trajectory, instabilities can arise within the wake as vorticity concentrations interact, and dissipation occurs as turbulent and molecular processes diffuse wake vorticity. These physics are important to measure, because these determine wake size and energy as it proceeds downstream and what impact it will have when it impinges on rotors farther downstream.
- **Wake impingement on downwind turbine.** In the multi-row wind plant environment, the wake produced by an upstream rotor may impinge on a downstream rotor, after undergoing the combined influences of skew, meander, instability, and dissipation. Coupled with impingement, the collective action of these four processes determines reductions in energy capture and amplification in fatigue loading.

Altogether, the most significant intended outcomes of the wind tunnel measurement activity, in connection with other previous and future measurement campaigns, are as follows. These will be explained and summarized in the conference presentation:

- Improved physical understanding of major wind plant fluid dynamic phenomena.
- High quality measured datasets suitable for validating wind turbine and plant models.
- Development and validation of wind turbine and plant computational models.

Acknowledgments

This research is supported by the United States Department of Energy, through the EERE Wind and Water Power Program's Atmosphere to Electrons (A2e) Initiative.

Analysis of Wind Turbine Stall with Per-Tuft Statistics

Tyler E. Gallant
University of Waterloo, Waterloo, Canada

Professor David A. Johnson
University of Waterloo, Waterloo, Canada

Introduction

A growing demand for wind turbine innovation has necessitated the development of analysis tools for measuring wind turbine blade performance. Currently, there exists few accurate, quantitative methods for measuring stall over a wind turbine blade. One technique, which has been used previously by Eggleston and Starcher [1], Haans *et. al.* [2] and others, is tuft flow visualization. This method consists of attaching short tufts of string to a surface immersed in a flow, and using their orientation and behavior to infer the flow behavior over the blade. Unfortunately, most tuft flow visualization studies in the literature provide only limited, qualitative data, as authors analyzed images manually.

To obtain objective, quantitative stall data, digital image processing algorithms were developed independently by Swytink-Binnema *et. al.* [1] and Vey *et. al.* [4]. The first is designed to analyze images taken from the root of the blade (as shown in Fig. 1), and calculates the fraction of tufts in each frame which are indicative of stall (*i.e.* the stall fraction, ζ) [1] In contrast, the Vey *et. al.* [4] algorithm is designed for images recorded from a ground mounted camera, and has only been used for phase averaged results at one blade positon. However, the Vey *et. al.* [4] algorithm is capable of logging per-tuft statistics, increasing the possibilities for data analysis. This paper presents the expansion of the Swytink-Binnema *et. al.* [1] algorithm to include per-tuft statistics, as well as its application to data measured at the University of Waterloo (UW).

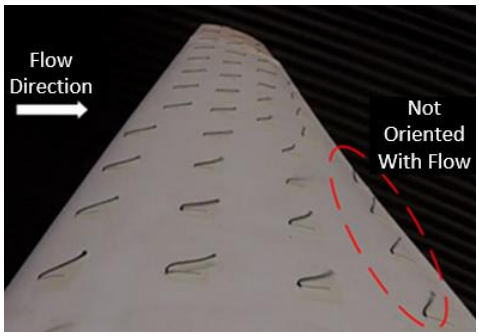

Fig. 1 Image of tufts on a wind turbine blade in a flow

Body

Tests were conducted at the UW Wind Generation Research Facility, which acts as an open circuit wind tunnel with a fan area of 11.4 m by 7.6 m capable of generating wind speeds up to 11 m/s [5]. The facility houses the UW Wind Energy Group test turbine, which was equipped with three 1.6 m long test blades [6], each with a tapered chord and a twist of approximately 19°. The blades are designed to operate at 200 rpm in a 6.5 m/s wind [6]. An image of the turbine used is provided in Fig. 2(a).

Approximately 40 tufts were attached to the blade surface aligned parallel to the quarter chord line and spaced 4 to 8 cm apart. A high-definition (HD) video camera was attached to the blade root via an adhesive mount to record the tufts movement. Video was recorded at 1080p resolution at a rate of 60 fps. An image of the camera and tufts attached to the blade is provided in Fig. 2(b).

Results from the study (available in [7]) showed that the amount of stall increased with wind speed, with ζ varying from approximately 18% at a tip speed ratio, λ, of 6.3 up to approximately 43% at $\lambda = 3.7$. As the turbine was yawed, it was found that ζ increased as the blade rotated toward the wind and decreased as the blade rotated away from the wind. This variation occurs due to how the angle of attack, α, varies throughout the rotation. As the blade travels toward the wind, the upstream wind vector is offset by the yaw angle such that the axial velocity on the blade is decreased and the tangential velocity is increased, reducing α. The opposite occurs as the blade travels away from the wind.

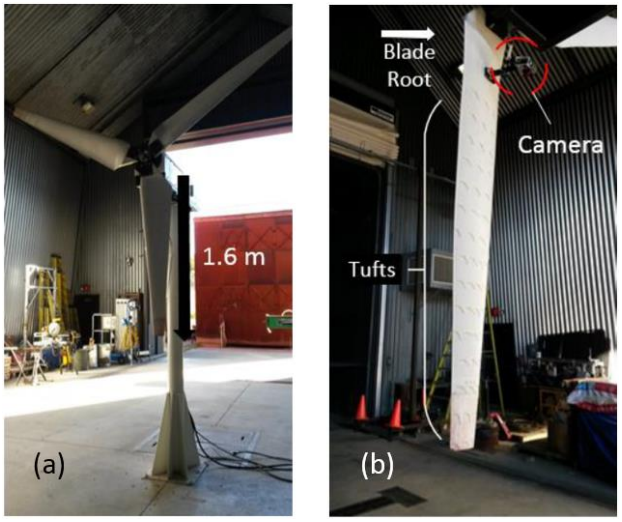

Fig. 2 (a) WEG Test Turbine (b) Tufted Blade

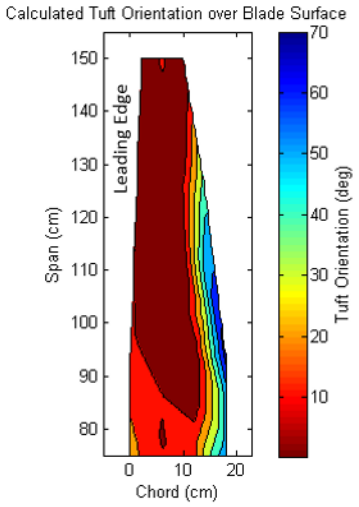

Fig. 3 Average tuft orientation at $\lambda = 6.3$.

The Swytink-Binnema *et. al.* **[1]** processing algorithm was expanded to include individual tuft tracking. This includes logging the orientation of every tuft in every frame such that the range of motion experienced by a tuft may indicate turbulence or oscillation between separated and attached flow. Per-tuft statistics also allow for the interpolation of data between tufts. Fig. 3 shows a contour map of the average tuft orientation experienced over the span of the blade, calculated by interpolating between the average tuft orientations for the 41 tufts observed. Attached flow is indicated by tufts with an average orientation less than 20° from horizontal, so the figure shows that at $\lambda = 6.3$, most of the blade experiences attached flow, with some stall being observed at the trailing edge.

Expanding the functionality of the Swytink-Binnema *et. al.* [1] algorithm has increased the potential for analysis and understanding when it comes to stall. Preliminary testing has shown that this algorithm can objectively and rapidly analyze tuft images to a depth not previously reported in the literature.

Acknowledgments

The authors would like to gratefully acknowledge support from NSERC and OCE.

References

[1] Eggleston, D. and Starcher, K. 1990, "A comparative study of the aerodynamics of several wind turbines using flow visualization," *J Sol Energy*, Vol. 112, no. 4, pp. 301-309. DOI: 10.1115/1.2929938.

[2] Haans, W., Sant, T., van Kuik, G. and van Bussel, G. 2006, "Stall in yawed flow conditions: a correlation of blade element momentum predictions with experiments," *Sol Energy Eng*, Vol. 128, pp. 472-480. DOI: 10.1115/1.2349545.

[3] Swytink-Binnema, N. and Johnson, D.A. 2015, "Digital tuft analysis of stall on operational wind turbines," *Wind Energy*, DOI: 10.1002/we.

[4] Vey, S., Lang, H.M., Nayeri, C.N., Paschereit, C.O. 2014, "Extracting quantitative data from tuft flow visualizations on utility scale wind turbines," *J Physics: Conference Series*, Vol. 524, 012011.

[5] "UW Live Fire Research Facility." UWaterloo Wind Energy Group. Available: windenergy.uwaterloo.ca. [Accessed Dec. 5, 2014].

[6] Gertz, D. and Johnson, D.A. 2011. "An evaluation testbed for wind turbine blade tip designs – baseline case," *Int. J. Energy Research*, Vol. 35, n. 15, pp. 1360-1370.

[7] Gallant, T.E. and Johnson, D.A. 2015. "Analysis of Wind turbine Stall using Tuft Flow Visualization," in *Proc. of the 25th CANCAM*, London, ON, pp. 113-116.

Large Eddy Simulation of Atmospheric Boundary Layer Flows over Complex Terrain

Yi Han, Michael Stoellinger
Department of Mechanical Engineering, University of Wyoming, Laramie, Wyoming, U.S.A

Introduction

In this work, we present a validation and some improvements to the atmospheric boundary layer (ABL) solver in the OpenFOAM-based simulator for on/offshore wind farm applications (SOWFA) [1], which was originally developed by the U.S. Department of Energy's National Renewable Energy Laboratory (NREL). SOWFA contains an incompressible flow solver for performing large-eddy simulation (LES) of wind flow through wind farms. So far the solver (named ABLSolver) has mostly been used for computing wind farm flows over the flat terrain. Recently, a new solver (named ABLTerrainSolver) has been added suitable for simulating flow over complex terrain and it has been applied to a simple terrain case consisting of several two-dimensional hills. Here we apply this new solver to a real three-dimensional complex terrain including hills and valleys located in southern Wyoming to predict effects like local acceleration, separation and recirculation. The focus of this work will be on evaluating different mechanisms for providing appropriate turbulent inflow conditions and also to study the effects of different boundary conditions for the top and sides of the domain.

Body

Mesh generation on the real complex terrain. This research work will mainly focus on the Sierra Madre wind farm site located in Carbon County, Wyoming. Firstly, a $3780\,m \times 3690\,m \times 1775\,m$ domain in the longitudinal(x), latitudinal(y), and altitudinal(z) directions where there are several meteorological towers inside is chosen. For the LES simulation, the topography is obtained from the fine-scale 1-arc-second terrain from the Shuttle Radar Topography Mission dataset (SRTM) with simulations down to the approximately 30-meter resolution for the section of the project site. Secondly, a mesh size of $190 \times 187 \times 100$, which is relatively coarse but suitable for this somewhat qualitative study, is created with the vertical stretching that allows a fine resolution near the ground where the first grid point at 5-meter above the terrain surface and the maximum height of the cell is about 70-meter. The mesh generations on and above the real terrain are shown in Fig. 1 and 2, respectively.

Fig.1 Structure mesh domain on the real terrain with resolution of $\Delta x \times \Delta y = 20m \times 20m$

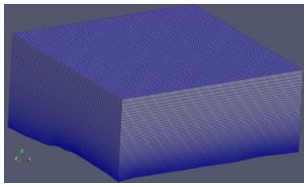

Fig.2 Structured mesh block of ABL over the terrain with vertical stretching Δz from 5m to 70m.

Boundary condition modifications to fit the real flow case. The tutorial cases in SOWFA are periodic, which means that the lateral boundaries are cyclic in OpenFOAM set up. This is obviously not the true situation in the real wind farm. In the current work, the west and east faces of the domain are modified as inlet and outlet boundaries, respectively. The north, south and upper faces are set as slip, zero stress boundaries. Wall stress conditions are applied at the terrain surface. Firstly, the uniform velocity and temperature profiles are specified at the inlet boundary and the simulation result can be seen in Fig. 3. Then, the Smirnov-Shi-Celik (SSC) procedure [2], which is a random flow generation (RFG) technique, is used for initial/inlet boundary generation in LES computation for turbulent flows. The SSC procedure offers a relatively inexpensive way to generate random velocity fluctuations, representing a turbulent inflow. It is a far more realistic representation of turbulence than can be obtained with a simple Gaussian velocity distribution using a random-number generator since the generated

velocity field satisfies prescirbed spatial and temporal correlation scales and is nearly divergence free. The preliminary simulation result of this boundary condition modification is shown in Fig. 4.

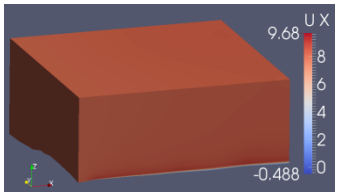

Fig. 3 The overview of along-wind (x-direction) velocity in simulation block under the inflow condition of uniform velocity (8 m/s) after running 15000 sec.

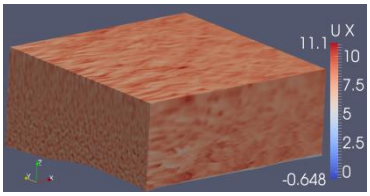

Fig.4. The overview of along-wind (x-direction) velocity in simulation block under the initial SCC turbulent inflow condition ($\overline{U}$ = 8m/s) after 15000 sec

Numerical methods. The filtered continuity, momentum and potential temperature equations are solved by using OpenFOAM's buoyantBoussinesqPimpleFoam, which is a transient solver for buoyant, turbulent flow of incompressible fluids. ABLTerrainSolver modified the solver metioned above by adding the effects of Coriolis forces, a large-scale driving-pressure gradient to achieve a desired wind speed at a given height, and specified surface stresses and temperature flux. For LES simulation, the Lagrangian-averaged scale-independent (LASI) dynamic Smagorinsky mode [3] is used to model the sub-grid-scale (SGS) stress tensor.

Projection for the final paper/presentation. (1) Based on the wind property data measured by the meteorological tower in the Sierra Madre wind farm provided by the Power Company of Wyoming, the speed and direction of the prevailing wind over this area in a period of time displaying close to neutral conditions will be analyzed. The rectangular cuboidal domain will then be rotated so that the x-axis will be aligned with the mean wind direction and the y-axis will become the crosswind direction. The structured mesh with stretching in vertical direction will be refined in order that more accurate simulation could be operated on it. (2) More practical boundary conditions of velocity and temperature will be specified. The combination of log wind profile with the SCC turbulence generating procedure will be utilized in the inlet velocity boundary condition. A second approach for inflow conditions will be generated based on the interpolated results from Weather Research and Forecasting (WRF) RANS output. (3) If the time permits, improvements to the ABLTerrainSolver are expected to be made such that a hybrid LES-RANS modeling approach can be used. The one-way coupled WRF-LES approach will be validated through comparison with time statistics from several meteorological towers located within the LES domain.

Acknowledgements

We would like to acknowledge the NREL for providing the open source SOWFA package online. This work was supported by the U.S. Department of Energy, Office of Science, Basic Energy Sciences, under Award # DE-SC0012671.

References

[1] Matthew J. Churchfield, Sang Lee, Patrick J. Moriarty. Adding complex terrain and stable atmospheric condition capability to the OpenFOAM-based flow solver of the simulator for on/offshore wind farm applications (SOWFA). ITM Web of Conference 2, 02001(2014).
[2] Smirnov, A., Shi, S., Celik, I. Random flow generation technique for large-eddy simulations and particle-dynamics modeling. *Journal of Fluids Engineering*. 123: 359-371, 2001.
[3] C. Meneveau, T. Lund, and W. Cabot. A lagrangian dynamic subgrid-scale model of turbulence. *Journal of Fluid Mechanics*, 319:353–385, 1996.

Flow-Induced Instabilities of Wind Turbine Blades

Yahya Modarres-Sadeghi
University of Massachusetts, Amherst, MA, USA

Pariya Pourazarm
University of Massachusetts, Amherst, MA, USA

Matthew Lackner
University of Massachusetts, Amherst, MA, USA

Introduction

Offshore wind turbine blades continue to grow in length, with the longest blades in operation now exceeding 70 m, and blades as long as 80 m in the prototype stage. This trend is driven by economics – wind turbine installation costs are substantially higher offshore than onshore, and so increased energy production and thus increased rotor areas are crucial for cost-effective offshore wind energy [1]. As blades become longer, however, they become more susceptible to various flow-induced dynamic instabilities [2]. Flow-induced instabilities occur due to the highly nonlinear interaction between the blade and the flow around it, and can lead to catastrophic failures of the blades. Furthermore, the blade's mass increases at a rate greater than the square of the increase in length, and so while there is tremendous motivation to make longer blades as light as possible, reducing a blade's mass further increases the potential for flow-induced instabilities. Thus, one of the major barriers to increased wind turbine rotor areas and decreased cost of energy is the limitation imposed by flow-induced instabilities.

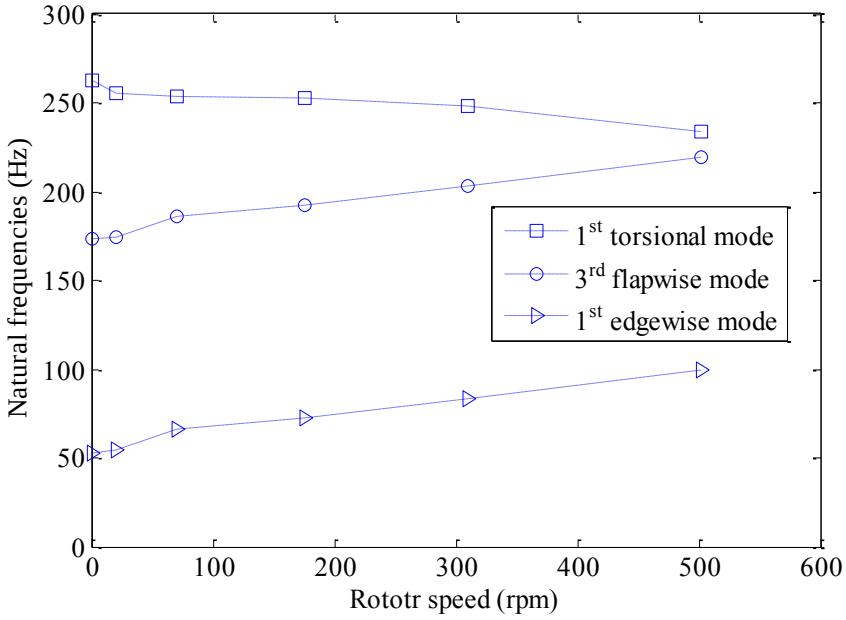

Fig. 1 An argand diagram based on experimental results for a rotating blade undergoing coupled-mode flutter.

Results

In the current work, the dynamic instabilities of parked and rotating wind turbine blades are studied using a numerical stability analysis and supported by experimental results. For the experimental component of the work, a series of tests were conducted in a wind tunnel. A three-bladed small scale wind turbine was designed for the

rotating blade experiments. To have the blades with the desired flexibility and aerodynamic properties, which matched the low Reynolds condition, the S3014 airfoil, with 9.5% thickness, was chosen to be utilized through the length of the blade. A piezo sensor was attached to the blade and the rotor speed was controlled by the eddy-current braking system. The wind speed was increased gradually and at each step data from the sensor attached to the blade were collected. As the oncoming wind speed was increased, the beam natural frequencies varied up to a critical wind speed at which two structural modes coalesced and resulted in coupled-mode flutter (Fig. 1). For the set of system parameters used in the experimental set-up, the first torsional beam mode and the third flapwise beam mode were combined to give rise to a flutter mode. A theoretical model based on coupled flexural-torsional beam equations subjected to aerodynamic loadings was derived and used to study the flow-induced instability for the designed blade.

To study the dynamic behavior of parked wind turbine blades, a new set of blades with a much higher flexibility were designed. The flexible blades were untwisted and had constant chords but different span to chord ratios. The experiments were conducted in an open-section wind tunnel and the flutter onset was found and recorded for each blade. The onset of flutter was also obtained theoretically and compared to the experimental results. It was observed that for all three blades the flutter mode was a combination of the 1st and the 2nd flapwise modes (bending-bending) and had a subcritical nature. Due to the high flexibility of the blades, a very small change in the angle of attack resulted in a large flapwise deflection, which altered the flutter characteristics significantly (more than 50% drop in the flutter critical speed).

Acknowledgments

The support provided by the Wind Technology Testing Center, a part of the Massachusetts Clean Energy Center is acknowledged. This work is supported in part by the National Science Foundation, award number CBET-1437988.

References

[1] S. Tegen, E. Lantz, M. Hand, B. Maples, A. Smith, and P. Schwabe, "2011 cost of wind energy," *Contract*, vol. 303, pp. 275–3000, 2013.
[2] M. H. Hansen, "Aeroelastic instability problems for wind turbines," *Wind Energy*, vol. 10, no. 6, pp. 551–577, 2007.

Variable, Large Feedback Wind Turbine Control Synthesis with Limited Plant Information

Yelena V. O'Brien
Wind Energy Research Center, University of Wyoming, Laramie, WY. U.S.

John F. O'Brien
Wind Energy Research Center, University of Wyoming, Laramie, WY. U.S.

Introduction

A method of control synthesis for a two-output blade pitch control with two unique features is presented. The first feature is a *variable loop transmission algorithm* that smoothly transitions feedback from the rotor regulation loop to the tower acceleration loop that enhances secondary performance if the primary variable is within prescribed limits. The second feature is large disturbance rejection achieved *without a linearized model of the wind turbine dynamics* available for purposes of loop shaping. This amalgam of novel capabilities provides control flexibility despite significant bandwidth limitations intrinsic to large wind turbines, and will be investigated in near-future research on wind farm control strategies.

Body

A variable loop transmission (VLT) strategy for single-input/two-output (SITO) controller is presented [1]. It is applied for illustrative purposes on the 1.5 MW turbine collective blade pitch to low speed shaft rate and tower fore/aft acceleration controller. Results presented in the sequel are acquired using the NREL FAST model of the turbine subject to 40 s of turbulent wind at principally region 3 speeds [2]. The control is applied simultaneously with the torque controller of Jonkman [2]. Region 2-3 transition and other specifics are considered beyond the scope of this work which serves to illustrate the potential of the variable SITO strategy for bandwidth limited, large turbine (and eventually turbine farm) control.

VLT is an algorithm that smoothly and stably reshapes the SITO loop transmission in closed loop so that the available feedback is transitioned between the two output paths. For the blade pitch controller, loop gain is shifted between the low frequency transmission of the shaft rate control and the bandpass transmission in an interval about the structure's first mode. These frequency intervals of negative feedback must be adequately separated (typically a few octaves) for stability, a feedback limiting feature for large wind turbines as their first mode is at low frequency (1-4 Hz). A fixed SITO system sacrifices rotor regulation performance for structural damping. A VLT system recovers this performance if rate error is large (effectively becoming a single output rate controller), and increases structural control by shifting loop gain to the modal frequency if the rate error is within prescribed limits. The algorithm is explained in detail in the full manuscript.

The proposed VLT system has a second distinctive feature in large feedback rotor rate control with high-order compensation synthesized without the benefit of a transfer function approximation of the turbine dynamics at a selected wind speed. This provides greater performance than the standard PI controller with a similar on-line tuning capability (a Ziegler-Nichols-like procedure for high-order compensation). The 40 s FAST simulation of the 1.5 MHz turbine operating in turbulent wind shows an 18% improvement of shaft rate error standard deviation compared to the PI controller *with the same bandwidth*. The algorithm is explained in detail in the full manuscript.

Fig. 1 shows weighting functions with inverse relationship used in the loop transmission shifting algorithm. Comparatively large values for the rotor loop are the result of the low speed shaft error exceeding a selected threshold (more feedback applied to the rate channel, e.g. 14-21 s); large values for the acceleration loop result when the shaft rate error is within the threshold (more feedback shifted to the first mode frequency). Fig. 2 shows

tower fore/aft acceleration (SITO versus SITO-VLT) in the interval between 20 and 25 s, in which the VLT algorithm shifts approximately 6 dB to the acceleration channel, reducing the acceleration standard deviation by 30% compared to the fixed two-output controller.

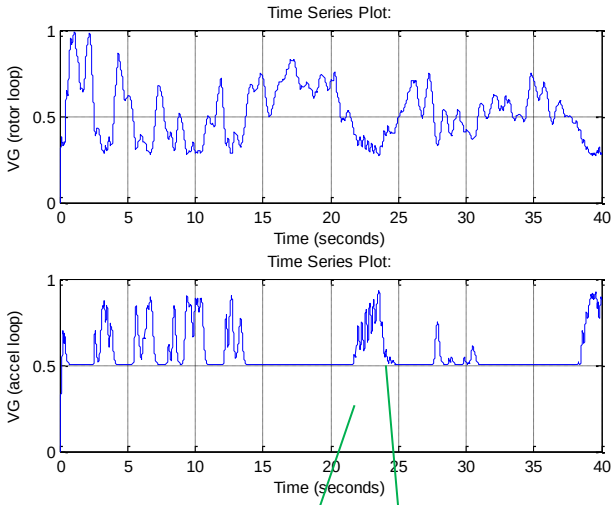

Fig. 1 Weighting functions for the 1.5 MW wind turbine SITO-VLT control system

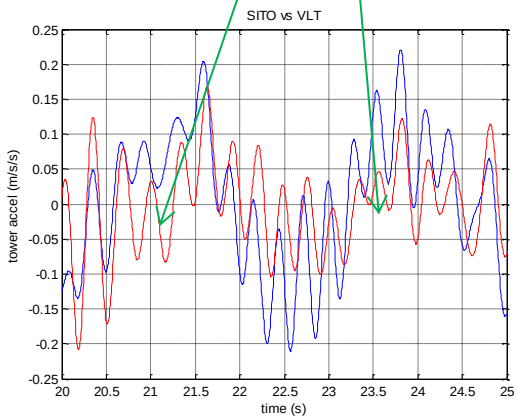

Fig. 2 Tower fore/aft acceleration in turbulent wind (blue SITO, red VLT-SITO)

Acknowledgments

The work is supported by grant 4201-11921-1002415 funded by the U.S. Department of Energy, Office of Science.

References

[1] O'Brien, J., Frequency-Domain Control Design for High-Performance Systems, IET, Stevenage, UK, 2012.
[2] Jonkman, J. and Buhr, M., "FAST Users Guide," Technical Report NREL/EL-500-38230, Aug. 2005.

Notes

CONFERENCE ABSTRACT REVIEW BOARD

Jubayer Chowdhury, WindEEE Research Institute, Canada

Yves Gagnon, Moncton University, Canada

Charlotte Bay Hasager, DTU Wind Energy, Denmark

Sue Haupt, National Center for Atmospheric Research, USA

David Johnson, University of Waterloo, Canada

Philippe Lavoie, University of Toronto, Canada

Maryam Refan, WindEEE Research Institute, Canada

Case van Dam, UC Davis, USA

LOCAL ORGANIZATION

WindEEE Research Institute

Western University

2535 Advanced Ave, London, ON

Canada N6M 0E2

www.windeee.ca

CONFERENCE OPERATIONS TEAM

Maryam Refan, Conference Coordinator

Adrian Costache, Production Coordinator

Jubayer Chowdhury, Operations Staff

Ahmed Elatar, Operations Staff

Julien LoTufo, Operations Staff

Mohammad Karami, Operations Staff

Karen Norman, Operations Staff

Kelly Garvey, SER Conference Coordinator

organizers

Western Wi Insti

Cornell University

University of Wyoming

DTU Technical University of Denmark

sponsors

Western

David R. Atkinson Center for a Sustainable Future

Wind Energy Research Center

School of Energy Resources

ISBN 978-0-7714-3099-2